

**ROTATIONAL SYMMETRIC POWER DIVIDER
AND
MULTIPOINT MICROSTRIP POWER DIVIDER**

LIM YEE BOON

**A project report submitted in partial fulfilment of the
requirements for the award of Bachelor of Engineering
(Hons.) Electrical and Electronic Engineering**

**Faculty of Engineering and Science
Universiti Tunku Abdul Rahman**

April 2012

DECLARATION

I hereby declare that this project report is based on my original work except for citations and quotations which have been duly acknowledged. I also declare that it has not been previously and concurrently submitted for any other degree or award at UTAR or other institutions.

Signature : _____

Name : LIM YEE BOON

ID No. : 08UEB07961

Date : _____

APPROVAL FOR SUBMISSION

I certify that this project report entitled **“ROTATIONAL SYMMETRIC POWER DIVIDER AND MULTIPORT MICROSTRIP POWER DIVIDER”** was prepared by **LIM YEE BOON** has met the required standard for submission in partial fulfilment of the requirements for the award of Bachelor of Engineering (Hons.) Electrical and Electronic Engineering at Universiti Tunku Abdul Rahman.

Approved by,

Signature : _____

Supervisor: Dr, Lim Eng Hock

Date : _____

The copyright of this report belongs to the author under the terms of the copyright Act 1987 as qualified by Intellectual Property Policy of University Tunku Abdul Rahman. Due acknowledgement shall always be made of the use of any material contained in, or derived from, this report.

© 2012, LIM YEE BOON. All right reserved.

ACKNOWLEDGEMENTS

First and foremost, I offer my sincerest gratitude to my dearest supervisor, Dr Lim Eng Hock who has supported me throughout my thesis with his patience and knowledge. With his valuable guidance and advices, I manage to complete this research project in time. I appreciated his dedication in answering my curiosity and questions whenever I had doubt and confused.

I would like to place acknowledgement to my respective senior and friends who have been doing their research under my project supervisor, Dr. Lim Eng Hock. They have shared their ideas and knowledge with me and provided me with help whenever I faced a problem. I would like to thank them who have assisted me in this project which enables the process toward completion was undergone smoothly.

Nevertheless, I would like to special thanks to University Tunku Abdul Rahman (UTAR) management for preparing a good environment for me to complete this project. Equipment, devices and materials have been prepared well. Moreover, they had prepared and set up the OPAC system which enables students to obtain the necessary journal and scientific papers to complete the thesis writing successfully.

Last but not the least, I would like to thank my parents and for their endless support and encouragement throughout my studies in UTAR. Their moral support and love help to make my thesis complete smoothly.

**ROTATIONAL SYMMETRIC POWER DIVIDER
AND
MULTIPORT MICROSTRIP POWER DIVIDER**

ABSTRACT

In nowadays, filters are essential in communication as they are playing an important role to select or confine the Radio Frequency (RF) signals within assigned spectral limits since the electromagnetic spectrum is limited by licensing issues and shared over different channels. This project research introduces a new design of band pass filter that that is fabricated with the Rogers Duroid F4003C substrate. The proposed filter is a Rotational Symmetric Power Divider and In-phase Multiport Power Divider . This design technique is further developed to propose a microwave power divider. Power divider is one of the important parts in microwave systems as it is often used to combine or divide the RF signals. They are usually used in antennas feeds, power amplifiers and so on. The basic approach to design a good power divider is to have a performance comparison on the basic type of the power divider like rotational symmetric and patch resonator power divider. The rotational symmetry power divider is preferable because of it geometry could achieve port alignments and structure compactness. The proposed power divider is aimed to have features of high isolation at the output ports, excellent phase and amplitude balance, low insertion loss, higher power handling capability, compact in size and wider bandwidth. Good power dividers allow the system to have better performance in its application by giving better signal clarity, low non-linear signal distortion, reduce number of amplifiers, lower investment and cost effectiveness.

TABLE OF CONTENTS

DECLARATION	ii
APPROVAL FOR SUBMISSION	iii
ACKNOWLEDGEMENTS	v
ABSTRACT	vi
TABLE OF CONTENTS	vii
LIST OF TABLES	x
LIST OF FIGURES	xi
LIST OF SYMBOLS / ABBREVIATIONS	xvi
LIST OF APPENDICES	Error! Bookmark not defined.

CHAPTER

1	INTRODUCTION	1
	1.1 Background	1
	1.2 Aims and Objectives	2
	1.3 Project Motivation	3
	1.4 Thesis Overview	4
	1.5 Design Methodology	5
2	LITERATURE REVIEW	6
	2.1 Background	6
	2.2 Microstrip Bandpass Filters	7
	2.3 Microstrip Resonators	8
	2.3.1 Theory	8
	2.3.2 Design Consideration	9
	2.4 Recent Developments	10

	2.4.1	Dual-Mode Patch Resonator-Based Microwave Filters	10
	2.4.2	Microstrip Square Patch Filters	12
2.5		Power Divider	14
	2.5.1	Theory	15
	2.5.2	T - Junction Power Divider	16
2.6		Wilkinson Power Divider	17
	2.6.1	Theory	18
	2.6.2	Recent Developments	19
2.7		Introduction of Simulation Tools	24
	2.7.1	High Frequency Simulation Structure	24
	2.7.2	Microwave Office	25
3		Rotational Symmetric Power Divider	26
	3.1	Background	26
	3.2	Configuration	26
	3.3	Results	28
	3.3.1	Discussion	30
	3.4	Parametric Analysis	31
	3.5	Discussion	42
4		Multi-port Microstrip Power Divider	43
	4.1	Background	43
	4.2	Three-port Microstrip Patch Power Divider	43
	4.2.1	Configuration	44
	4.2.2	Results	45
	4.2.3	Discussion	47
	4.3	Parametric Analysis	48
	4.4	Discussion	59
	4.5	Four-port Microstrip Patch Power Divider	59
	4.5.1	Configuration	60
	4.5.2	Results	61
	4.5.3	Discussion	63

4.6	Parametric Analysis	65
4.7	Discussion	82
5	Future Work and Recommendations	83
5.1	Achievements	83
5.2	Future Work	84
5.3	Conclusion	84
	REFERENCES	85

LIST OF TABLES

TABLE	TITLE	PAGE
Table 3.1	The dimension of the Rotational Symmetric Power Divider	27
Table 3.2	Comparison between the measure and simulated S-parameter	31
Table 4.1	The dimension of Three-port Microstrip Patch Power Divider	44
Table 4.2	Comparison between the measure and simulated S-parameter	47
Table 4.3	The dimension of Four -port Microstrip Patch Power Divider	60
Table 4.4	Comparison between the measure and simulated S-parameter	64

LIST OF FIGURES

FIGURE	TITLE	PAGE
Figure 1.1	Diagram of Proposed Power Divider Design (a) Rotational Symmetric Power Divider , (b) One-to-two Power divider and (c) One-to-three Power Divider	5
Figure 2.1	Microstrip design	7
Figure 2.2	Proposed dimension of a square patch filter	10
Figure 2.3	S-parameter of the comparison between measurement and simulation	11
Figure 2.4	Proposed dimension of a square patch filter	12
Figure 2.5	S-parameter for the square patch filter with stub	13
Figure 2.6	Proposed dimension and S-parameter for the cascade square patch with stub	13
Figure 2.7	(a) Diagram of T-junction Power Divider and (b) Equivalent circuit of T-junction Power Divider	16
Figure 2.8	Diagram of the Wilkinson Power Divider equivalent circuit	18
Figure 2.9	Proposed design for multiway Wilkinson power divider	19
Figure 2.10	Proposed transition design of a multiway Wilkinson power divider	21
Figure 2.11	S-parameter and Phase of the Multiway Wilkinson power divider	22
Figure 2.12	Proposed design for the Y-junction Power Divider	22
Figure 2.13	S-parameter for the Y-junction Power Divider	23

Figure 3.1	Top down view of the Rotational Symmetric Power Divider	27
Figure 3.2	Magnitude of Rotational Symmetric Power Divider (Simulation)	28
Figure 3.3	Phase of Rotational Symmetric Power Divider (Simulation)	28
Figure 3.4	Magnitude of Rotational Symmetric Power Divider (Experimental)	29
Figure 3.5	Phase of Rotational Symmetric Power Divider (Experimental)	29
Figure 3.6	Configuration of the Rotational Symmetric Power Divider	31
Figure 3.7	Effect of the changes of via position of Dx_1 and Dx_2 (Magnitude)	32
Figure 3.8	Effect of the changes of via position of Dx_1 and Dx_2 (Phase)	33
Figure 3.9	Effect of the changes of via position of Dx_3 and Dx_4 (Magnitude)	34
Figure 3.10	Effect of the changes of via position of Dx_3 and Dx_4 (Phase)	34
Figure 3.11	Effect of the changes of via position of Dx_5 and Dx_6 (Magnitude)	35
Figure 3.12	Effect of the changes of via position of Dx_5 and Dx_6 (Phase)	36
Figure 3.13	Effect of the changes of via position of $Dx_7, Dx_8, Dx_9,$ and Dx_{10} (Magnitude)	37
Figure 3.14	Effect of the changes of via position of $Dx_7, Dx_8, Dx_9,$ and Dx_{10} (Phase)	37
Figure 3.15	Effect of the changes of via position of Dl_2 (Magnitude)	38
Figure 3.16	Effect of the changes of via position of Dl_2 (Phase)	39
Figure 3.17	Effect of the changes of via position of Dl_4 (Magnitude)	40

Figure 3.18	Effect of the changes of via position of DI_4 (Phase)	40
Figure 3.19	Effect of the changes of via position of DI_6 (Magnitude)	41
Figure 3.20	Effect of the changes of via position of DI_6 (Phase)	42
Figure 4.1	Top down view of Three-port Microstrip Patch Power Divider	44
Figure 4.2	Magnitude of Three-port Microstrip Patch Power Divider (Simulation)	45
Figure 4.3	Phase of Three-port Microstrip Patch Power Divider (Simulation)	45
Figure 4.4	Magnitude of Three-port Microstrip Patch Power Divider (Experimental)	46
Figure 4.5	Phase of Three-port Microstrip Patch Power Divider (Experimental)	46
Figure 4.6	Configuration of the Three-port Microstrip Patch Power Divider	48
Figure 4.7	Effect of changes in length L_2 (Magnitude)	49
Figure 4.8	Effect of changes in length L_2 (Phase)	49
Figure 4.9	Effect of changes in length L_4 (Magnitude)	50
Figure 4.10	Effect of changes in length L_4 (Phase)	51
Figure 4.11	Effect of changes in width W_2 (Magnitude)	52
Figure 4.12	Effect of changes in width W_2 (Phase)	52
Figure 4.13	Effect of changes in width W_3 (Magnitude)	53
Figure 4.14	Effect of changes in width W_3 (Phase)	54
Figure 4.15	Effect of changes in width W_5 (Magnitude)	55
Figure 4.16	Effect of changes in width W_5 (Phase)	55
Figure 4.17	Effect of changes in width W_6 (Magnitude)	56
Figure 4.18	Effect of changes in width W_6 (Phase)	57
Figure 4.19	Effect of changes in width W_7 (Magnitude)	58

Figure 4.20	Effect of changes in width W_7 (Phase)	58
Figure 4.21	Top down view of Four-port Microstrip Patch Power Divider	60
Figure 4.22	Magnitude of Four-port Microstrip Patch Power Divider (Simulation)	61
Figure 4.23	Phase of Four-port Microstrip Patch Power Divider (Simulation)	61
Figure 4.24	Magnitude of Four-port Microstrip Patch Power Divider (Experimental)	62
Figure 4.25	Phase of Four-port Microstrip Patch Power Divider (Experimental)	62
Figure 4.26	S-parameter for the triangular gap is filled	64
Figure 4.27	Configuration of the Four-port Microstrip Patch Power Divider	65
Figure 4.28	Effect of changes in length L_2 (Magnitude)	66
Figure 4.29	Effect of changes in length L_2 (Phase)	66
Figure 4.30	Effect of changes in length L_3 (Magnitude)	67
Figure 4.31	Effect of changes in length L_3 (Phase)	68
Figure 4.32	Effect of changes in length L_7 (Magnitude)	69
Figure 4.33	Effect of changes in length L_7 (Phase)	69
Figure 4.34	Effect of changes in length L_8 (Magnitude)	70
Figure 4.35	Effect of changes in length L_8 (Phase)	71
Figure 4.36	Effect of changes in width W_1 (Magnitude)	72
Figure 4.37	Effect of changes in width W_1 (Phase)	72
Figure 4.38	Effect of changes in width W_2 (Magnitude)	73
Figure 4.39	Effect of changes in width W_3 (Magnitude)	75
Figure 4.40	Effect of changes in width W_3 (Phase)	75
Figure 4.41	Effect of changes in width W_3 (Magnitude)	76

Figure 4.42	Effect of changes in width W_3 (Phase)	77
Figure 4.43	Effect of changes in width W_5 (Magnitude)	78
Figure 4.44	Effect of changes in width W_5 (Phase)	78
Figure 4.45	Effect of changes in width W_6 (Magnitude)	79
Figure 4.46	Effect of changes in width W_6 (Phase)	80
Figure 4.47	Effect of changes in width W_8 (Magnitude)	81
Figure 4.48	Effect of changes in width W_8 (Phase)	81

LIST OF SYMBOLS / ABBREVIATIONS

h	Height of the substrate
t	Thickness of the microstrip
θ	Phase
λ	Wavelength
ϵ_{eff}	effective dielectric constant
c	Speed of light
f	Frequency of wavelength
f_c	Centre frequency
Z_{in}	Input impedance, Ω
S_{11}	Reflection loss, dB
S_{21}	Insertion loss, dB

CHAPTER 1

INTRODUCTION

1.1 Background

Rapid advancement in microwave engineering has brought in significant development to wireless communications. Research works in many wireless gadgets such as mobile phones, wireless routers, and mobile tablets are now of great interest. All the devices use conventional bandpass filters to remove the unwanted signals and allow only a certain band of spectrum to pass through. In order to fully utilise the spectrum more effectively, a bandpass filter with a wider band is more preferable. Microstrip bandpass filters can be easily mounted on a dielectric substrate and can provide a more flexible design of the circuit layout. Many types of microwave components such as bandpass filter, circulator, power divider, and directional coupler have been proposed for different wireless systems.

Power divider is widely used nowadays as the design itself has the ability to divide the input power equally by turning the ratio of impedance, based on the numbers of output. Other than that, poor isolation can be avoided as the power reflected from the output port can be minimised through this design. Filter size has been a big aspect in the filter design since century ago. Miniaturization of the circuit design is preferable in accordance with the current trend of technology. It helps to save space. In short, many devices can be connected parallel at the same time. Due to the smaller size of the filter, the cost of the material used in fabrication also reduced.

1.2 Aims and Objectives

The main objective of this project is to propose and construct a new bandpass filter design which can offer a better performance than the previous and present filters available in the market. Before a proposal has been made, several researches and studies are carried out through IEEE Xplorer database under the UTAR OPAC system as it provides thousands of published journal for student reference. Since the author would like to design one-to-two and one-to-three power dividers, broad knowledge and understanding in Microstrip Filter design are highly required for implementation in the later design. Those journals available in the database provide related articles on the filter design which helps to initiate new ideas and concepts for the proposal.

This project is divided into 3 sections. The first part of the project is to design an In-Phase Rotational Symmetry three-port Power Divider. At first, it is aimed to resonated at the frequency from 1.5 Ghz till 4.0 Ghz with a sharp roll-off. From the finding, the designated filter has the property of a single-band with dual modes which resonates at the frequency between 2.5 Ghz till 3.5 Ghz, which is inside the acceptable range.

The second part of the project is to design a Three-Port Microstrip Power Divider with a single-band and dual-mode characteristic. This designated filter resonates at the frequency between 1.5 Ghz till 2.5 Ghz. For the last section of this project is to design a Four-Port Microstrip Power Divider with a single-band and dual-mode characteristic. This designated filter resonates at the frequency between 1.5 Ghz till 2.5 Ghz.

All the proposed designs mentioned above are constructed using Copper board with the substrate dielectric of 3.38 and the thickness of the substrate is 0.8128mm. After the proposal, author ought to learn how to use Ansoft HFSS software to do the simulation on the proposed design. The optimization of the filter design will be carried out by using this software to prove the probability of chances that the proposed design shall work as expected. This software is used to designed the microstrip filters before it is ready for fabrication. Involvement in handling the

fabrication of the microstrip is also important as it gives the author a hands-on experience.

Not only that, author will learnt how to use the VNA (Vector Network Analyzer) to take measurement of the fabricated filter and make comparison with the proposed filter in HFSS to see the difference. From here, author will learn not only theoretical knowledge, but also hardware analysis. After the completion of the project, author will have a better understanding of the microstrip resonator and power divider properties.

1.3 Project Motivation

The motivation of this project is to design several types of power divider with different designs which can work effectively in real. The performance of the filter is justified from the impedance matching and insertion loss. Usually a filter with a low insertion loss and good impedance matching will be considered as good filter. In the IEEE Xplorer database, most filters are found to be performing well but not used. It is mainly because of the complexity of the proposed design and large in size, which are not fit for commercial purpose.

Simplicity and small size will be the prioritised and considered when comes to filter design so that the result is comparable to the published journal design. Although there are many types of design when comes to power divider, and yet there is no resonator with via published in IEEE Xplorer database. With these, it motivates the author to carry out the research on power dividers so that it can be implemented in real word technologies.

1.4 Thesis Overview

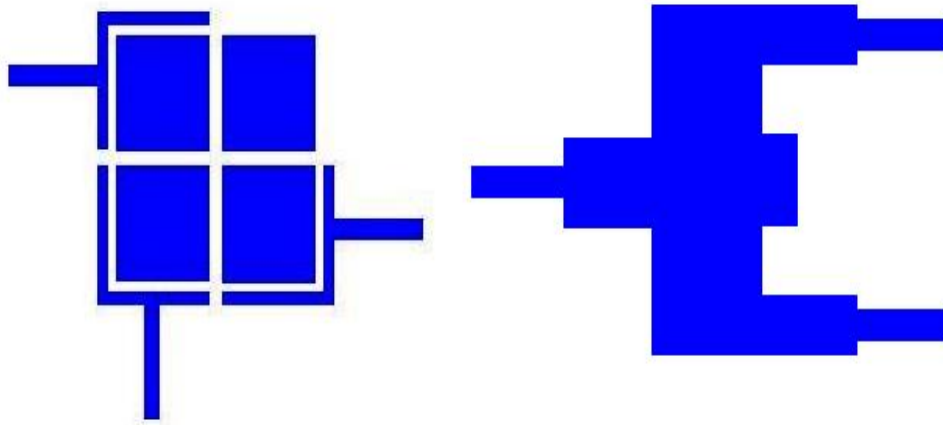
Throughout the thesis writing, there consists of 5 chapters which will discuss the overall progress of the final year project in detail. Chapter 1 is discussing about the background of the filter in microwave engineering, issues that has been arise in the market, aims and objectives to construct filters, project motivation and, overall thesis overview. It gives reader a very basic guideline for what is going on for the next few chapters.

Chapter 2 is mainly about the literature review of the final year project. This section is discussing about the types of filters available in the market and discuss the property and characteristic of it. It consists of the background of Microstrip filters, theory, design consideration and issues of Microstrip loop resonator. Other than that, recent development on filters in microwave engineering will be further discussed in this section. Power divider will be the main issue that will be further explored in detail such as Wilkinson Power Divider. Theory, design consideration and issues, and and recent development of Wilkinson Power Divider available in the global market will be elaborated in this section. There will be an introduction of simulation tools such as High Frequency Simulation Structure (HFSS) and Microwave Office.

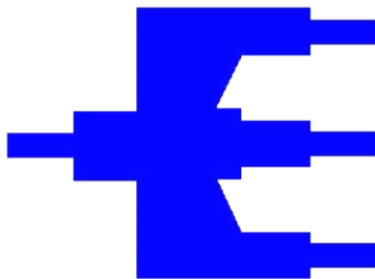
Chapter 3 will be elaborating the theory, configuration, synthesis , results, parametric analysis and discussion of actual proposed design filter, under the Rotational Symmetric Power Divider category. Chapter 4 will be dealing with the Multiport Microstrip Power Divider such as One-to-two Patch Power Divider and One-to-three Patch Power Divider. Both projects will be elaborated on the same analysis as Rotational Symmetric Power Divider. Future work and recommendation will fall in Chapter 5 which discussing more on achievement, future work and conclusion of this entire Final Year Project.

1.5 Design Methodology

This section will briefly explain the configuration for the proposed filter design as shown in Figure 1.1.



(a) Rotational Symmetry Power Divider (b) One-to-two Power Divider



(c) One-to-three Power Divider

Figure 1.1 Diagram of Proposed Power Divider Design (a) Rotational Symmetric Power Divider , (b) One-to-two Power divider and (c) One-to-three Power Divider

The application of the power divider will be further discussed in chapter 3 onwards. Simulation and optimisation of the power divider will also be carried out at the fabrication stage to obtain the optimum performance of the power divider.

CHAPTER 2

LITERATURE REVIEW

2.1 Background

Microstrip bandpass filter has been greatly implemented in modern technology since few tenth years back. It is mainly due to the rapid growth in development of the RF applications. In order to competent with the global trait, most of the wireless communications has seek for a higher level of improvement in filtering effect and smaller in size for design. A high performance and small size designed filters are now greatly demanded by global market. The design of the filter mostly depends on the requirement needed for the RF application, such as square patch filter, rectangular patch filter, circular ring filter and triangular patch filter. Each of the proposed design has its own characteristic and properties, which can be studied through analysis and research.

A proposed design will be rendered useless without proper simulation tools. HFSS software has been a great simulation tool that contribute in designation work of the microstrip filters and antenna. Apart from that. it runs in the virtual world as it has the ability to draw out the pattern of the design exactly for the fabrication part as well. Only the fully optimized design will be fabricated to ensure the final product can be operated. Furthermore, the accuracy of the simulation tools can be as high as 95%, compared to the fabricated filter. This is to ensure the failure rate in fabrication and the fabrication cost of the filter are as low as possible.

2.2 Microstrip Bandpass Filters

As circuits have been reduced in size with integrated semiconductor electron devices, a transmission structure was so that it is compatible with circuit construction techniques to provide guided waves over limited distances. A single-wire transmission line over a ground plane in a planar form had been constructed, which called Microstrip.

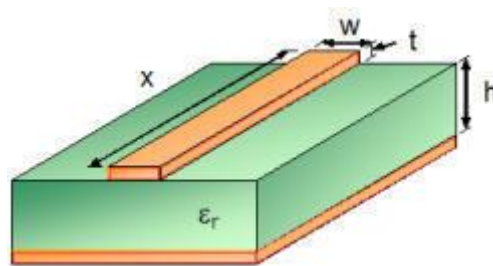


Figure 2.1 Microstrip design

Microstrip employs a flat strip conductor suspended above a ground plane by a low-loss dielectric material. The size of the circuit can be reduced through judicious use of a dielectric constant some 2-10 times that of free space (or air), with a penalty that the existence of two different dielectric constants (below and above the strip) makes the circuit difficult to analyze in closed form (and also introduces a variability of propagation velocity with frequency that can be a limitation on some applications).

The advantages of microstrip have been well established, and it is a convenient form of transmission line structure for probe measurements of voltage, current and waves. Microstrip structures are also used in integrated semiconductor form, directly interconnected in microwave integrated circuits. There are several formula that can be used in calculating the respective variables such as effective width and height, wave length and phase of the transmission line.

Width of the transmission line ;

$$W = w + \frac{t}{\pi} \left[\ln \left(\frac{2h}{t} \right) + 1 \right]$$

Height of the transmission line ;

$$H = h - 2t$$

Phase of the transmission line;

$$\theta = \frac{2\pi}{\lambda}$$

Wavelength of the transmission line;

$$\lambda = \frac{c}{f\sqrt{\epsilon_{eff}}}$$

2.3 Microstrip Resonators

2.3.1 Theory

There are many types of microstrip resonator had been published in IEEE Xplorer database. Resonator works as the fundamental element in a filter. It is used to determine the size of a filter. Since the advancement in microwave application demands a smaller and effective filter, resonator plays an important role in miniaturize the filter size.

There are many ways in reducing a filter size. The common way to reduce filter size will be modifying the physical structure of it. It can be a dual-mode circular patch, dual-mode triangular patch and even dual-mode rectangular patch resonator. The performance of a filter is greatly rely on the design of the resonator. A slight changes in the resonator will affect the result of the filter.

2.3.2 Design Consideration

There are several important parameters and general characteristics that affect the performance of the proposed design filters. The common properties desired for power divider which has a very wide operational bandwidth, good matching for all ports and high insertion loss.

Insertion loss is the loss of signal power resulting from the insertion of a device in a transmission line or optical fibre and is usually expressed in decibels (dB). If the power transmitted to the load before insertion is P_T and the power received by the load after insertion is P_R , then the insertion loss in dB is given by,

$$10 \log_{10} \frac{P_T}{P_R}$$

Return loss is the loss of signal power resulting from the reflection caused at a discontinuity in a transmission line or optical fiber. This discontinuity can be a mismatch with the terminating load or with a device inserted in the line. It is usually expressed as a ratio in decibels (dB);

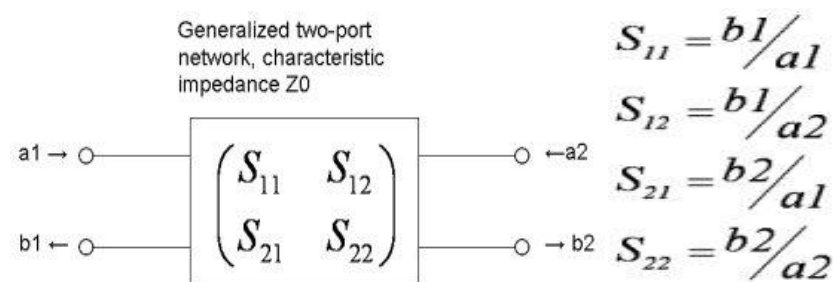
$$RL(\text{dB}) = 10 \log_{10} \frac{P_i}{P_r}$$

where $RL(\text{dB})$ is the return loss in dB, P_i is the incident power and P_r is the reflected power.

Bandwidth of a filter is defined as the difference between the upper and the lower cutoff frequencies. The shape factor is the ratio of bandwidths measured using two attenuation values to determine the cutoff frequency.

S-parameters describe the response of an N-port network to voltage signals at each port. The first number in the subscript refers to the responding port, while the second number refers to the incident port. Thus S_{21} means the response at port 2 due to a signal at port 1. The most common "N-port" in microwaves are one-ports and

two-ports, three-port network S-parameters are easy to model with software such as HFSS software and measured using VNA .



In a power splitter, the ability to keep signals (including any reflected signals) at the output ports separate from one another; to prevent cross-talk between ports. In a power combiner, the ability to prevent signals at an input port from appearing at any other input port. Isolation is achieved through the use of a Wilkinson type design employing resistor(s) of precisely calculated values placed at the terminus of transformer sections between port pairs.

2.4 Recent Developments

2.4.1 Dual-Mode Patch Resonator-Based Microwave Filters

The author has reviewed a paper entitled "Dual-Mode Patch Resonator-Based Microwave Filters" by Jia-Lin Li, Jian-Peng Wang, Xue-Song Yang, and Bing-Zhong Wang. In this journal, a square patch with a circle perturbation to study single and dual mode properties had been proposed .

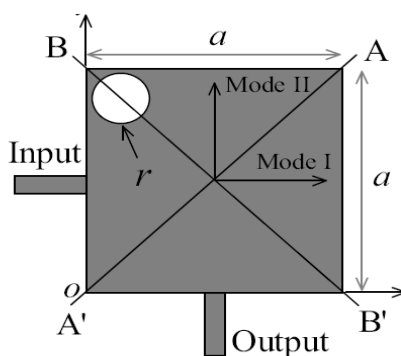


Figure 2.2 Proposed dimension of a square patch filter

This journal covers some theory on resonator and coupling. The rectangle patch is a transmission line for resonating purpose. The power is fed through a fed line with a standard width from input A and coupled into the square patch. A perturbation of radius r is etched away to observe the effect of it. The design has the optimised centre frequency of 2.45 GHz. This design has a very low insertion loss, shape rejection and low cost due to a compact size of design. This filter also has a very good selectivity with a sharp roll-off at the transmission between the passband and rejection band.

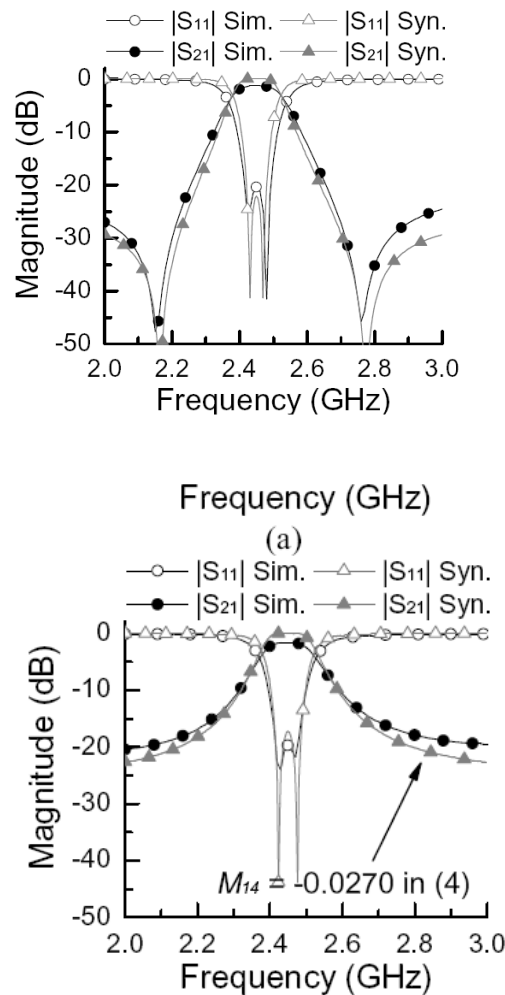


Figure 2.3 S-parameter of the comparison between measurement and simulation

Another set of experiment also been conducted to place the perturbation to another side with the angle of 90 degree. From the investigation, it proves that the pair of degenerate modes can be excited. It shows that both filters exhibit symmetry

response. Both of the transmission zeros adjacent to the lower and upper cut-off frequency with attenuations over 40 dB. The pair of transmission zeros improve the passband selectivity, even only using one patch as resonator. It also shows that the perturbation with a larger hole area leads to a wider resonance between two modes.

From the studies, the relationship of perturbation with the patch resonator has been studied. It is very important for a filter to know some of the basic parameter and characteristic of a filter design, such as filter size and usage of perturbation. It is also important to determine the resonant frequency of the filter. Designer can refer to the calculated electrical length as a guidance to design microstrip square patch filter with another extra features. Since the gap of the coupler will affect the bandwidth of the resonator, coupling gap and electrical length of the design shall be concluded into the design consideration.

2.4.2 Microstrip Square Patch Filters

The author has reviewed a paper entitled "Microstrip Square Patch Filter" by Guang Xue, Dexun Qu, Xiaojun Qiu and Chuanjia Zheng. In this journal, a square patch with a square perturbation to study single and dual mode properties had been proposed. It has dimension of unfixed length and width of a , dielectric constant of 6.15 and substrate thickness of 0.635mm.

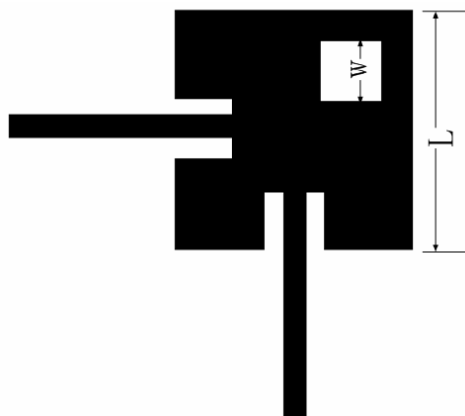


Figure 2.4 Proposed dimension of a square patch filter

This journal is reviewing on the relationship between the resonant frequency and perturbation size. When a square of $w \times w$ dimension etched away from the

patch, it shows 2 transmission zeroes in the s-parameter, which gives the filter a better selectivity. The position of the feeder also plays the important role in adjusting the performance of the filter. When 2 feeders are placed close to each other, the left side of the passband will become steep. In contrast, the right side of the passband will attenuate more.

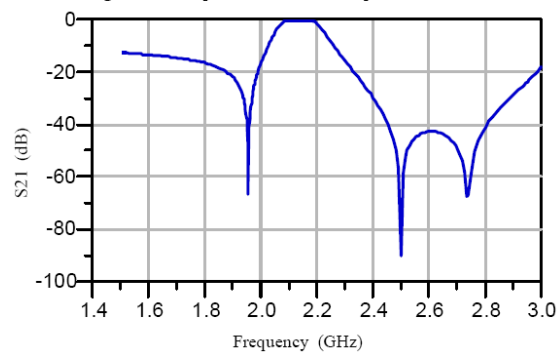


Figure 2.5 S-parameter for the square patch filter with stub

From the design, coupling strength mostly depends on the perturbation size. It means that precision in adjusting the perturbation size will result in better matching and coupling. It was found that the resonant frequency decreases in accordance with the increase in the size of the perturbation. A cascaded design of the filter has been proposed after the analysis as the sideband does not achieve an optimum result.

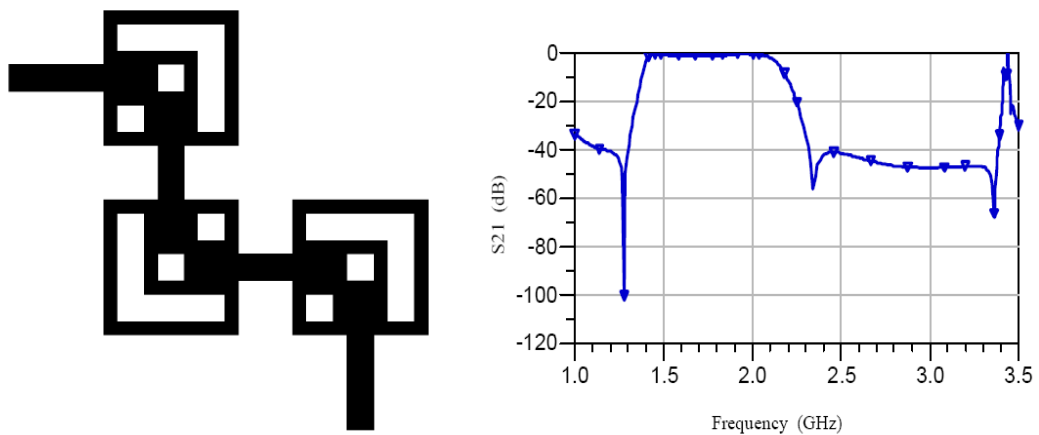


Figure 2.6 Proposed dimension and S-parameter for the cascade square patch with stub

From the chart, it shows that the s-parameter reached a low insertion loss of 0.2 dB and attenuate more than 40 dB. In this project, cascade form can be used in order to form a dual-mode filter. However, connect the resonators in cascade may caused the filter size larger. Many complicated calculations may involve in order creating a cascade form patch resonator. Hence, cascade patch resonators filter design would be considered in my project.

2.5 Power Divider

Power dividers (also power splitters and, when used in reverse, power combiners) and directional couplers are passive devices used in the field of radio technology. They couple a defined amount of the electromagnetic power in a transmission line to another port where it can be used in another circuit. An essential feature of directional couplers is that they only couple power flowing in one direction. Power entering the output port is not coupled.

The earliest transmission line power dividers were simple T-junctions. These suffer from very poor isolation between the output ports – a large part of the power reflected back from port 2 finds its way into port 3. It can be shown that it is not theoretically possible to simultaneously match all three ports of a passive, lossless three-port and poor isolation is unavoidable. It is, however, possible with four-ports and this is the fundamental reason why four-port devices are used to implement three-port power dividers: four-port devices can be designed so that power arriving at port 2 is split between port 1 and port 4 (which is terminated with a matching load) and none (in the ideal case) goes to port 3.

The term hybrid coupler originally applied to 3 dB coupled line directional couplers, that is, directional couplers in which the two outputs are each half the input power. This synonymously meant a quadrature 3 dB coupler with outputs 90° out of phase. Now any matched 4-port with isolated arms and equal power division is called a hybrid or hybrid coupler. Other types can have different phase relationships. If 90° , it is a 90° hybrid, if 180° , a 180° hybrid and so on. In this article hybrid coupler without qualification means a coupled line hybrid.

2.5.1 Theory

There are nine independent variables of scattering matrix describe the behaviour of the simplest power three ports divider circuit written as:

$$[S] = \begin{bmatrix} S_{11} & S_{12} & S_{13} \\ S_{21} & S_{22} & S_{23} \\ S_{31} & S_{32} & S_{33} \end{bmatrix}$$

In order to get maximum impedance matched and minimum reflection occurred at each port, the three port network must reciprocal and its scattering matrix will be symmetric. For a network to be well-matched, it should have reflection coefficients $S_{ij} = 0$ for $i = j$ and the matrix rewritten as:

$$[S] = \begin{bmatrix} 0 & S_{12} & S_{13} \\ S_{12} & 0 & S_{23} \\ S_{13} & S_{23} & 0 \end{bmatrix}$$

Reciprocal property was very important to ensure two ports suffer similar power losses despite having different propagation directions. Reciprocal networks have symmetrical scattering matrix across the diagonal from up left to the bottom right and written as:

$$[S] = \begin{bmatrix} S_{11} & S_{12} & S_{13} \\ S_{12} & S_{22} & S_{23} \\ S_{13} & S_{23} & S_{33} \end{bmatrix}$$

However, it is impossible to construct a three port lossless reciprocal network that is matched at all ports. For lossless network in ideal case, the scattering matrix is unity and leads to

$$S_{12}S_{12}^* + S_{13}S_{13}^* = |S_{12}|^2 + |S_{13}|^2 = 1$$

$$S_{21}S_{21}^* + S_{23}S_{23}^* = |S_{21}|^2 + |S_{23}|^2 = 1$$

$$S_{31}S_{31}^* + S_{32}S_{32}^* = |S_{31}|^2 + |S_{32}|^2 = 1$$

$$S_{13}^* S_{23} = 0$$

$$S_{23}^* S_{12} = 0$$

$$S_{12}^* S_{13} = 0$$

$$S_{12} \neq 0$$

$$S_{13} S_{12}^* = 0, S_{13} = 0$$

$$S_{23}^* S_{12} = 0, S_{23}^* = 0$$

This asserts that $|S_{13}|^2 + |S_{23}|^2 = 0$ and therefore contradicts $|S_{31}|^2 + |S_{32}|^2 = 0$. If the three-port network is allowed to be lossy it can be reciprocal and matched at all ports.

2.5.2 T - Junction Power Divider

The T-junction power divider is defined as a simple three-port network that can be used for power dividing or even power combining. In ideal case, T-junction power divider is treated as lossless divider. A lossless divider means that there are no resistive element inside the design so that there will be no loss in power transferring from input port to output port, with the equation of $P_1 = P_2 + P_3$. P_1 indicates the incident power whereas P_2 and P_3 are defined as absorbed power at the match loads.

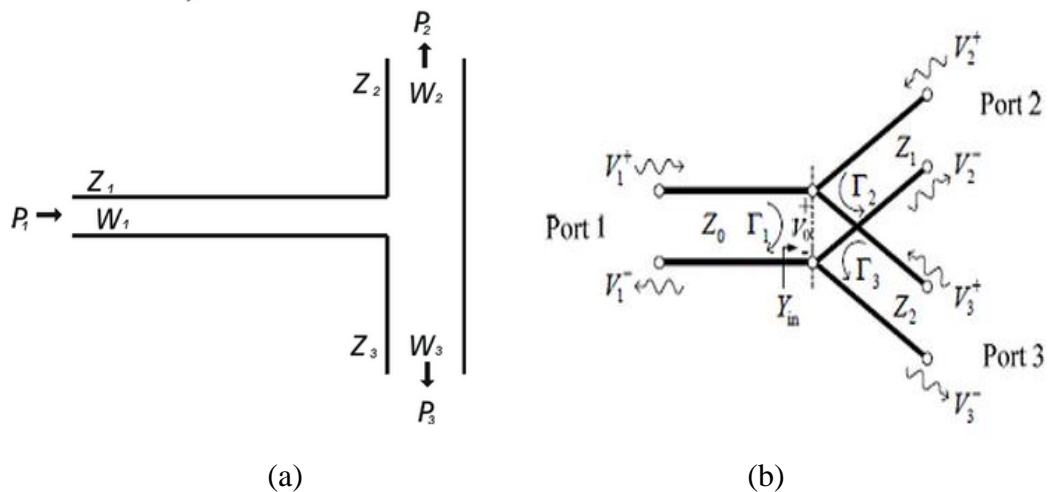


Figure 2.7 (a) Diagram of T-junction Power Divider and (b) Equivalent circuit of T-junction Power Divider

$$Y_{in} = jB + \frac{1}{Z_1} + \frac{1}{Z_2} = \frac{1}{Z_0}$$

Generally, there are some stray fields that associated with the discontinuity at the junction, which might lead to stored energy that can be accounted for by a lumped susceptance, B. Since the transmission line is assumed to be lossless, only real part of the characteristic impedance will be taken into calculation . The equation will becomes as shown below ;

$$\frac{1}{Z_1} + \frac{1}{Z_2} = \frac{1}{Z_0}$$

Z1 represents the impedance at port 2 and Z2 represents the impedance at port 3. The power absorbed by 2 output ports must be equal , P2 = P3 to divide the power equally at both ends. It also means that the characteristic impedance for both output ports must be equal.

There is some condition that the design is built to have different output power for both ports. In order to have different power ratio, the characteristic impedance would be adjusted by using some equations as shown below;

$$P_1 = P_2 + P_3 = \alpha P_1 + \beta P_1 \quad \alpha + \beta = 1$$

$$P_2 = \frac{1}{2} \frac{V_o^2}{Z_2} = \alpha P_1 = \alpha \frac{1}{2} \frac{V_o^2}{Z_1} \quad \Rightarrow \quad \alpha = \frac{Z_1}{Z_2}$$

$$P_3 = \frac{1}{2} \frac{V_o^2}{Z_3} = \beta P_1 = \beta \frac{1}{2} \frac{V_o^2}{Z_1} \quad \Rightarrow \quad \beta = \frac{Z_1}{Z_3}$$

2.6 Wilkinson Power Divider

The Wilkinson power divider consists of two parallel uncoupled $\lambda/4$ transmission lines. The input is fed to both lines in parallel and the outputs are terminated with twice the system impedance bridged between them. The design can be realised in planar format but it has a more natural implementation in coax – in planar, the two lines have to be kept apart so they do not couple but have to be brought together at their outputs so they can be terminated whereas in coax the lines can be run side-by-side relying on the coax outer conductors for screening.

The Wilkinson power divider solves the matching problem of the simple T-junction: it has low VSWR at all ports and high isolation between output ports. The input and output impedances at each port are designed to be equal to the characteristic impedance of the microwave system. This is achieved by making the line impedance of the system impedance – for a $50\ \Omega$ system the Wilkinson lines are approximately $70\ \Omega$.

2.6.1 Theory

In the field of microwave engineering and circuit design, the Wilkinson Power Divider is a specific class of power divider circuit that can achieve isolation between the output ports while maintaining a matched condition on all ports. The Wilkinson design can also be used as a power combiner because it is made up of passive components and hence reciprocal. First published by Ernest J. Wilkinson in 1960, this circuit finds wide use in radio frequency communication systems utilizing multiple channels since the high degree of isolation between the output ports prevents crosstalk between the individual channels.

Meanwhile, the microstrip power dividers are useful for dividing & combining signals. The most widely used power divider is the Wilkinson power divider. The Wilkinson power divider splits an input signal into two equal phase output signals. It may also work as a combiner in which case it is used to combine two equal-phase signals into a single signal in the opposite direction. There is an ideal configuration of the Wilkinson Power Divider as shown below;

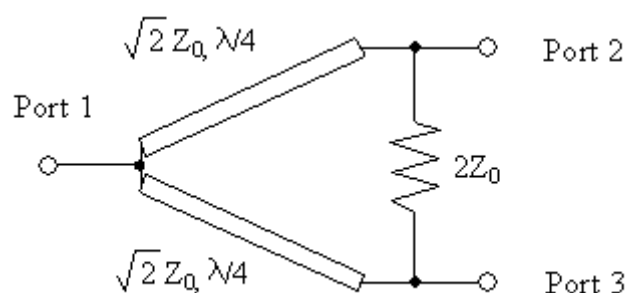


Figure 2.8 Diagram of the Wilkinson Power Divider equivalent circuit

When a signal enters port 1, it splits into equal-amplitude, equal-phase output signals at ports 2 and 3. Since each end of the isolation resistor between ports 2 and 3 is at the same potential, no current flows through it and therefore the resistor is decoupled from the input. The two output port terminations will add in parallel at the input, so they must be transformed to $2 \times Z_0$ each at the input port to combine to Z_0 .

The quarter-wave transformers in each leg accomplish this; without the quarter-wave transformers, the combined impedance of the two outputs at port 1 would be $Z_0/2$. The characteristic impedance of the quarter-wave lines must be equal to $1.414 \times Z_0$ so that the input is matched when ports 2 and 3 are terminated in Z_0 . With this, Wilkinson splitter works like a power divider.

2.6.2 Recent Developments

2.6.2.1 Multiway Dual-Band Planar Power Dividers with Arbitrary Power Division

The author has reviewed a paper entitled "Multiway Dual-Band Planar Power Dividers with Arbitrary Power Division" by Yongle Wu, Quan Xue, Shulan Li and Cuiping Yu. In this journal, a novel closed-form design method of generalized Wilkinson Power Dividers is proposed. The power divider can be designed in arbitrary-way with arbitrary power division in a pure planar structure.

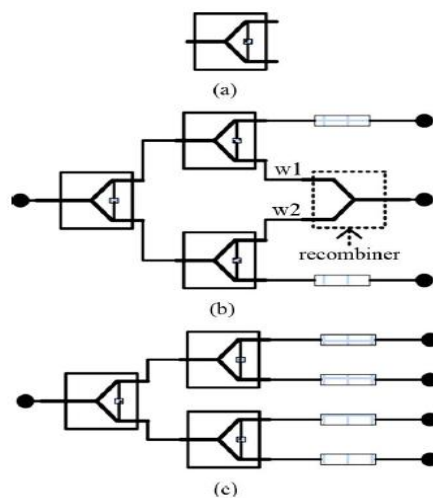


Figure 2.9 Proposed design for multiway Wilkinson power divider

Several 3-way and 4-way power dividers with different dual-band applications are designed. 3-way power divider operates at the frequency of 0.6 GHz and 2.45 GHz with a power dividing ratio of 3 :5 :1. The combination of W1 and W2 will not degrade the performance of the power combiner efficiencies. Dual-band impedance feeder with equal electrical lengths are utilized to make all the output signals in-phase and the output ports matched at the desired 2 bands. All the output ports can be isolated effectively because each two-way dual-band unequal power divider cell in the whole circuit has ideal isolation performance.

When the number of ways increases, the planar configurations of multiway dual-band arbitrary power dividers will become more flexible. For example, there are three typical planar configurations of five-way generalized power dividers, which are shown in Figs. 2(a)–2(c). Similarly, additional interconnecting transmission lines should be used to obtain in-phase characteristics in dual-band applications.

Here, there are two kinds of interconnecting transmission lines: 1) compulsory lines which are used as phase shifters to achieve in-phase (such as Line 1 in Fig. 2) or as impedance transformers to realize dual-band matching (such as Line 2 in Fig. 2); 2) optional lines (not shown in Figs. 1 and 2) which are just used to modify the total external characteristic and enhance implementation flexibility of the proposed power dividers such as the interconnecting transmission lines.

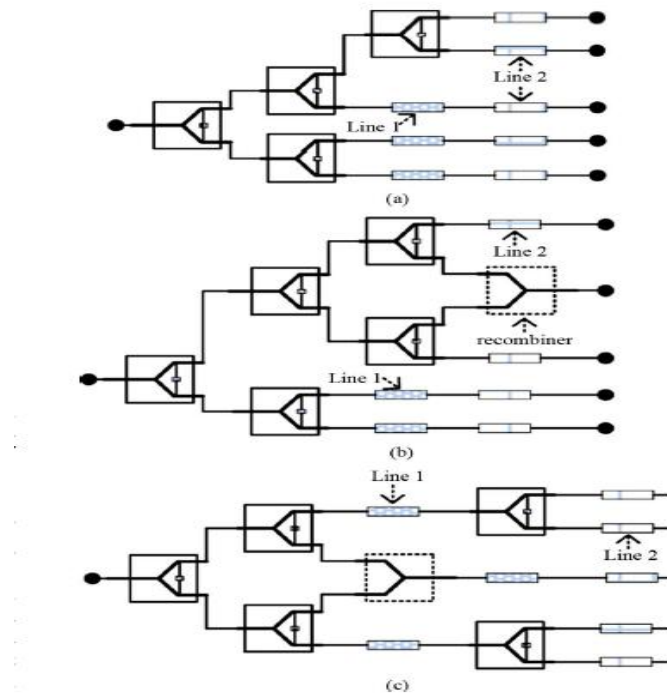


Figure 2.10 Proposed transition design of a multiway Wilkinson power divider

From the studies, proposed generalized Wilkinson power divider simultaneously has four main characteristics: planar structure if implemented by microstrip or stripline, multiple ways, arbitrary power dividing, and dual-band operations. In this journal, there are several unexplained tolerance which remain unsolved and it can only be used for references. Authors plan to use this journal as a reference in designing 3 ports and 4 ports multiway power dividers by feeding in the same length of transmission line to obtain the same in-phase effect.

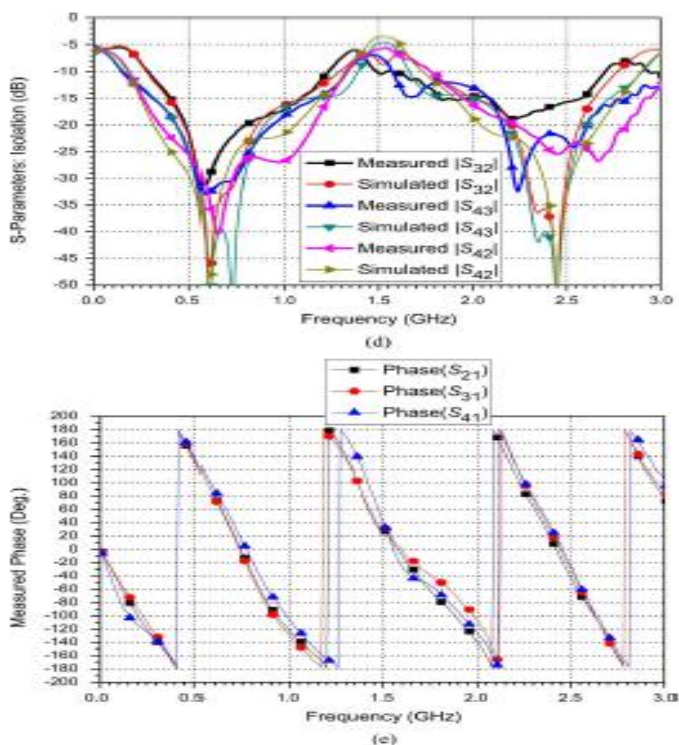


Figure 2.11 S-parameter and Phase of the Multiway Wilkinson power divider

2.6.2.2 Y-Junction Power Divider

The author has reviewed a paper entitled " Y-Junction Power Divider" by X.Zou , C.M Tong and D.W. Yu. This journal is reviewing on the role of substrate integrated waveguide in millimetre-wave and microwave IC as it has a very low return loss and high Q-factor.

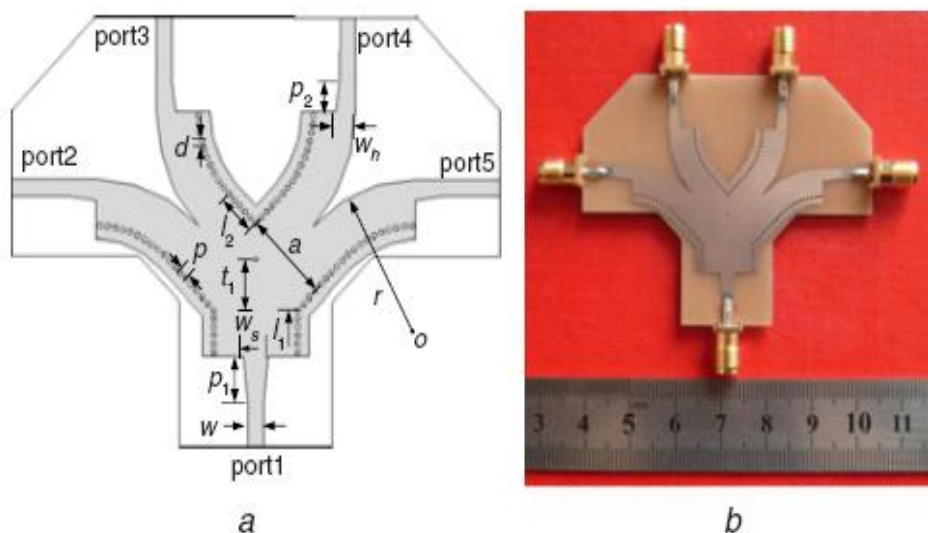


Figure 2.12 Proposed design for the Y-junction Power Divider

The power divider is built on a 1.0 mm-thick substrate with relative permittivity of 4.3 and loss tangent of 0.001 at 10 GHz. Measured return loss is very similar to the simulated result, 215 dB bandwidth can reach 3.6 GHz (8.6–12.2 GHz). The measured transmissions are about 27.6 dB+0.2 dB in the passband. Compared with the simulated result, the measured transmissions are a bit lower, about 0.7 dB, owing to the dielectric loss and the insertion loss of the SIW-microstrip transitions and SMA connectors.

One important factor is the discontinuity of the Y-junction, causing different wave distances for the four outputs. Another factor is the testing port should be transferred when the apparatus tests the multi-port circuit. However, this kind of difference is allowable, below +0.3 dB. Compared with the traditional Y-junction SIW four-way power divider, the structure of the power divider is simpler, and the circuit area is reduced. So, the new power divider can be used in miniaturised microwave systems.

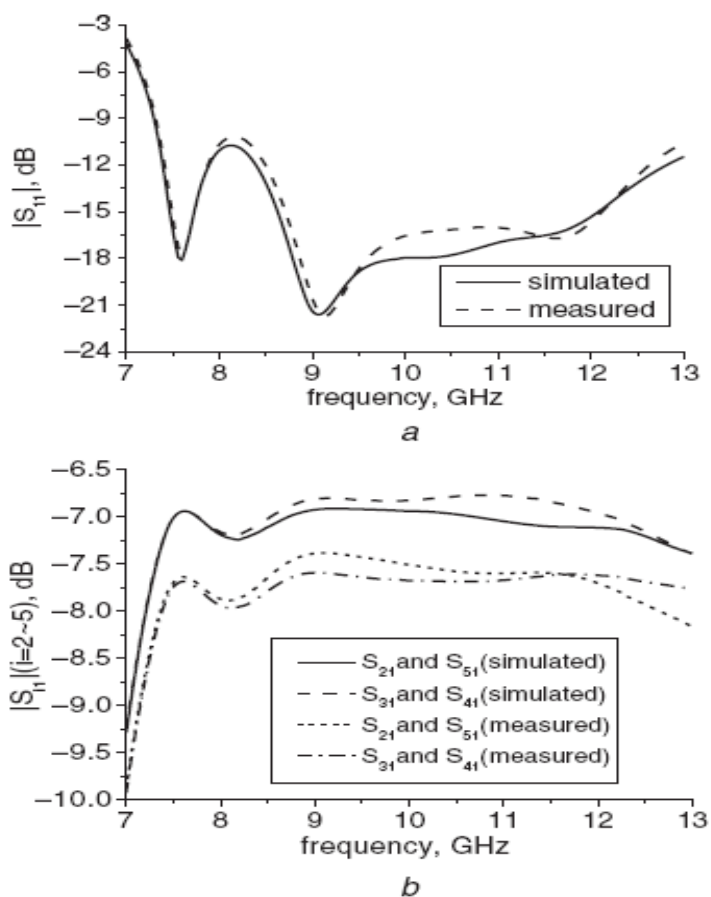


Figure 2.13 S-parameter for the Y-junction Power Divider

From this journal, the design theory and processing of a 90° Y-junction SIW power divider and a HMSIW power divider, and a novel Y-junction four-way power divider is fabricated by investigating them properly. Simulated and measured results show that it makes the 6 dB power divider work preferably in a broad bandwidth. The new power divider can be produced with batches and can be widely used in millimetre-wave and microwave circuits owing to its simple and novel structure. The author uses this concept in designing a similar structure of E-shape power divider in order to obtain a better matching and low return loss, compared to this journal.

2.7 Introduction of Simulation Tools

2.7.1 High Frequency Simulation Structure

ANSYS HFSS software is the industry-standard simulation tool for 3-D full-wave electromagnetic field simulation and is essential for the design of high-frequency and high-speed component design. HFSS offers multiple state-of-the-art solver technologies based on either the proven finite element method or the well established integral equation method. You can select the appropriate solver for the type of simulation you are performing.

Each HFSS solver is based on a powerful, automated solution process where you are only required to specify geometry, material properties and the desired output. From there HFSS will automatically generate an appropriate, efficient and accurate mesh for solving the problem using the selected solution technology. With HFSS the physics defines the mesh; the mesh does not define the physics.

There are several deciding factors on why Ansoft HFSS has been chosen as the simulation software to design the microwave bandpass filter. HFSS allowed the construction of bandpass filter in virtual world and provides several optimised result for the user to decide which configuration to be taken as the best example for fabrication in reality. With this, a lot of valuable times and materials that is used to construct the filter can be saved. Besides, this simulation software is capable of plotting electromagnetic field in 3 Dimension and this enable us to study on the behaviour of the radiation so that we can identify the best way to optimise the filter.

HFSS is powerful software that is able to produce the most accurate and consistent result and it also required the user to have some knowledge that can understand the simulation procedures and ways to get the best simulated results from the filter. Therefore, the tutorials of HFSS are studied to familiarise the user with the environment of the simulation software. The tutorials studied include “*Ansoft HFSS Training Example: Aperture-Coupled Patch Antenna*” and “*Ansoft HFSS Software Demonstration Example: Microstrip Transmission Line*”.

2.7.2 Microwave Office

Microwave Office RF/microwave design software is the industry's fastest growing microwave design platform. Microwave Office has revolutionized the communications design world by providing users with a superior choice. Built on the unique AWR high-frequency design environment platform with its unique unified data model™, Microwave Office offers unparalleled intuitiveness, powerful and innovative technologies, and unprecedented openness and interoperability, enabling integration with best-in-class tools for each part of the design process.

Microwave Office design suite encompasses all the tools essential for high-frequency IC, PCB and module design, including, linear circuit simulators, non-linear circuit, simulators, electromagnetic (EM) analysis tools, integrated schematic and layout, statistical design capabilities and parametric cell libraries with built-in design-rule check (DRC). Microwave Office AWR has several advantages, such as faster marketing , improvement in efficiency and accuracy , and quick learning curve.

CHAPTER 3

Rotational Symmetric Power Divider

3.1 Background

The fundamental design of the Rotational Symmetric Power Divider is mainly based on the published journal paper from IEEE Xplorer database, which known as " Dual-Mode Patch Resonator-Based Microwave Filters" by Jia-Lin Li, Jian-Peng Wang, Xue-Song Yang, and Bing-Zhong Wang. The geometrical layout of the proposed design from the paper are shown in Figure 2.2. It is a simple square patch with a circular hole as perturbation and 2 coupling line as transmission line.

3.2 Configuration

There are several tutorials that have been carried out by the author so that the author will be more proficient in using the HFSS software tool. In order to let the author to familiarise the software tool, a published journal entitled " Design of Tri-band Microstrip Bandpass Filter Using Folded Tri-Section Stepped-Impedance Resonator" by Haiwen Liu. This tutorial has last for 2 weeks as the author need to do the simulation by referring to the journal and construct the exact dimension of the proposed design. The toughest part of the design is to plot out the simulated result together with the journal simulated result and make comparison between the two. Although there are some difference in the results, and yet it is still in the acceptable range.

There is also another software called TXline which determines the dimension of the transmission line. The proposed design is using 50Ω impedance line. From the software tool, it is found that 50Ω impedance line of a F4003C substrate with the dielectric constant of 3.38 and thickness of 0.8128 mm has the width of 1.80 mm. For Rotational Symmetric Power Divider, the dimension is stated as below, together with the top down view of the filter design ;

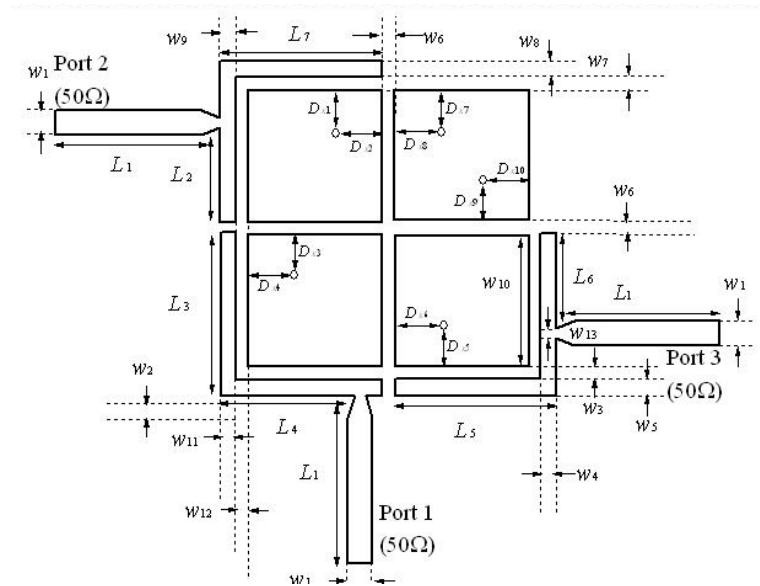


Figure 3.1 Top down view of the Rotational Symmetric Power Divider

Variable	Value (mm)	Variable	Value (mm)
D_{x1}	0.25	L_6	5.30
D_{x2}	0.65	L_7	8.35
D_{x3}	0.65	W_1	1.80
D_{x4}	0.25	W_2	0.45
D_{x5}	0.25	W_3	0.10
D_{x6}	0.65	W_4	0.45
D_{x7}	0.65	W_5	0.40
D_{x8}	0.25	W_6	0.30
D_{x9}	0.65	W_7	0.10
D_{x10}	0.25	W_8	0.30
L_1	15.40	W_9	0.45
L_2	5.30	W_{10}	7.70
L_3	8.30	W_{11}	0.20
L_4	6.55	W_{12}	0.15
L_5	8.35	W_{13}	1.20

Table 3.1 The dimension of the Rotational Symmetric Power Divider

3.3 Results

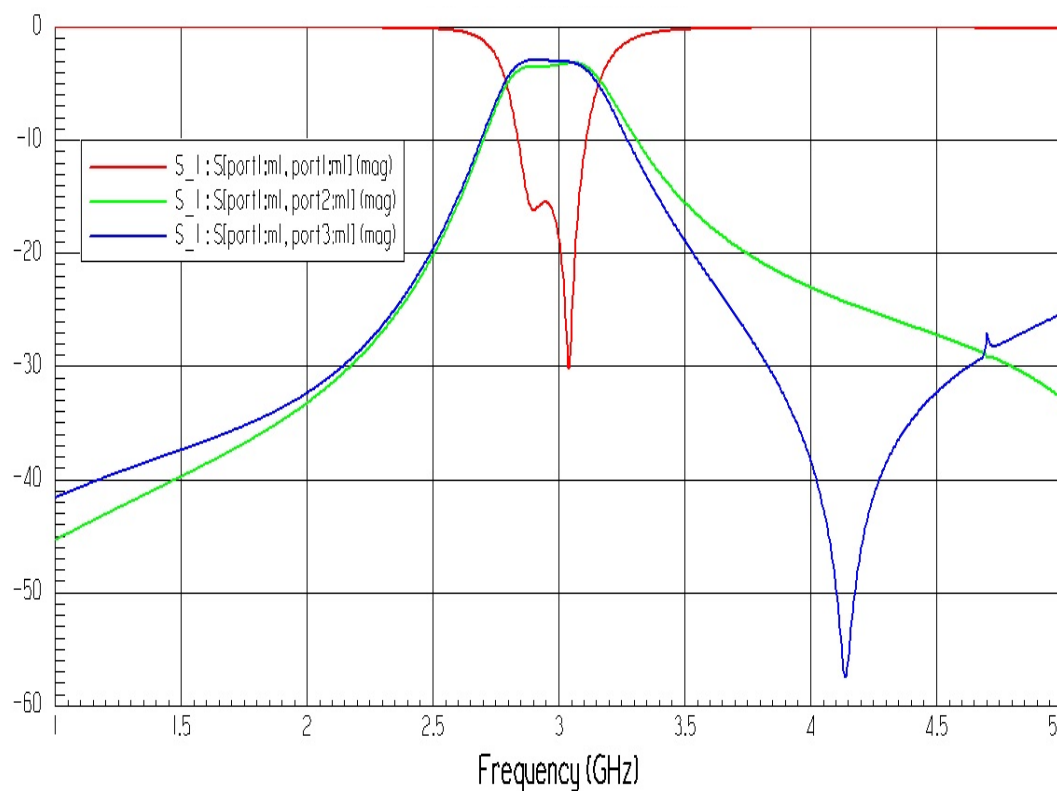


Figure 3.2 Magnitude of Rotational Symmetric Power Divider (Simulation)

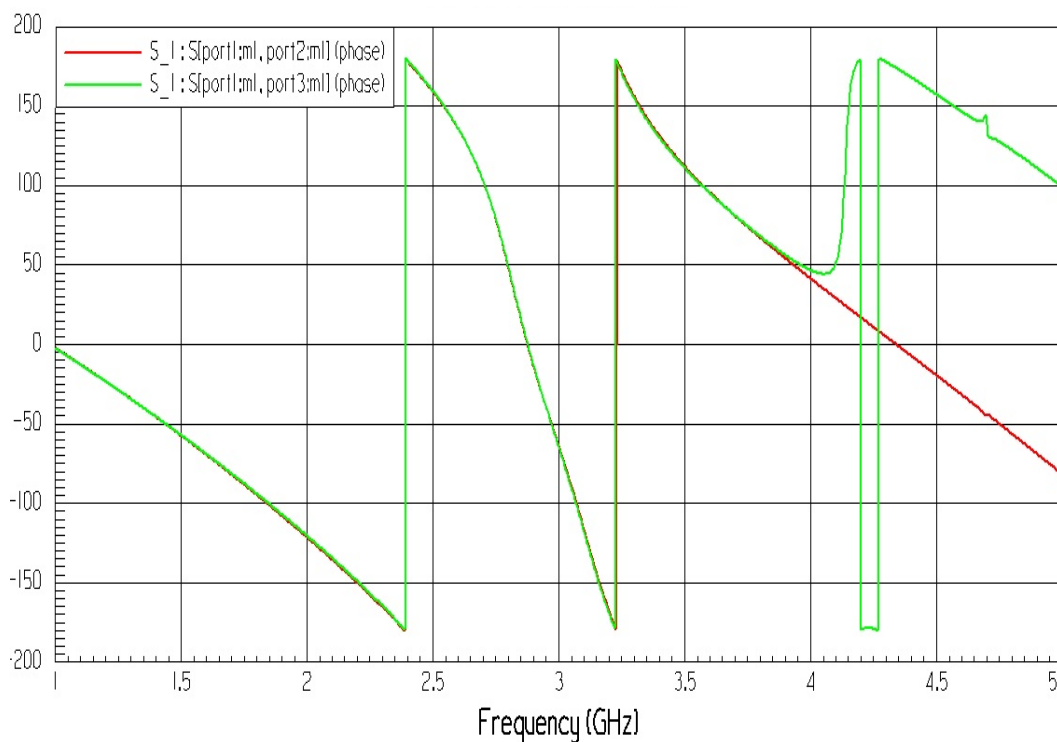


Figure 3.3 Phase of Rotational Symmetric Power Divider (Simulation)

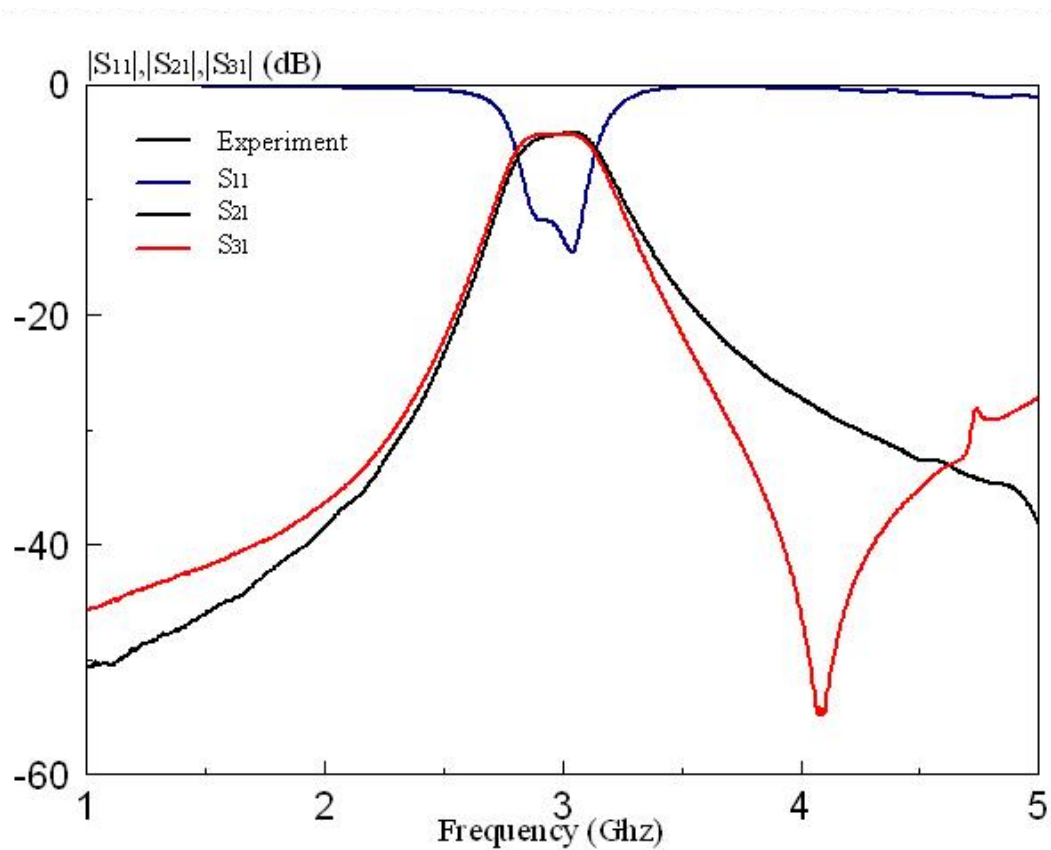


Figure 3.4 Magnitude of Rotational Symmetric Power Divider (Experimental)

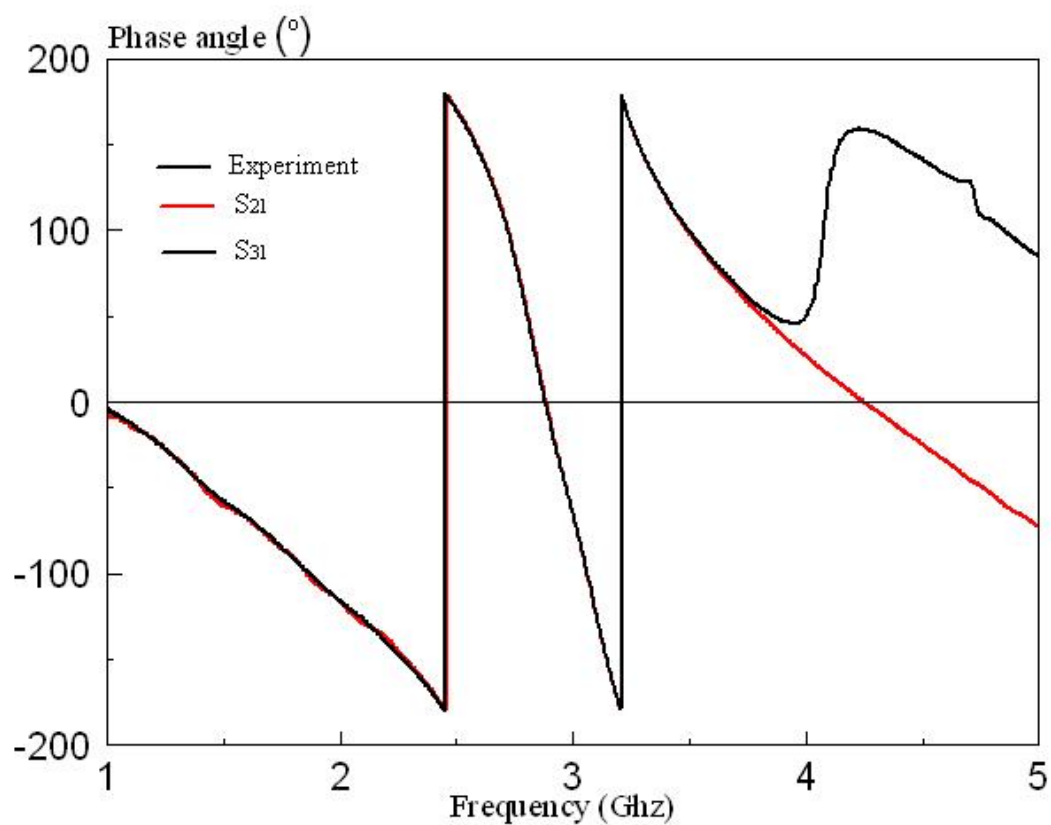


Figure 3.5 Phase of Rotational Symmetric Power Divider (Experimental)

3.3.1 Discussion

Experimental measurements had been carried out using the Rohde & Schwarz ZVB8 Vector Network Analyzer to inspect the proposed design filter. Several readings had been taken and compared the simulation result from HFSS. Figure 3.2 and Figure 3.4 shows the comparison between measured and predicted S parameter S_{11} , S_{21} and S_{31} of the proposed prototype. From the result, it clearly showed that there is a good agreement between simulations and the experimental result and this further justified the functionality and capability of the fabricated rotational symmetric power divider.

From Figure 3.2, it shows that the insertion loss from -2.92dB till -3.74 dB for S_{21} and -3.17 dB to -3.84 dB for S_{31} . The centre frequency for the simulated result is -2.947 GHz. From Figure 3.4, it shows that the insertion loss from -4.19 dB till -5.17 dB for S_{21} and -4.28 dB to -4.82 dB for S_{31} . The centre frequency for the experimental result is -2.937GHz. Although there is a shifting of insertion loss from -3dB to -4 dB, the result for experimental still acceptable due to the existence of via holes which grounding the patch resonator improperly. Improprate soldering on the via holes will affect the matching and the insertion loss.

The center frequency f_c , fractional bandwidth and error between measured and simulated result can be calculated by using the formula shown below. In fact, central frequency of a filter is a measurement of a central frequency between the upper and lower cutoff frequencies while the fractional bandwidth is the difference between the upper and lower frequencies in a contiguous set of frequencies divide by the center frequency. The comparison between the measurement and simulation results is summarized in table 3.2.

$$\text{Center frequency} = \frac{\text{Lower Frequency, } f_L + \text{High Frequency, } f_H}{2}$$

$$\text{Fractional Bandwidth} = \frac{\text{High Frequency, } f_H - \text{Lowe Frequency, } f_L}{\text{center frequency, } f_c} \times 100\%$$

$$\text{Error} = \frac{|f_c(\text{measured}) - f_c(\text{simulated})|}{f_c(\text{measured})} \times 100\%$$

	Measured		HFSS	
	S_{21}	S_{31}	S_{21}	S_{31}
Minimum Insertion Loss (dB)	-4.19	-4.28	-2.92	-3.17
3-dB Reference (dB)	-7.19	-7.28	-5.92	-6.17
f_L (GHz) / f_H (GHz)	2.857/3.092	2.857/3.092	2.842/3.107	2.842/3.107
f_c (GHz)	2.975	2.975	2.975	2.975
Fractional Bandwidth (%)	7.899	7.899	8.908	8.908
Error (%)	0.00	0.00	0.00	0.00

Table 3.2 Comparison between the measure and simulated S-parameter

3.4 Parametric Analysis

This section is about the case studies where author will need to carry out several simulation on the proposed design filter by changing the value of the variable such as patch length and width. The main purpose of this studies being carried out is to observe the changes of the s-parameter with the changes of the variables, whether it produces a better or worst result. Other parameter such as frequency range and centre frequency will be remained. The configuration of the proposed design filter shown below ;

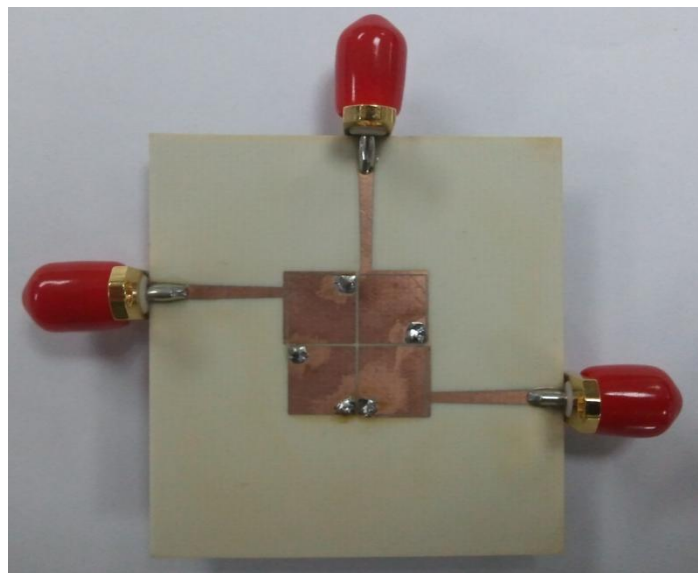


Figure 3.6 Configuration of the Rotational Symmetric Power Divider

Effect of Dx_1 and Dx_2

From the Table 3.1, when the via position Dx_1 changes from 0.25mm to 0.55mm and Dx_2 changes from 0.65mm to 0.35mm, the magnitude of S_{11} changes a little from -15.467 dB to -15.085 dB inside the passband ranging from 2.843 GHz to 3.107 GHz.

When the via position Dx_1 changes from 0.25mm to 0.85mm and Dx_2 changes from 0.65mm to 0.135mm, the magnitude of S_{11} changes a little from -15.467 dB to -15.083 dB inside the passband ranging from 2.843 GHz to 3.107 GHz.

2 modes of the proposed design do not shift, remain at the point of 2.903 GHz (-16.142 dB) and 3.037 GHz (-30.133 dB). No transmission zero is observed from the result but the Q - factor of the s-parameter is quite high. The attenuation also quite low. The phase of the proposed design is in-phase and same as the optimised result. The changes of variable Dx_1 and Dx_2 do not contribute much in affecting the result of the proposed power divider design.

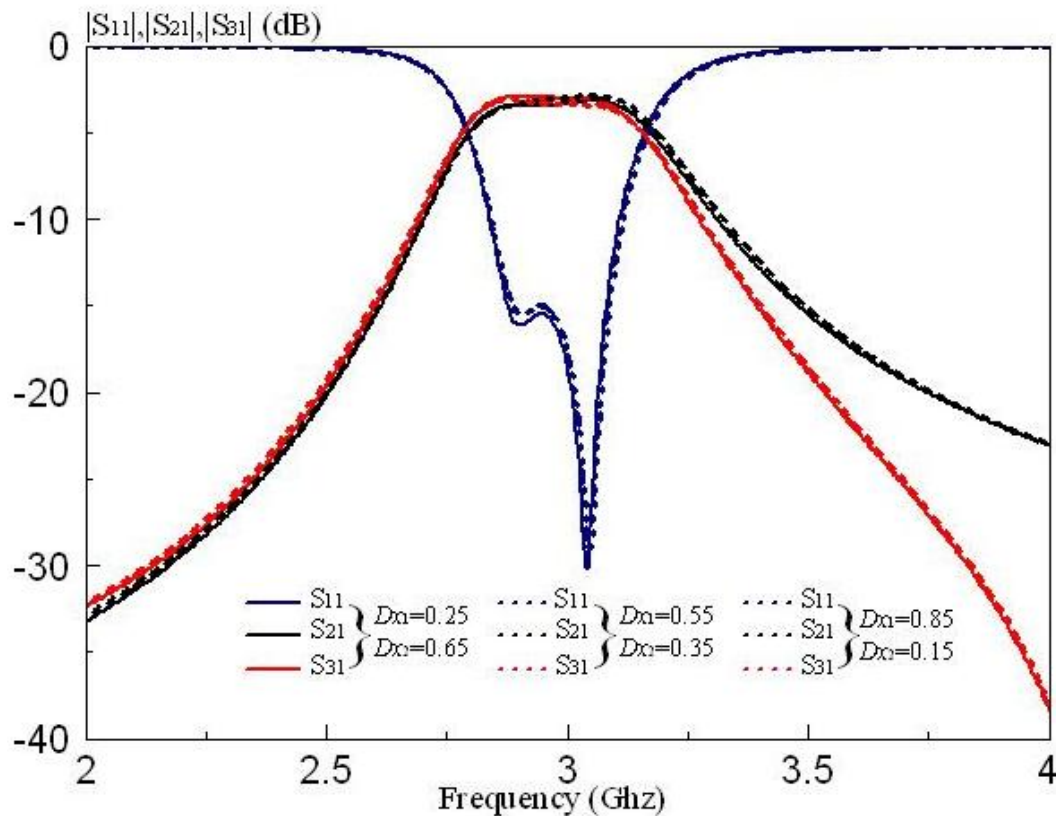


Figure 3.7 Effect of the changes of via position of Dx_1 and Dx_2 (Magnitude)

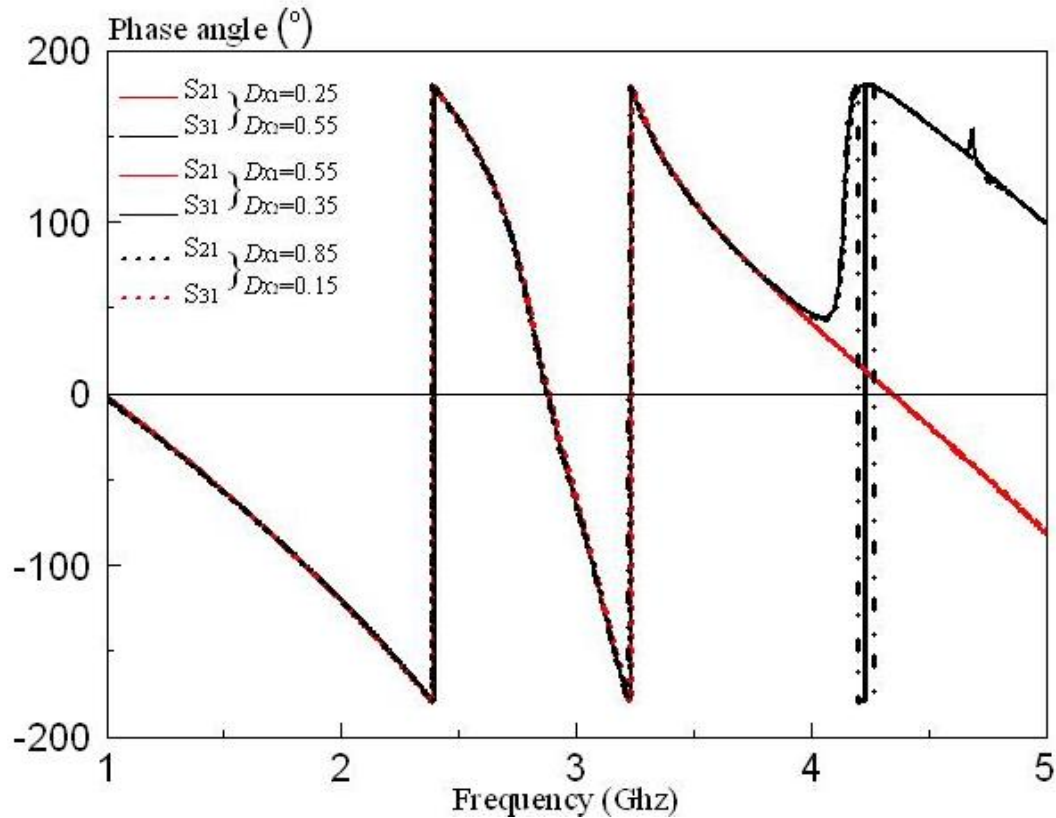


Figure 3.8 Effect of the changes of via position of Dx_1 and Dx_2 (Phase)

Effect of Dx_3 and Dx_4

From the Table 3.1, when the via position Dx_3 changes from 0.65mm to 0.95mm and Dx_4 changes from 0.25mm to 0.55mm , the magnitude of S_{11} changes from -15.467 dB to -7.956 dB inside the passband ranging from 2.843 Ghz to 3.107 Ghz .

When the via position Dx_3 changes from 0.65mm to 1.00 mm and Dx_4 changes from 0.25mm to 0.60 mm , the magnitude of S_{11} changes from -15.467 dB to -7.313 dB inside the passband ranging from 2.843 Ghz to 3.107 Ghz .

2 modes of the design as shifted higher than -8 dB. No transmission zero is observed and phase of the proposed design shifted to left side. This indicates that the increment of the Dx_3 and Dx_4 will result in higher reflection of signal in transmission.

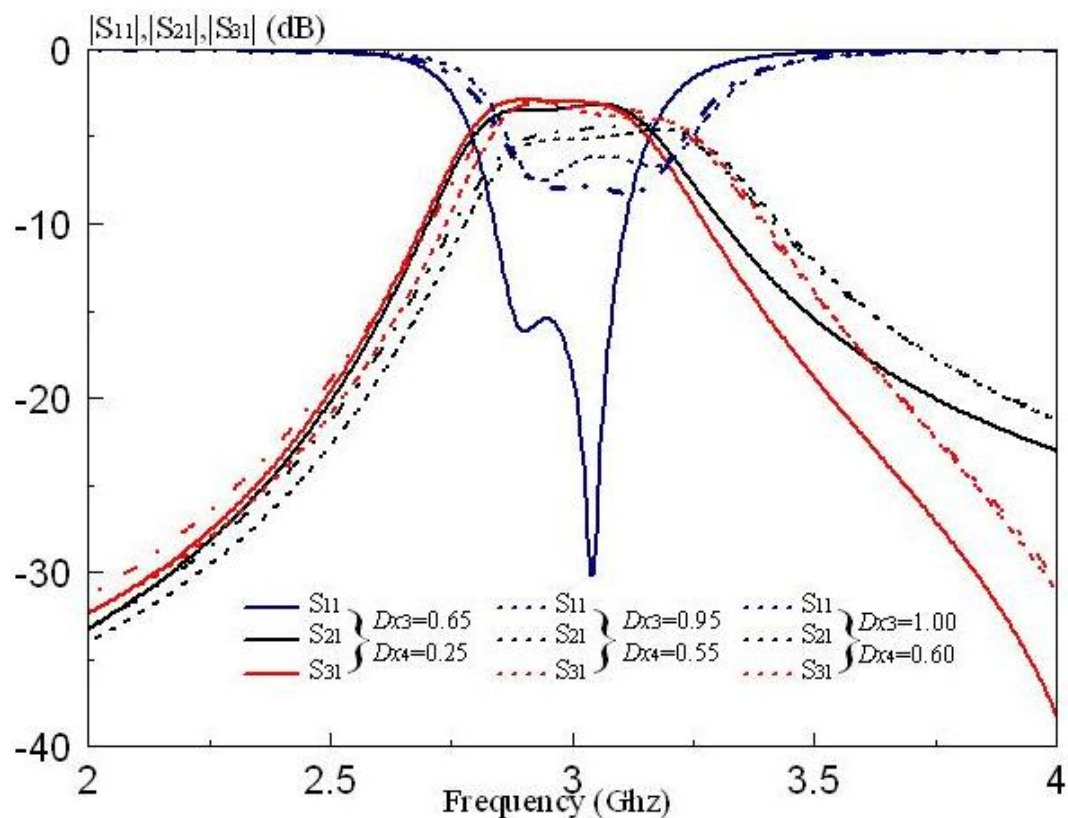


Figure 3.9 Effect of the changes of via position of Dx_3 and Dx_4 (Magnitude)

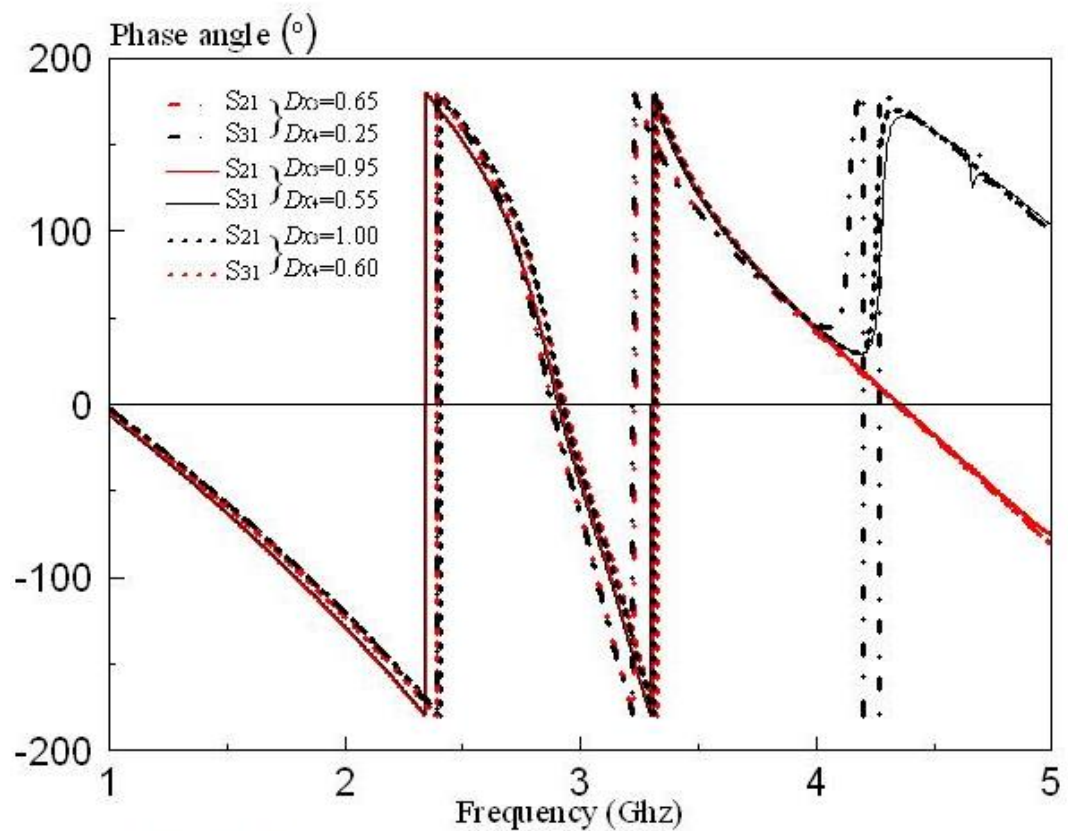


Figure 3.10 Effect of the changes of via position of Dx_3 and Dx_4 (Phase)

Effect of Dx_5 and Dx_6

From the Table 3.1, when the via position Dx_5 changes from 0.25mm to 0.55mm and Dx_6 changes from 0.65mm to 0.35mm , the magnitude of S_{11} changes from -15.467 dB to -14.829 dB inside the passband ranging from 2.843 Ghz to 3.107 Ghz .

When the via position Dx_5 changes from 0.65mm to 0.10 mm and Dx_6 changes from 0.25mm to 0.80 mm , the magnitude of S_{11} changes from -15.467 dB to -16.317 dB inside the passband ranging from 2.843 Ghz to 3.107 Ghz .

2 modes of the proposed design do not shift, remain at the point of 2.903 Ghz (-16.142 dB) and 3.037 Ghz (-30.133 dB). The Q - factor remains as well. It appears that later changes of via position has a better matching than the previous simulated result. The magnitude of the -3dB for S_{21} and S_{31} are flatter than the previous simulated result.

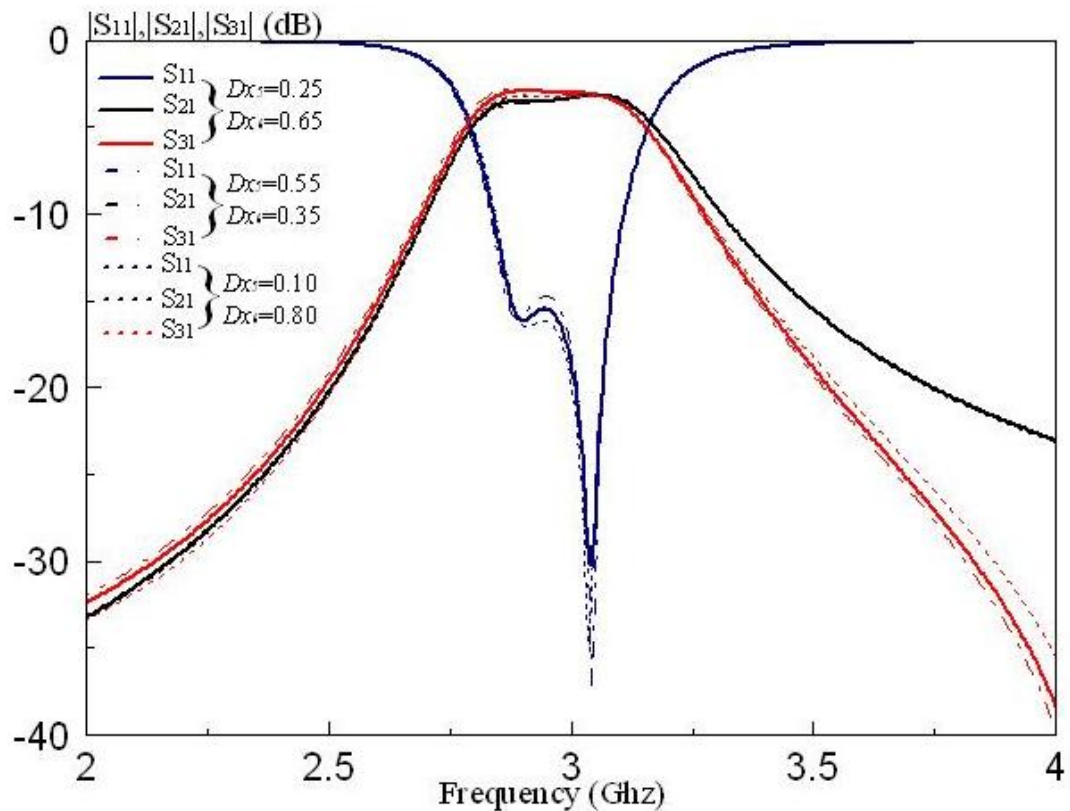


Figure 3.11 Effect of the changes of via position of Dx_5 and Dx_6 (Magnitude)

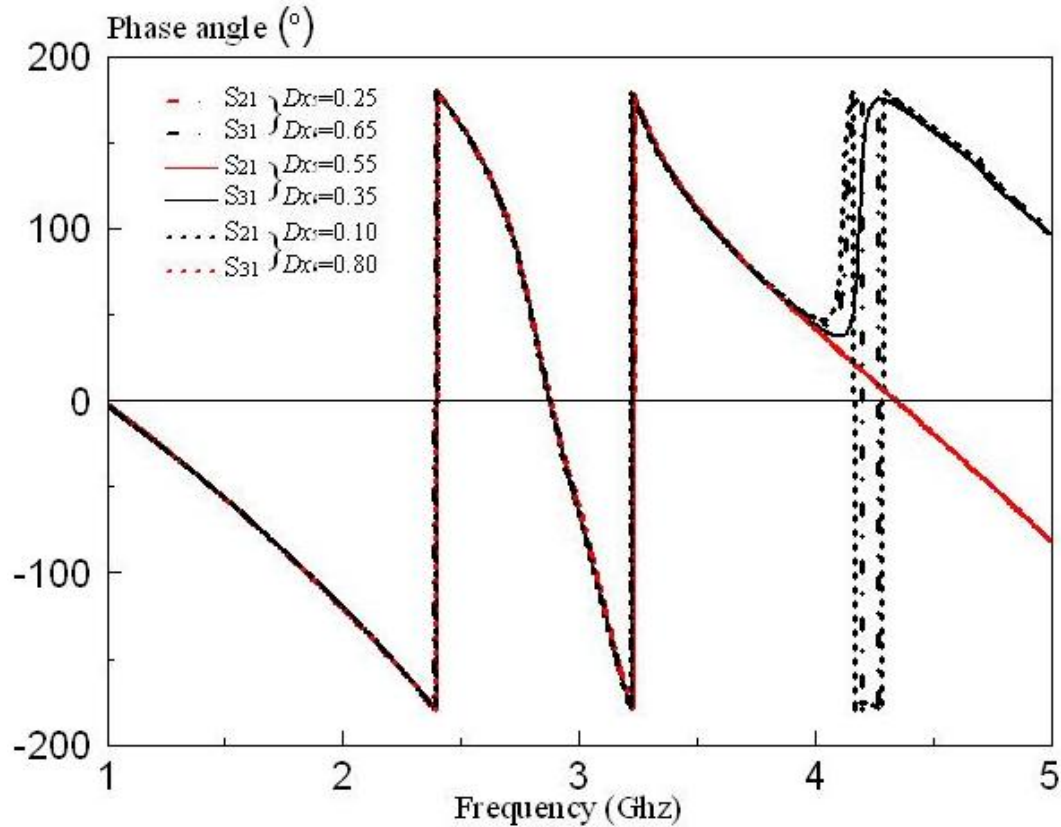


Figure 3.12 Effect of the changes of via position of Dx_5 and Dx_6 (Phase)

Effect of Dx_7 , Dx_8 , Dx_9 , and Dx_{10}

From the Table 3.1, when the via position Dx_7 and Dx_{10} changes from 0.25mm to 0.55mm and Dx_8 and Dx_9 changes from 0.65mm to 0.95mm, the magnitude of S_{11} changes from -15.467 dB to -15.589 dB inside the passband ranging from 2.843 GHz to 3.107 GHz.

When the via position Dx_7 and Dx_{10} changes from 0.25mm to 1.25 mm and Dx_8 and Dx_9 changes from 0.65mm to 0.80 mm, the magnitude of S_{11} changes from -15.467 dB to -17.032 dB inside the passband ranging from 2.843 GHz to 3.107 GHz.

2 modes of the proposed design do not shift, remain at the point of 2.903 GHz (-16.142 dB) and 3.037 GHz (-30.133 dB). The Q-factor remains as well. It appears that later changes of via position has a better matching than the previous simulated result. The magnitude of the -3dB for S_{21} and S_{31} are flatter than the previous simulated result.

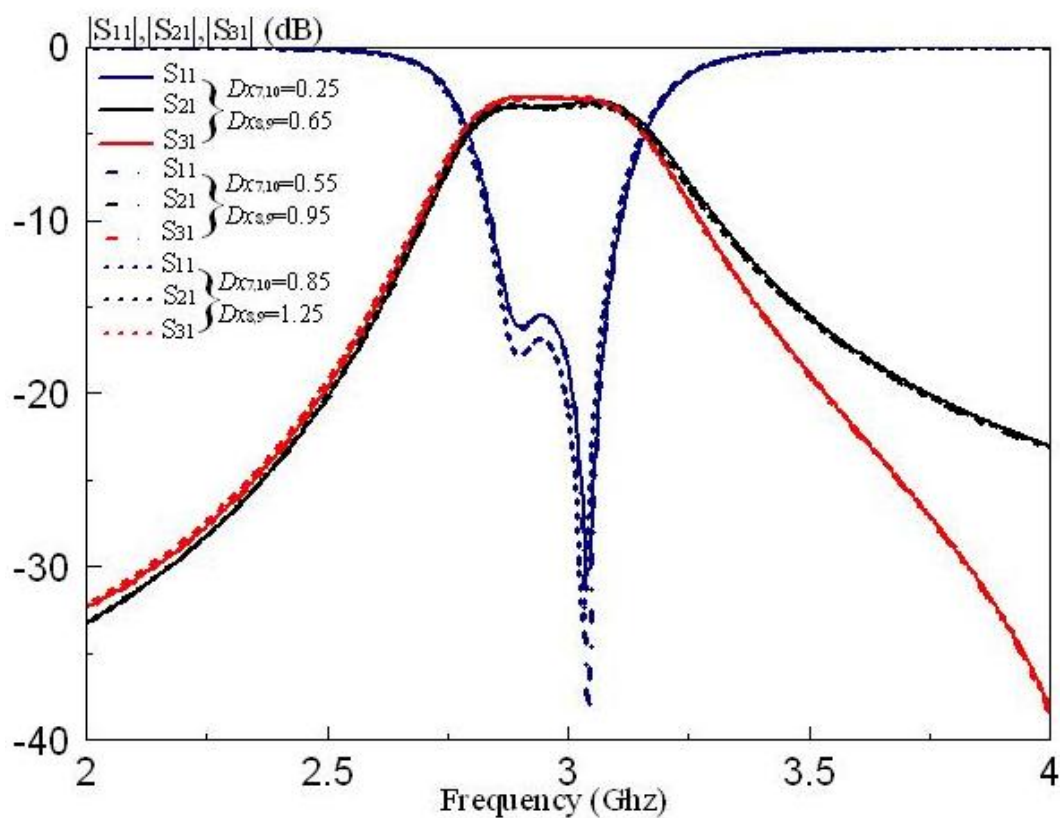


Figure 3.13 Effect of the changes of via position of Dx_7 , Dx_8 , Dx_9 , and Dx_{10} (Magnitude)

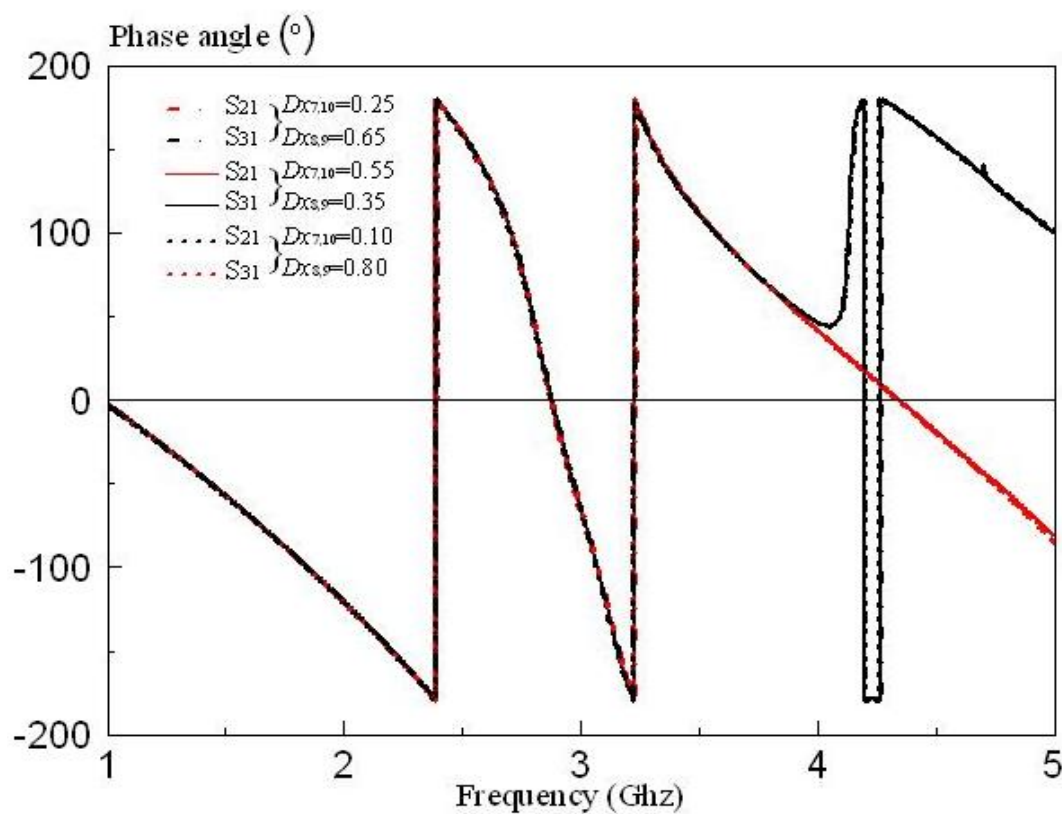


Figure 3.14 Effect of the changes of via position of Dx_7 , Dx_8 , Dx_9 , and Dx_{10} (Phase)

Effect of Dl_2

From the Table 3.1, when the via position Dl_2 changes from 5.30 mm to 4.10 mm, the magnitude of S_{11} changes from -15.467 dB to -16.286 dB inside the passband ranging from 2.843 GHz to 3.107 GHz .

When the via position Dl_2 changes from 5.30 mm to 6.50 mm, the magnitude of S_{11} changes from -15.467 dB to -16.633 dB inside the passband ranging from 2.843 GHz to 3.107 GHz .

2 modes of the proposed design shift a bit, from the point of 2.903 GHz (-16.142 dB) to 2.898 GHz (-17.417 dB) and from the point 3.037 GHz (-30.133 dB) to 3.032 (-27.020 dB). The Q - factor remains as well. It appears that later changes of via position has a better matching than the previous simulated result. The magnitude of the -3dB for S_{21} and S_{31} are flatter than the previous simulated result.

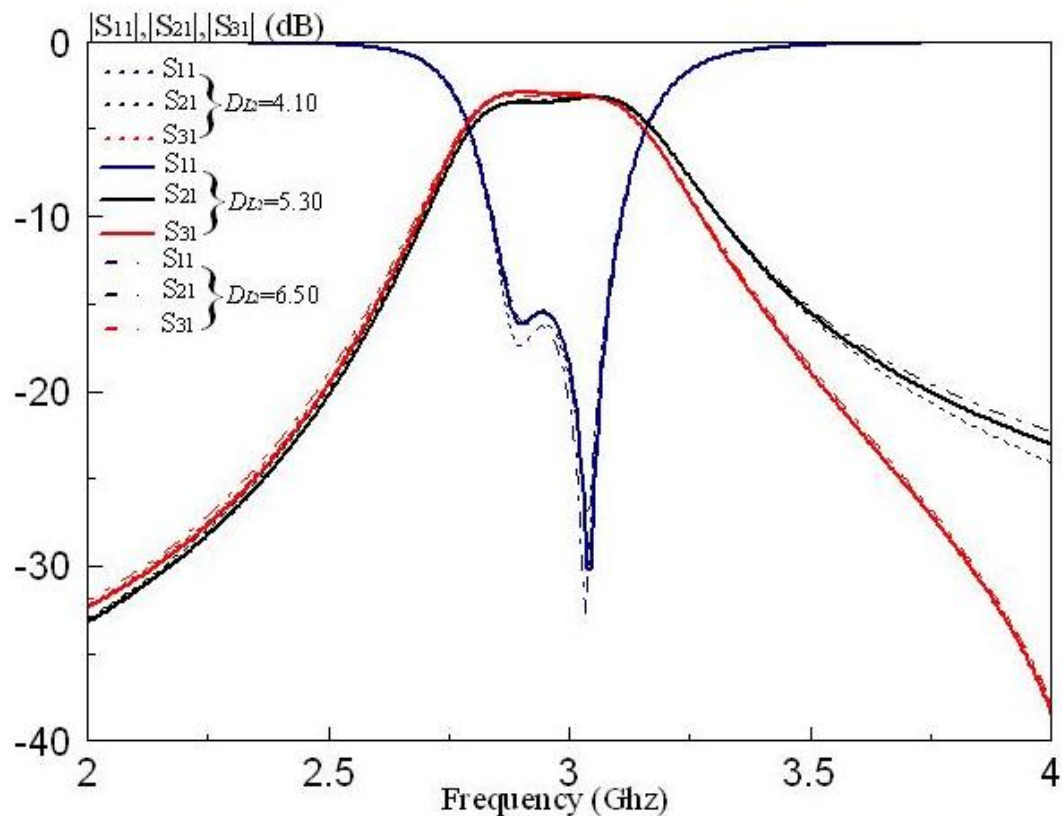


Figure 3.15 Effect of the changes of via position of Dl_2 (Magnitude)

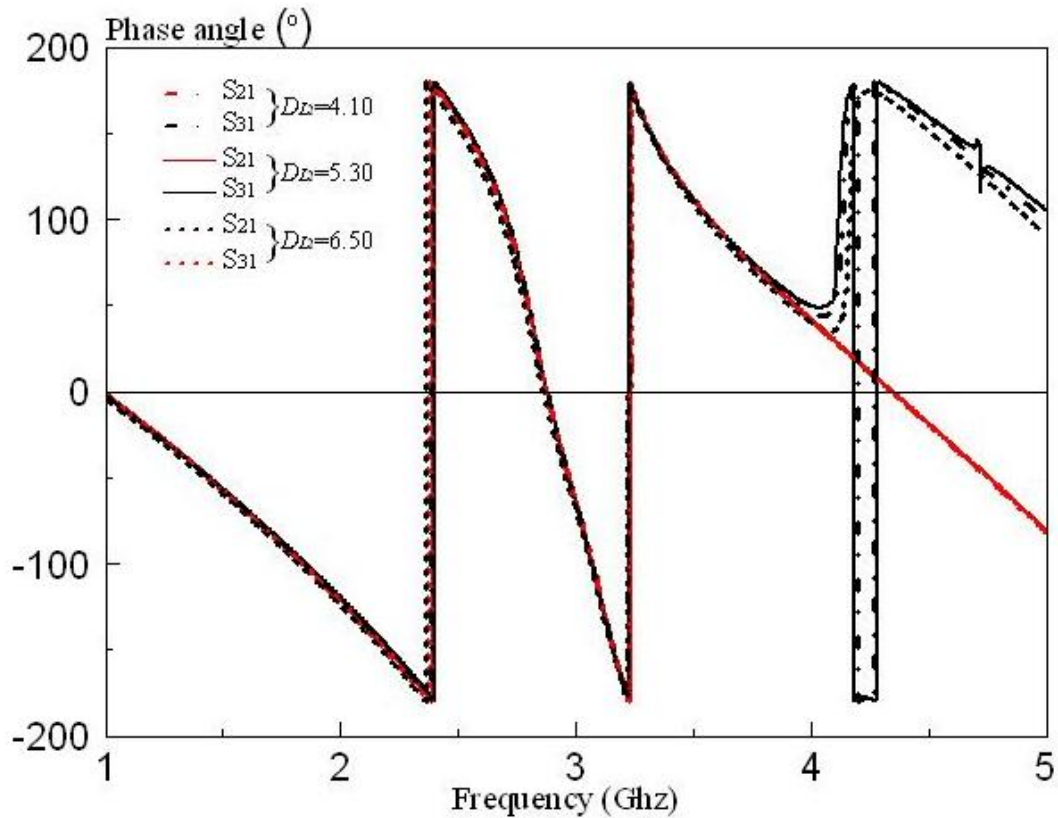


Figure 3.16 Effect of the changes of via position of DL_2 (Phase)

Effect of DL_4

From the Table 3.1, when the via position DL_4 changes from 6.55 mm to 5.55 mm, the magnitude of S_{11} changes from -15.467 dB to -12.335 dB inside the passband ranging from 2.843 GHz to 3.107 GHz .

When the via position DL_4 changes from 6.55 mm to 6.70 mm, the magnitude of S_{11} changes from -15.467 dB to -16.093 dB inside the passband ranging from 2.843 GHz to 3.107 GHz .

2 modes of the proposed design at $DL_4 = 6.55$ mm and 6.70 mm do not shift and remain at the point of 2.903 GHz (-16.142 dB) and 3.037 GHz (-30.133 dB) whereas the 2 modes of the proposed design at $DL_4 = 5.55$ mm change to 2.877 GHz (-14.136 dB). and 3.047 GHz (-22.923 dB) . It appears that later changes of via position has a better matching than the previous simulated result. The magnitude of the -3dB for S_{21} and S_{31} are flatter than the previous simulated result and acceptable.

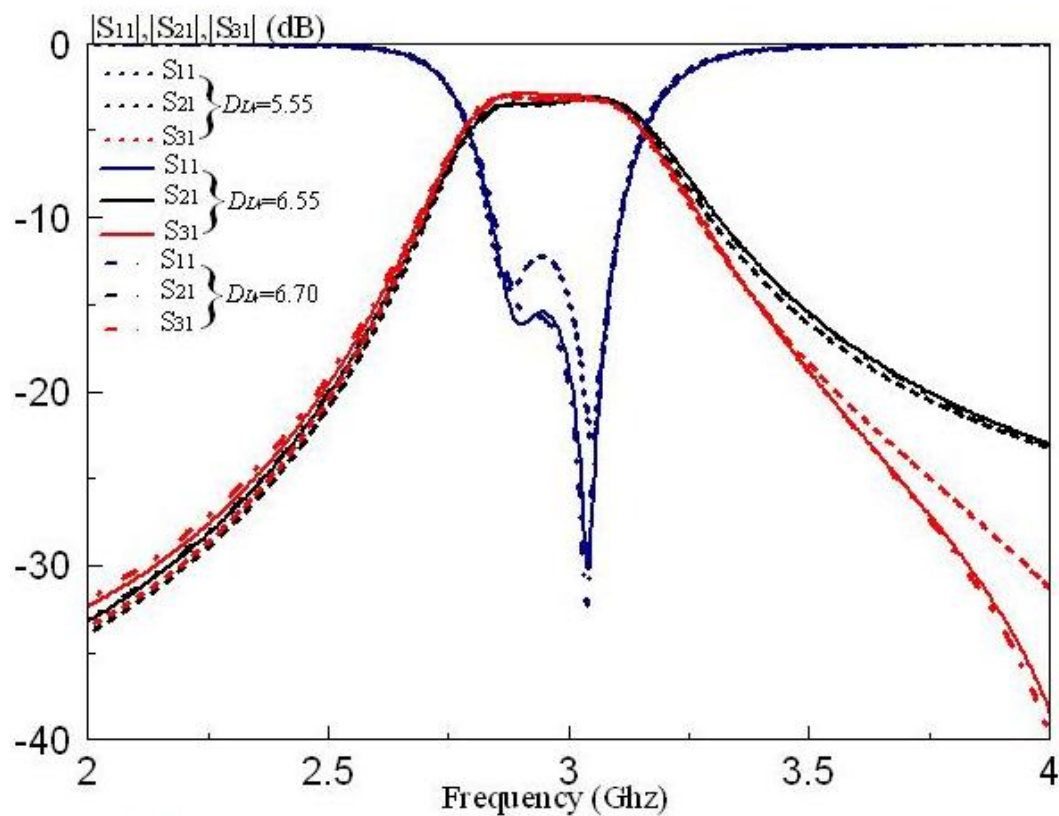


Figure 3.17 Effect of the changes of via position of DL_4 (Magnitude)

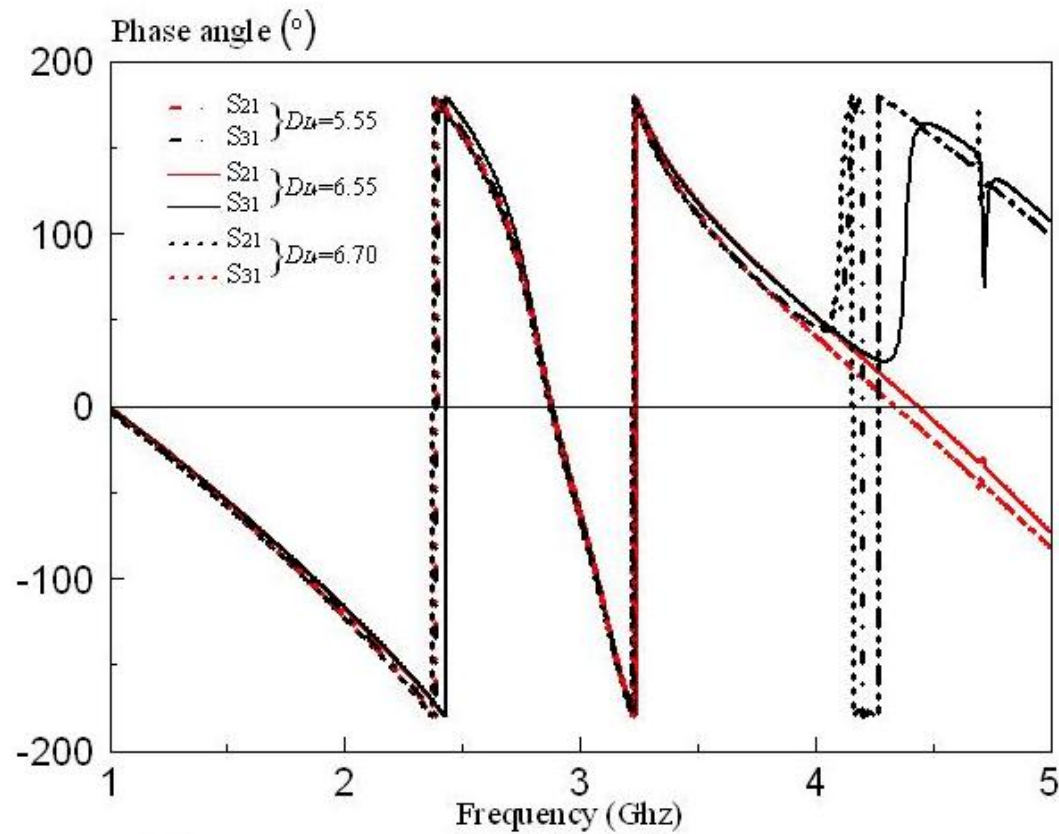


Figure 3.18 Effect of the changes of via position of DL_4 (Phase)

Effect of DI_6

From the Table 3.1, when the via position DI_6 changes from 5.30 mm to 4.30 mm, the magnitude of S_{11} changes from -15.467 dB to -18.410 dB inside the passband ranging from 2.843 GHz to 3.107 GHz .

When the via position DI_6 changes from 5.30 mm to 6.30 mm, the magnitude of S_{11} changes from -15.467 dB to -13.980 dB inside the passband ranging from 2.843 GHz to 3.107 GHz .

2 modes of the proposed design shifted. For $DI_6 = 4.30$ mm, the first mode increase to -14.123dB and the second mode increases to -32.874 dB. For $DI_6 = 6.30$ mm, the first mode decreases to -18.466 dB and the second mode decreases to -26.749 dB. It appears that first changes of via position has a better matching than the previous simulated result. The magnitude of the -3dB for S_{21} and S_{31} are flatter than the previous simulated result.

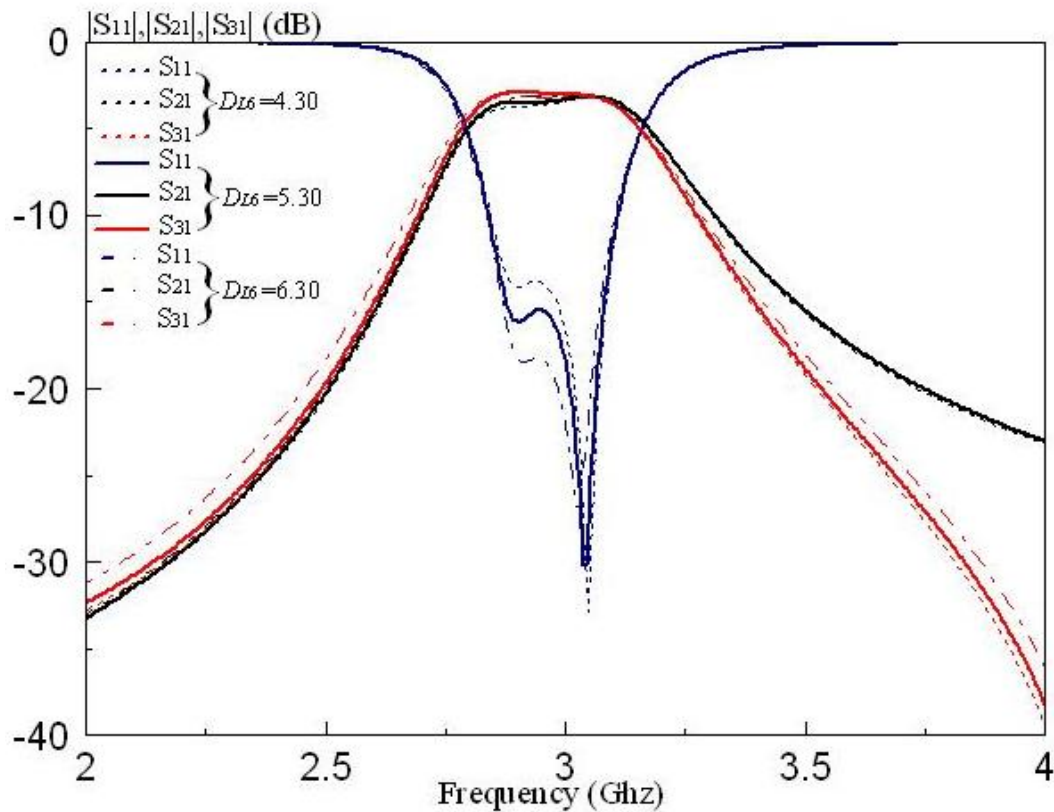


Figure 3.19 Effect of the changes of via position of DI_6 (Magnitude)

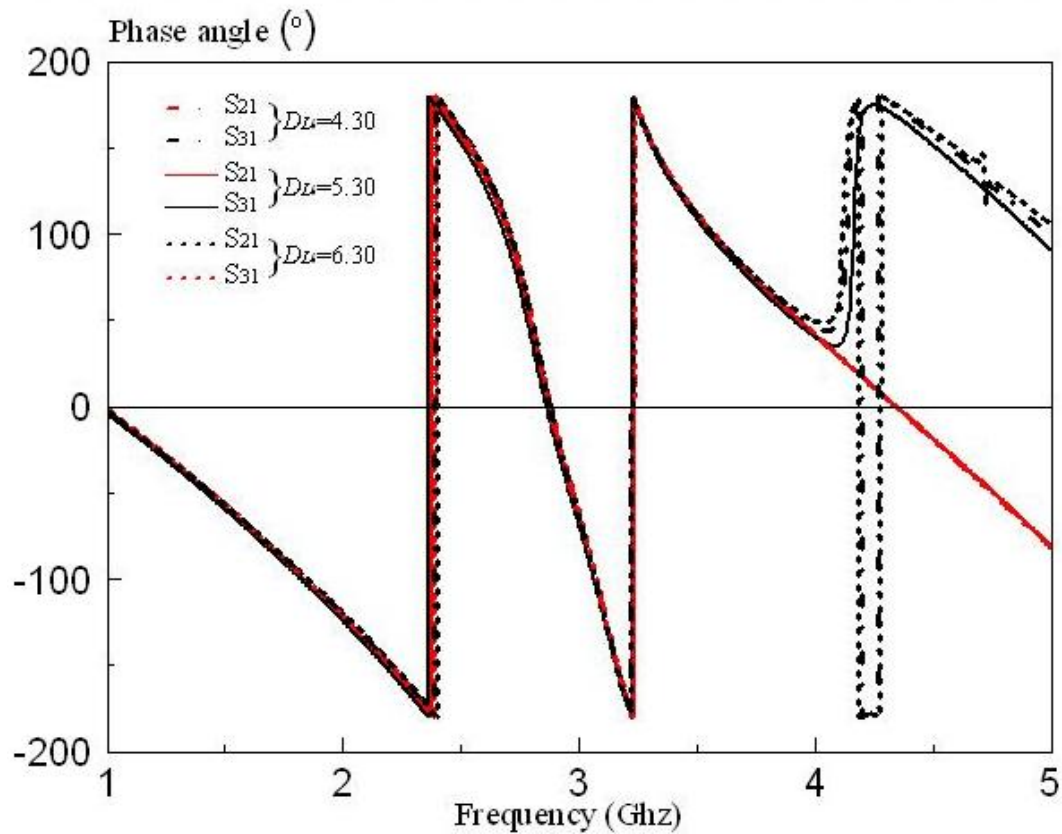


Figure 3.20 Effect of the changes of via position of DL_6 (Phase)

3.5 Discussion

Rotational symmetric power divider is a new concept in microwave application. The usage of via hole as grounding and wave guide is also a new approach in this design. It is proved that this proposed design can produce equal power at the output using the resonating concept

. It is very hard to tune the position of via holes as a little shifting in drilling and an equal soldering will affect the experimental result of the power divider. There is a lot of parameter analysis that can be done to tune the power divider in terms of s-parameter and phase. It happens that at certain level of tuning, the matching will become better but the phase will run off and vice versa. This is an unexplained situation as it could be loss at resonating patch or even coupler. This problem might be solved by using synthesis method which convert the schematic to equivalent circuit as representative for analysis. It is not done as this process is time consuming and it can hardly be done in this few months at 2nd semester.

CHAPTER 4

Multi-port Microstrip Power Divider

4.1 Background

Recent years, multiport power divider has been a hot issue which often discussed in microwave application . As mentioned in Chapter 2.5, there are lots of different power divider, such as hybrid ring power divider and Wilkinson Power Divider. Since the concept of Wilkinson Power Divider is an old concept, supervisor hopes the author will use the resonator concept to prove the filter design works out by resonance, rather than varying the width of the transmission line which change the impedance and the power ratio of the output. With the resonator concept, it is also important to ensure the power transfer from the input to the output has the lowest loss as possible. Lossless power divider is much preferable in the global market nowadays to improve the efficiency and effectiveness of the performance in microwave application.

4.2 Three-port Microstrip Patch Power Divider

To prove the concept of resonating works in real world, a rough proposed design of the filter has been given to the author by supervisor. It is a simple patch resonator as power divider by using similar to Wilkinson power divider configuration with one-to-two ports and the configuration of the design will be shown in Chapter 4.2.1 .

4.2.1 Configuration

The configuration of the proposed design is as shown below;

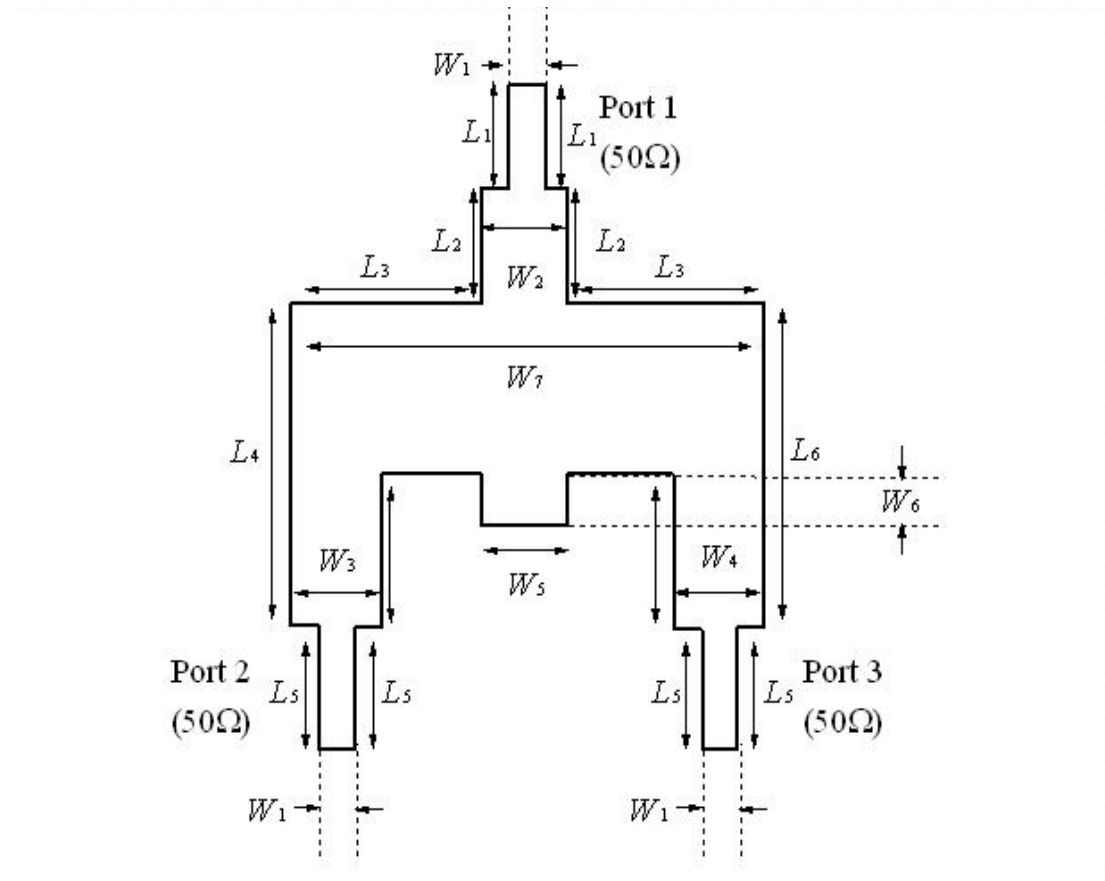


Figure 4.1 Top down view of Three-port Microstrip Patch Power Divider

L_1	11.50
L_2	20.00
L_3	20.00
L_4	37.00
L_5	11.50
L_6	37.00
W_1	1.80
W_2	10.00
W_3	10.00
W_4	10.00
W_5	10.00
W_6	6.50
W_7	50.00

Table 4.1 The dimension of Three-port Microstrip Patch Power Divider

4.2.2 Results

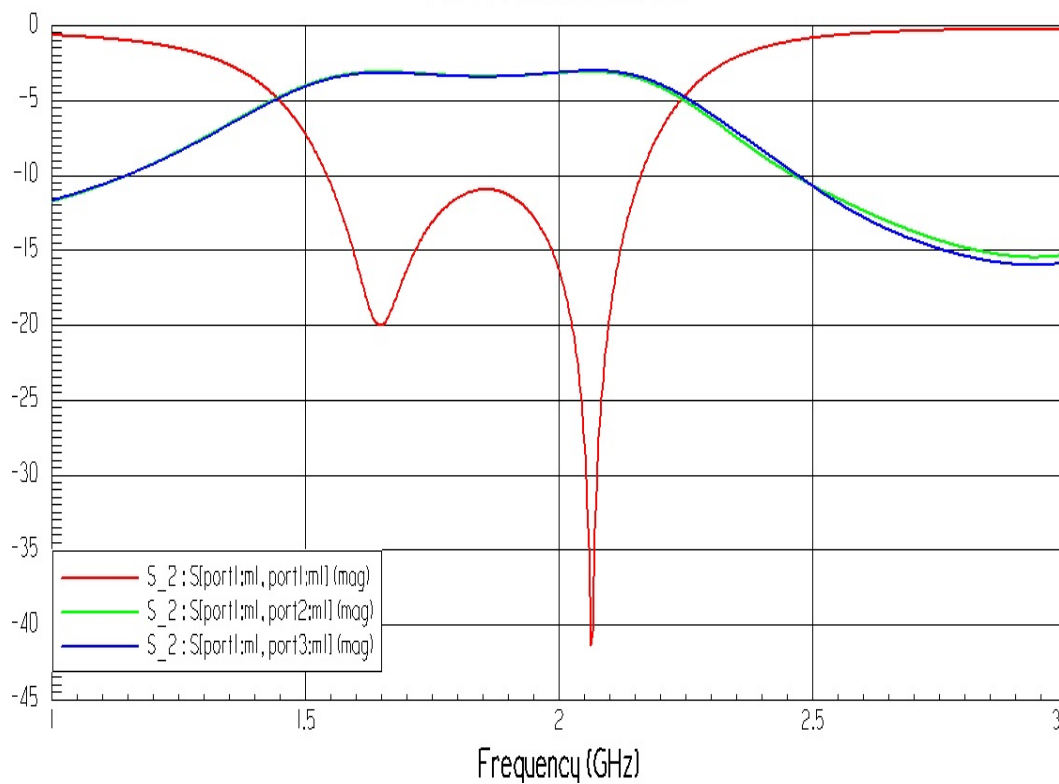


Figure 4.2 Magnitude of Three-port Microstrip Patch Power Divider (Simulation)

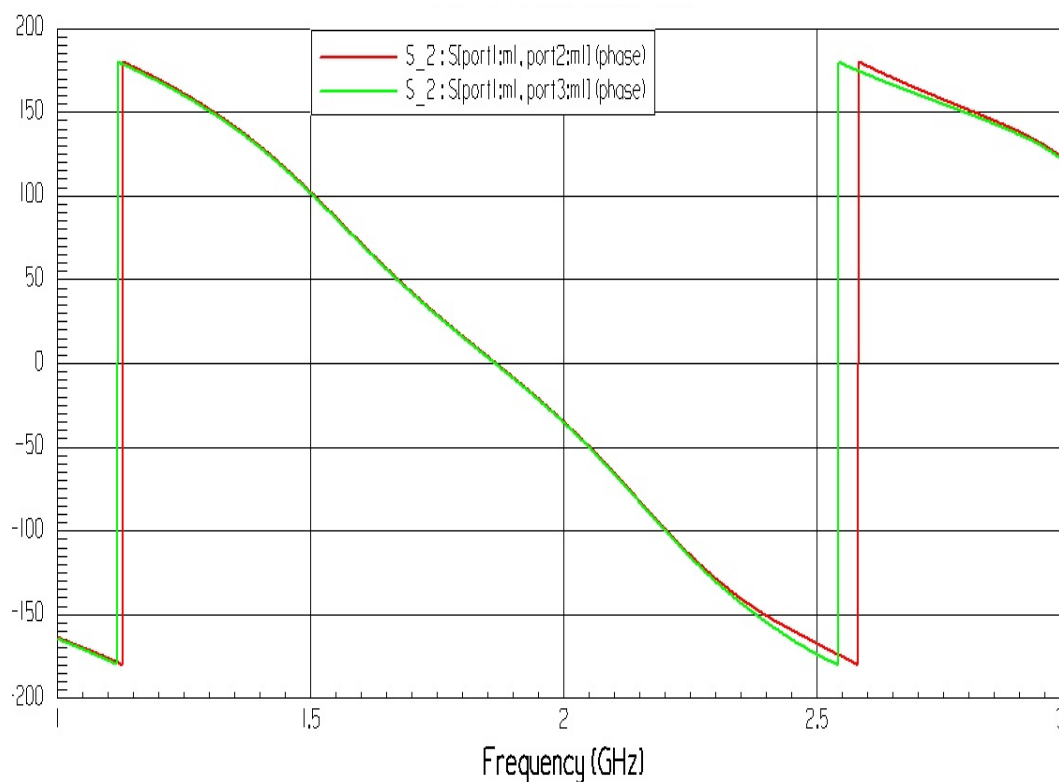


Figure 4.3 Phase of Three-port Microstrip Patch Power Divider (Simulation)

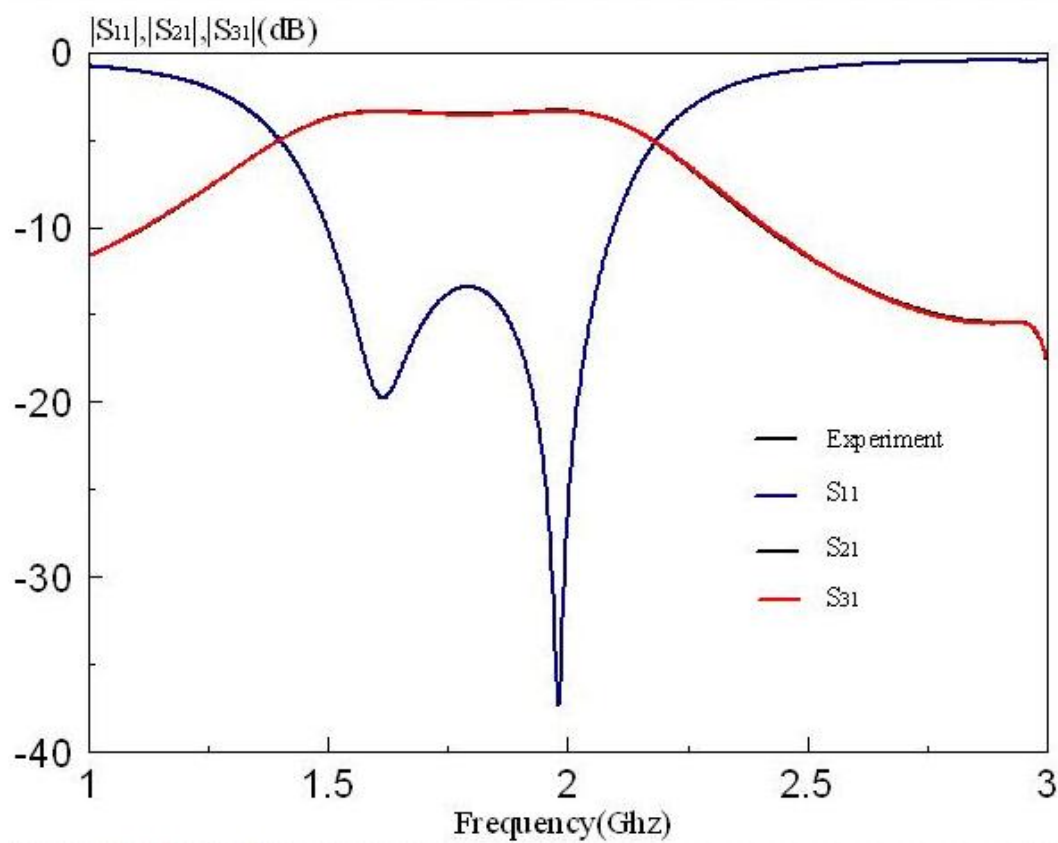


Figure 4.4 Magnitude of Three-port Microstrip Patch Power Divider (Experimental)

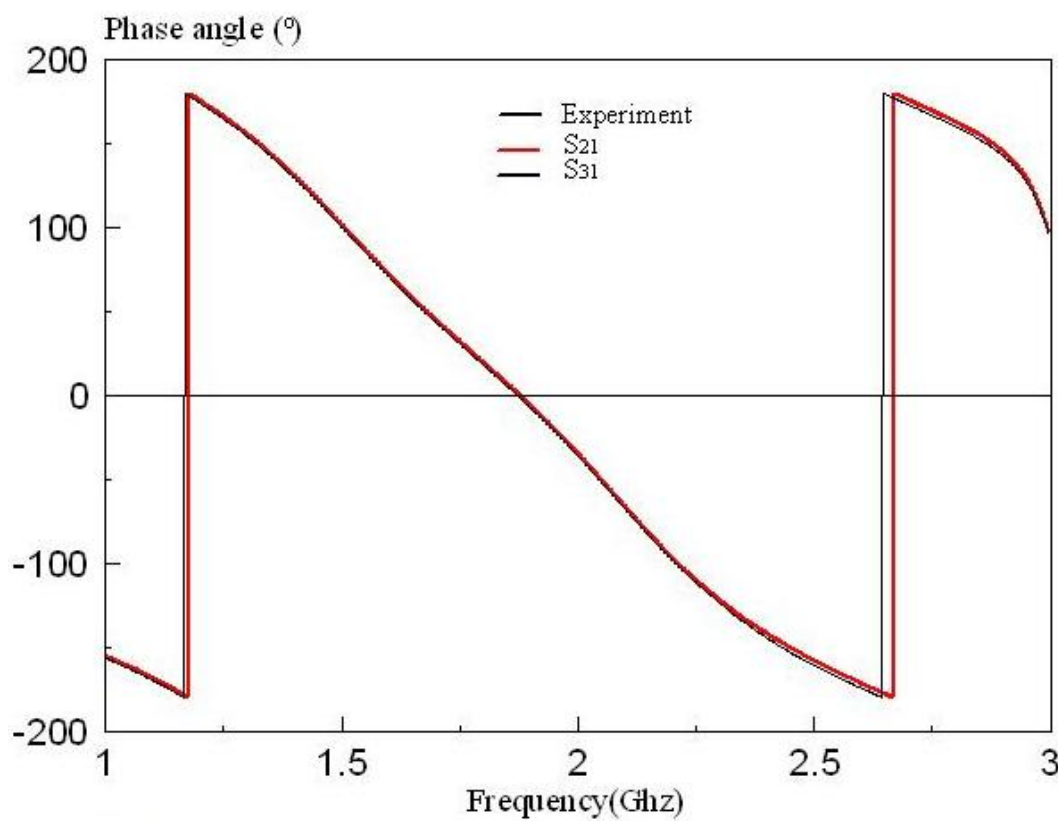


Figure 4.5 Phase of Three-port Microstrip Patch Power Divider (Experimental)

4.2.3 Discussion

Figure 4.2 and Figure 4.4 shows the comparison between measured and predicted S parameter S_{11} , S_{21} and S_{31} of the proposed prototype. The result from the experiment is quite promising as it has a better matching compared to the result from the simulation. One transmission zero can be obtained from the experimental result which proves that this proposed design power divider has a better selectivity.

From Figure 3.2, it shows that the insertion loss from -3.048 dB till -3.519 dB for S_{21} and -3.089 dB to -3.637 dB for S_{31} . The centre frequency for the simulated result is -1.846 GHz. From Figure 3.4, it shows that the insertion loss from -3.333 dB till -3.87 dB for S_{21} and -3.370 dB to -3.893 dB for S_{31} . The centre frequency for the experimental result is -1.784 GHz. Experimental phase result shows a good agreement with the simulation.

A better matching has been encountered mostly due to the centre stub of the design. Slight changes of the stub size will affect the result quite a lot. For this proposed design, the stub size is 10.00 mm x 6.50 mm which is the best configuration that can be found from the simulation. Without the centre stub, the insertion loss of the S_{21} , S_{31} and S_{41} will not be equal. The phase of the proposed will also be affected as well. Effect of the stub will be further discussed in the next section of this chapter. The comparison between the measurement and simulation results is summarized in table 4.2.

	Measured		HFSS	
	S_{21}	S_{31}	S_{21}	S_{31}
Minimum Insertion Loss (dB)	-3.333	-3.370	-3.048	-3.089
3-dB Reference (dB)	-6.333	-6.370	-6.048	-6.089
f_L (GHz) / f_H (GHz)	1.499/2.094	1.499/2.094	1.532/2.151	1.532/2.151
f_c (GHz)	1.797	1.797	1.842	1.842
Fractional Bandwidth (%)	33.11	33.11	33.60	33.60
Error (%)	2.50	2.50	2.44	2.44

Table 4.2 Comparison between the measure and simulated S-parameter

4.3 Parametric Analysis

This section of Chapter 4 is about the case studies on Three-port Microstrip Patch Power Divider by changing the value of the variable such as patch length and width. The main purpose of this studies being carried out is to observe the changes of the s-parameter with the changes of the variables, whether it produces a better or worst result. Other parameter such as frequency range and centre frequency will be remained. The configuration of the proposed design filter shown below ;

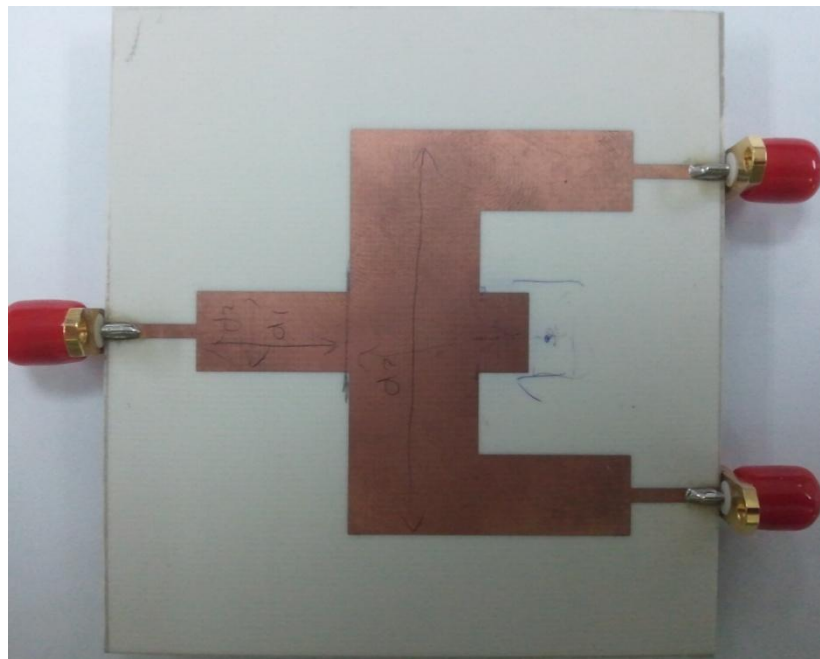
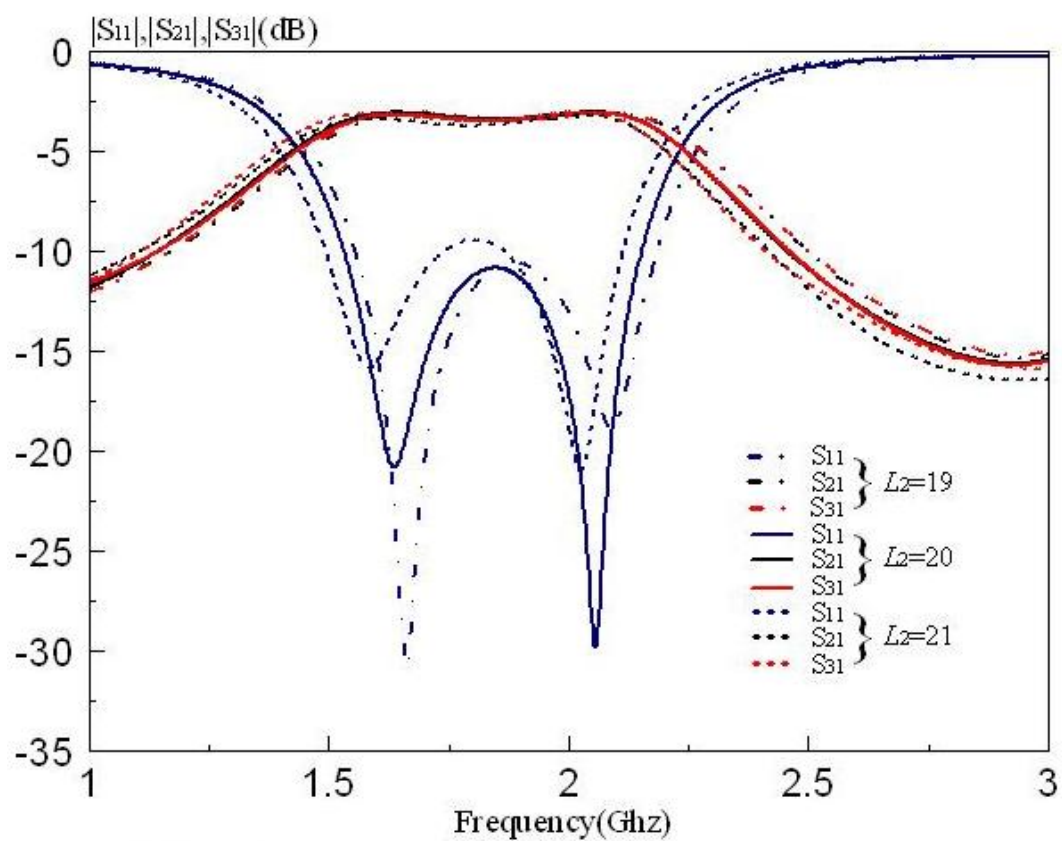
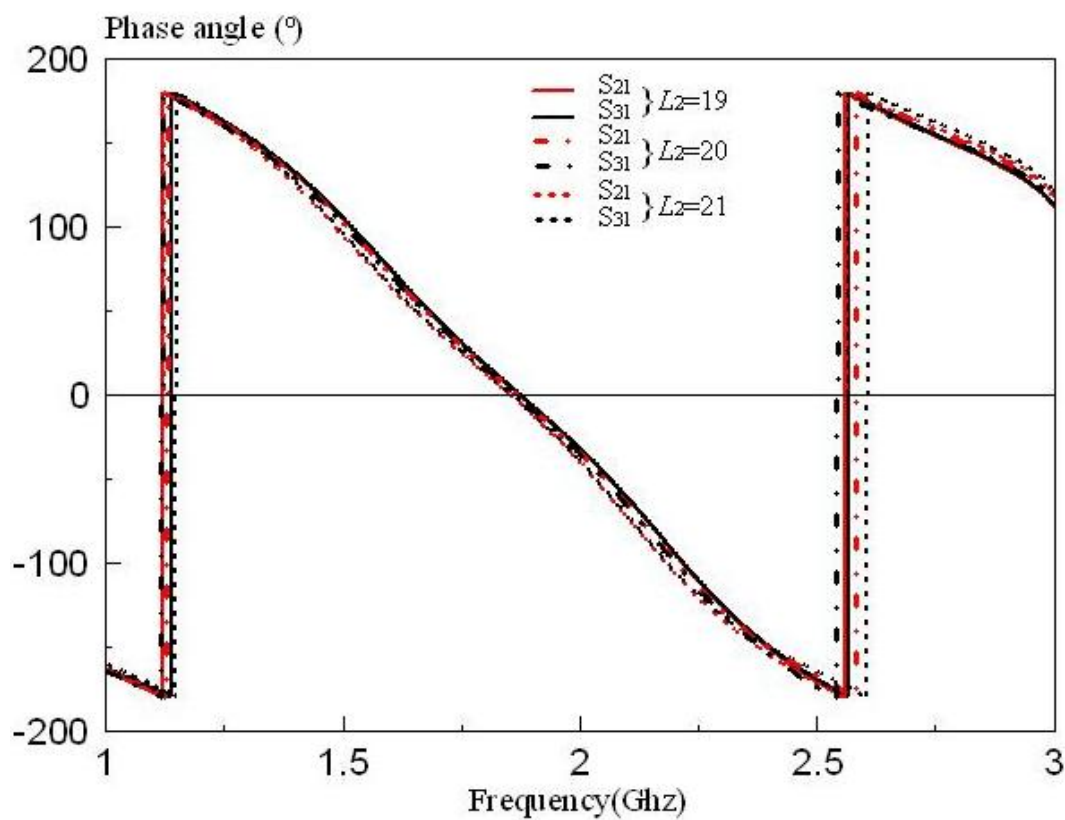


Figure 4.6 Configuration of the Three-port Microstrip Patch Power Divider

Effect of changes in length L_2

From the Table 4.1, when the length L_2 changes from 20 mm to 19 mm, the magnitude of S_{11} changes a little from -10.945 dB to -10.722 dB inside the passband ranging from 1.544 Ghz to 2.161 Ghz . When the length L_2 changes from 20 mm to 21 mm, the magnitude of S_{11} changes a little from -10.945 dB to -9.423 dB inside the passband ranging from 1.494 Ghz to 2.114 Ghz . The later change of length L_2 cause the passband shifted to left side. The result is ideal at $L_2 = 20$ mm and no changes should be applied for this parameter.

Figure 4.7 Effect of changes in length L_2 (Magnitude)Figure 4.8 Effect of changes in length L_2 (Phase)

Effect of changes in length L_4

From the Table 4.1, when the length L_4 changes from 37 mm to 36 mm, the magnitude of S_{11} changes a little from -10.945 dB to -9.981 dB inside the passband ranging from 1.544 GHz to 2.161 GHz .

When the length L_4 changes from 37 mm to 38 mm, the magnitude of S_{11} remain no changes inside the passband ranging from 1.544 GHz to 2.161 GHz. There is a changes of mode position in dB.

At $L_4 = 36$ mm, the first mode increase to -16.055 dB whereas the second mode increases to -23.270 dB. At $L_4 = 38$ mm, the first mode decreases to -24.088 dB whereas the second mode increases to -22.814 dB. No transmission zero can be observed. The result is ideal at $L_4 = 37$ mm and no further changes should be applied for this parameter.

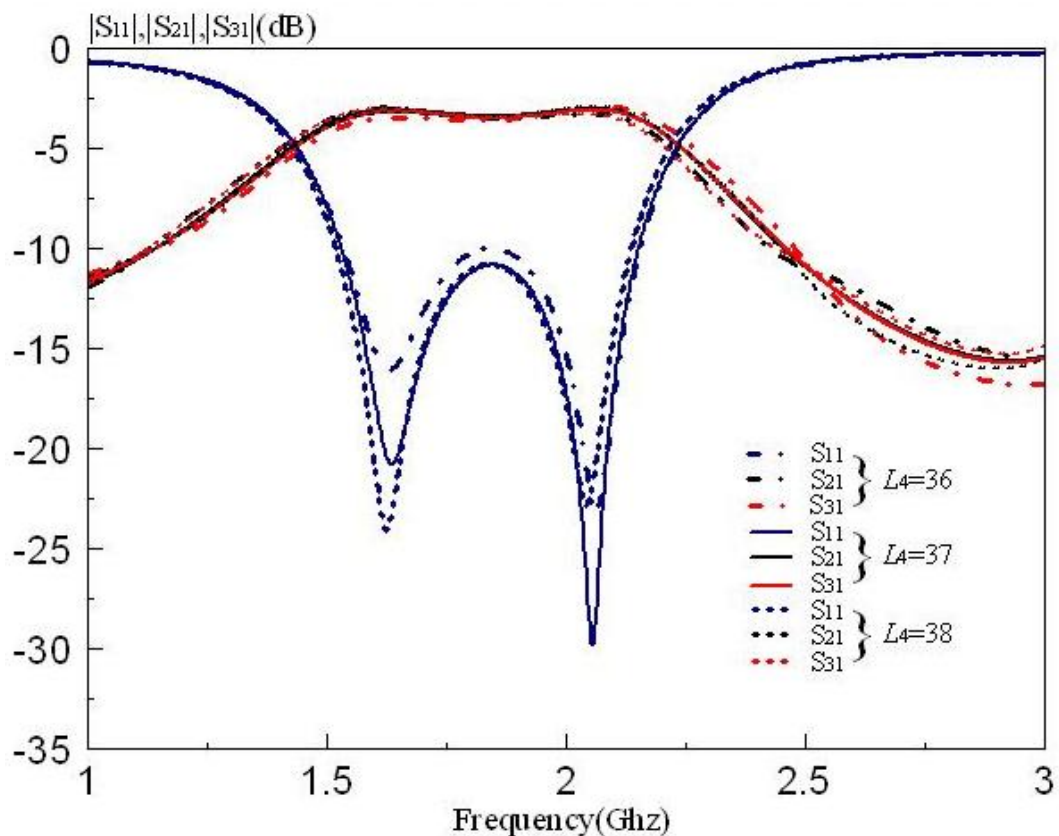


Figure 4.9 Effect of changes in length L_4 (Magnitude)

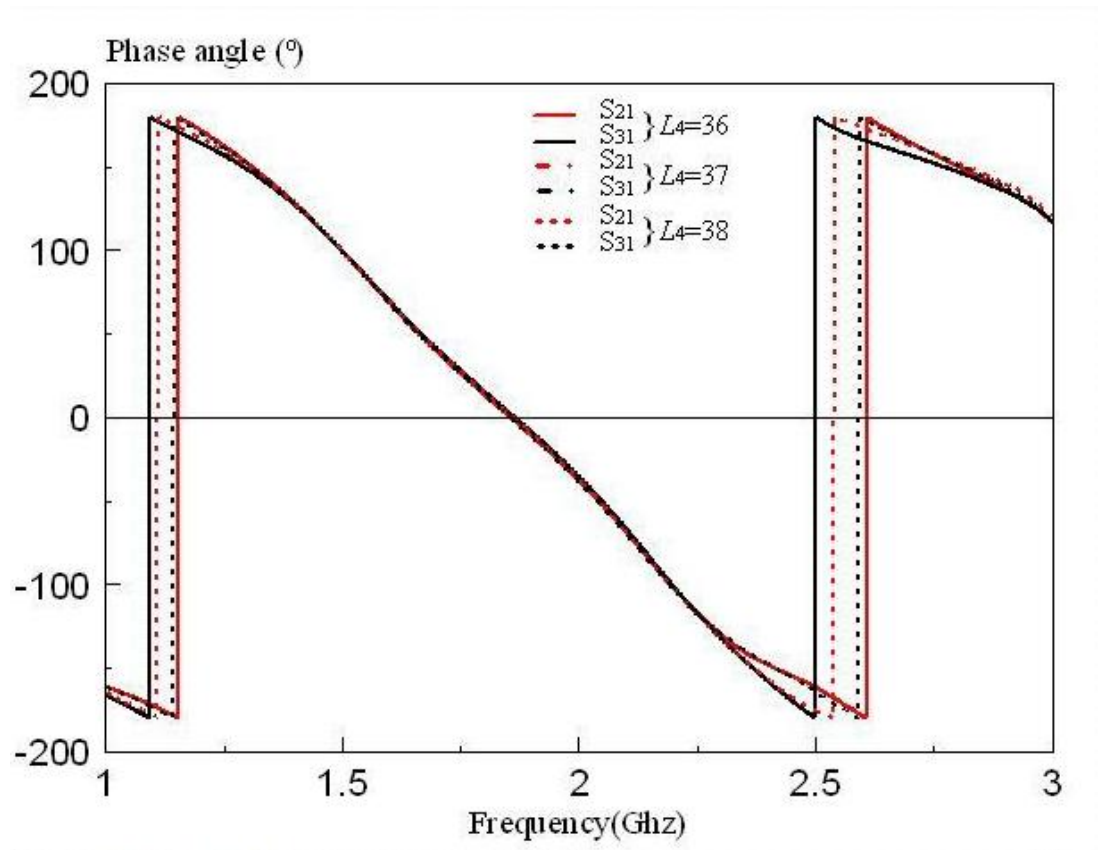


Figure 4.10 Effect of changes in length L_4 (Phase)

Effect of changes in width W_2

From the Table 4.1, when the width W_2 changes from 10 mm to 8 mm, the magnitude of S_{11} remain no changes inside the passband ranging from 1.544 GHz to 2.161 GHz . When the width W_2 changes from 10 mm to 12 mm, the magnitude of S_{11} changes from -10.945 dB to -7.437 dB inside the passband ranging from 1.497 GHz to 2.181 GHz.

2 modes changes when $W_2 = 12$ mm. The first mode decreases to -27.365 dB whereas the second mode increases to -22.667 dB. No transmission zero is observed and the phase do not shift inside the passband. The insertion loss at $W_2 = 12$ mm is attenuate around 4 dB which is barely acceptable.

From the result, there is no significant change of modes when $W_2 = 8$ mm and $W_2 = 10$ mm , so it is considered as ideal and no further changes should be applied.

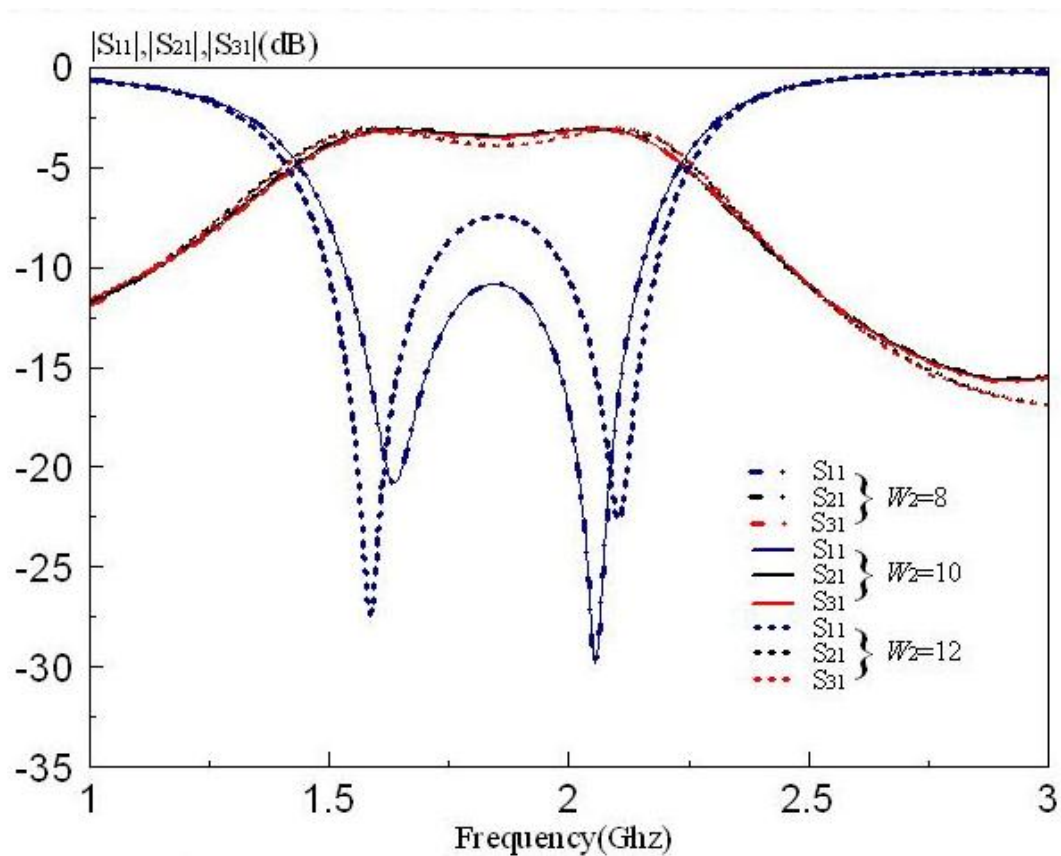


Figure 4.11 Effect of changes in width W_2 (Magnitude)

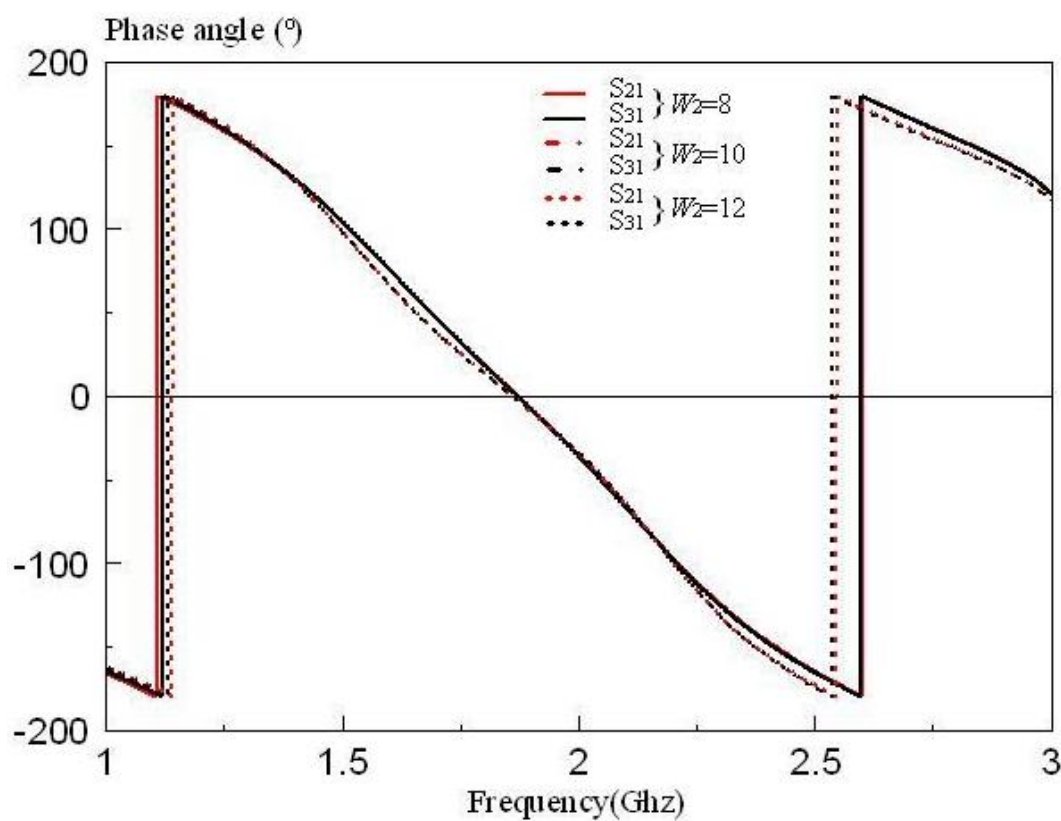


Figure 4.12 Effect of changes in width W_2 (Phase)

Effect of changes in width W_3

From the Table 4.1, when the width W_3 changes from 10 mm to 9 mm, the magnitude of S_{11} remain no changes inside the passband ranging from 1.544 GHz to 2.161 GHz .

When the width W_3 changes from 10 mm to 11 mm, the magnitude of S_{11} changes from -10.945 dB to -7.858 dB inside the passband ranging from 1.509 GHz to 2.158 GHz.

2 modes for the $W_3 = 11$ mm shifted. The first mode increase to -14.423 dB whereas the second mode decreases to -32.407 dB. No transmission zero is observed and the phase do not shift inside the passband. The result is considered to be ideal at $W_3 = 9$ mm and $W_3 = 10$ mm.

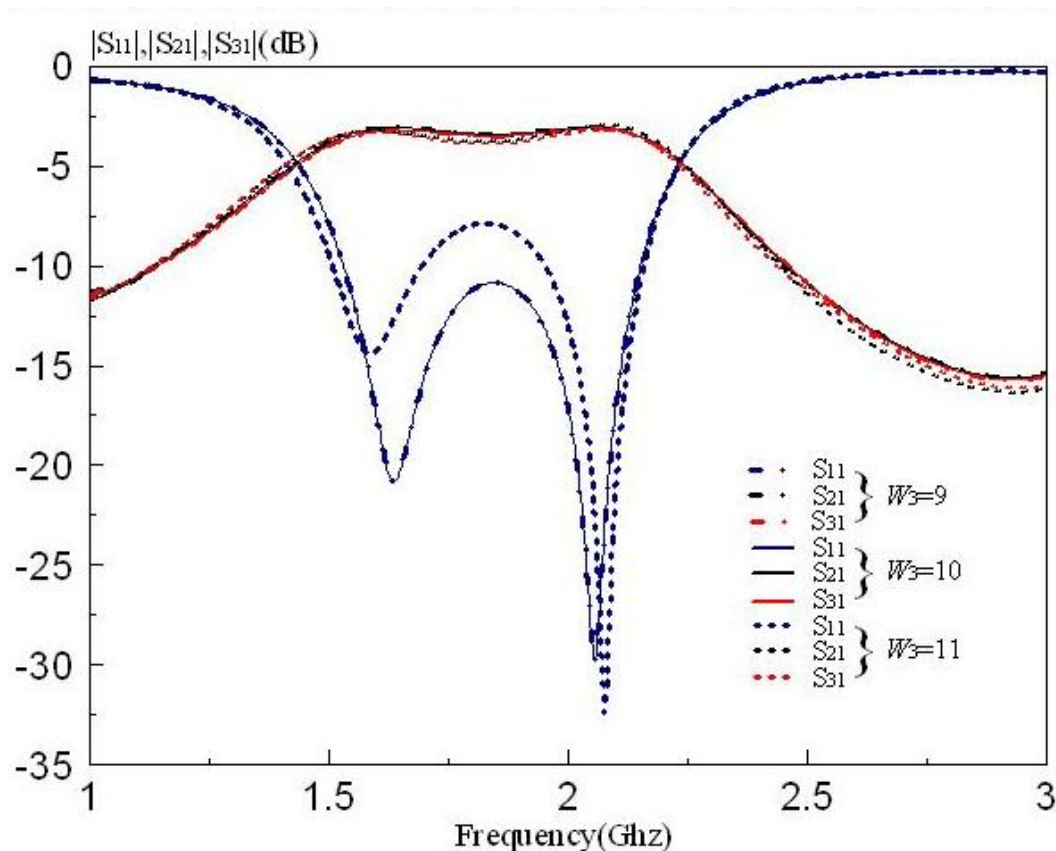


Figure 4.13 Effect of changes in width W_3 (Magnitude)

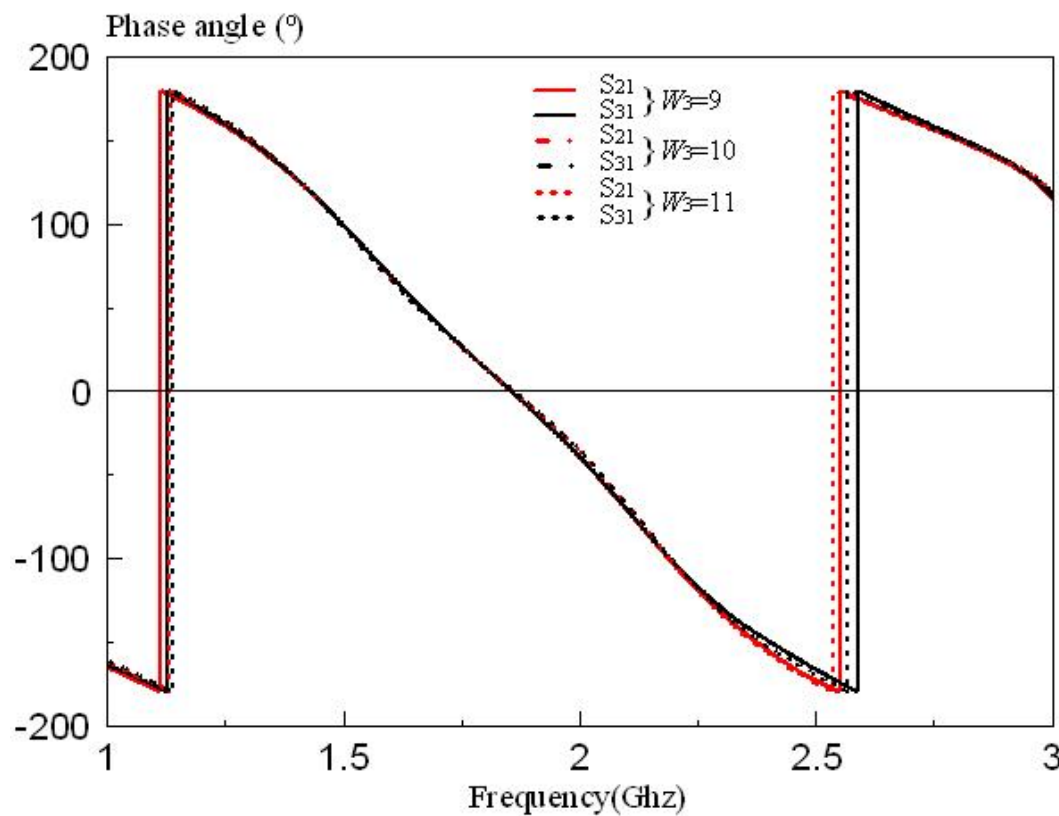
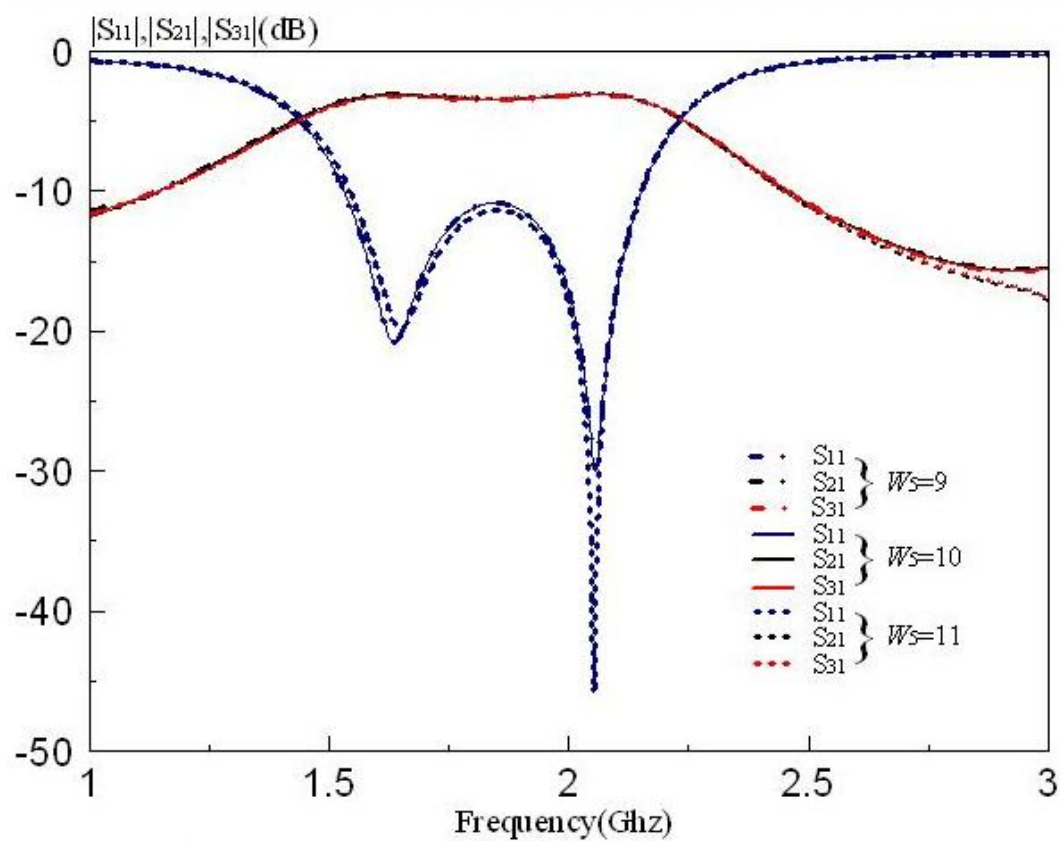
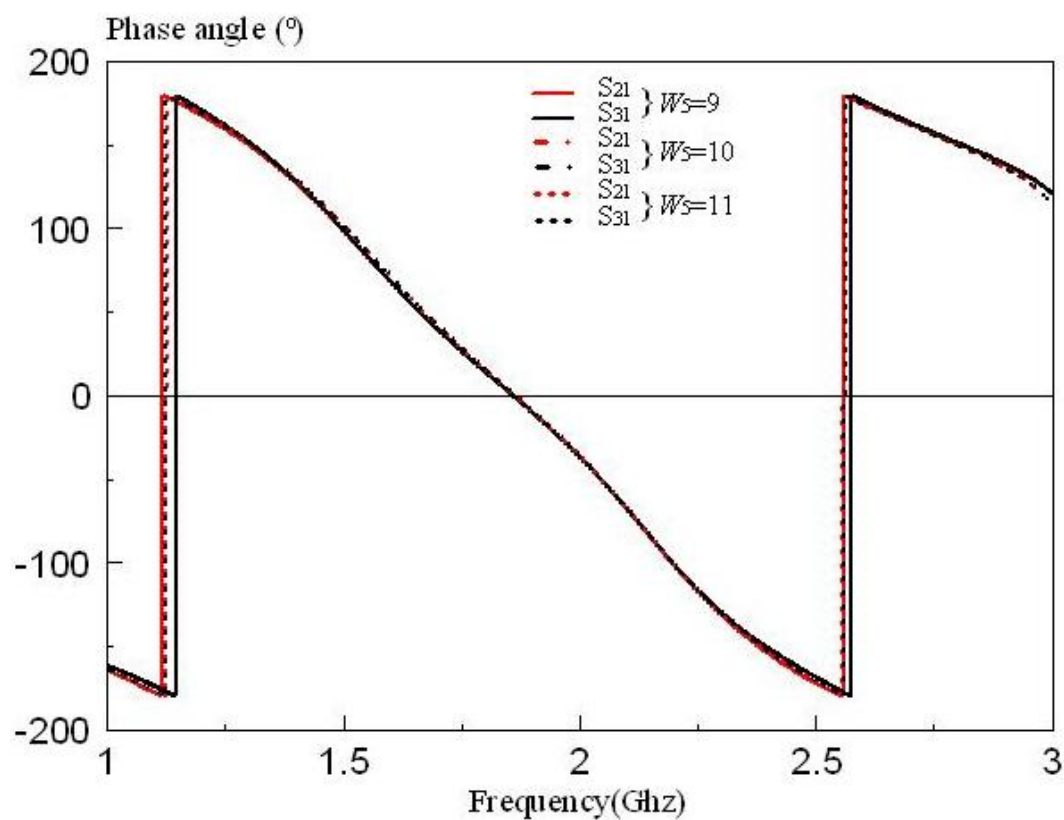


Figure 4.14 Effect of changes in width W_3 (Phase)

Effect of changes in width W_5

From the Table 4.1, when the width W_5 changes from 10 mm to 9 mm, the magnitude of S_{11} remain no changes inside the passband ranging from 1.544 GHz to 2.161 GHz .

When the width W_5 changes from 10 mm to 11 mm, the magnitude of S_{11} remain no changes inside the passband ranging from 1.544 GHz to 2.161 GHz . The significant change is on the second mode when $W_5 = 11$ mm which it changes to -45.750 dB. Changes in this parameter will not affect the matching of the simulated result

Figure 4.15 Effect of changes in width W_5 (Magnitude)Figure 4.16 Effect of changes in width W_5 (Phase)

Effect of changes in width W_6

From the Table 4.1, when the width W_6 changes from 6.5 mm to 5.5 mm, the magnitude of S_{11} changes from -10.945 dB to -9.288 dB inside the passband ranging from 1.544 GHz to 2.161 GHz .

The first resonant mode has shifted at $W_6 = 5.5$ mm. It increases to -16.789 dB. The second resonant mode does not changed. When the width W_6 changes from 6.5 mm to 7.5 mm, the magnitude of S_{11} changes from -10.945 dB to -11.062 dB inside the passband ranging from 1.544 GHz to 2.161 GHz .

The phase of this proposed design does not change when there is a changes in W_6 . The later changes in width W_6 to 7.5 mm will resulted in better matching. One zero has shifted nearer to the right of the passband. It gives the filter a better selectivity.

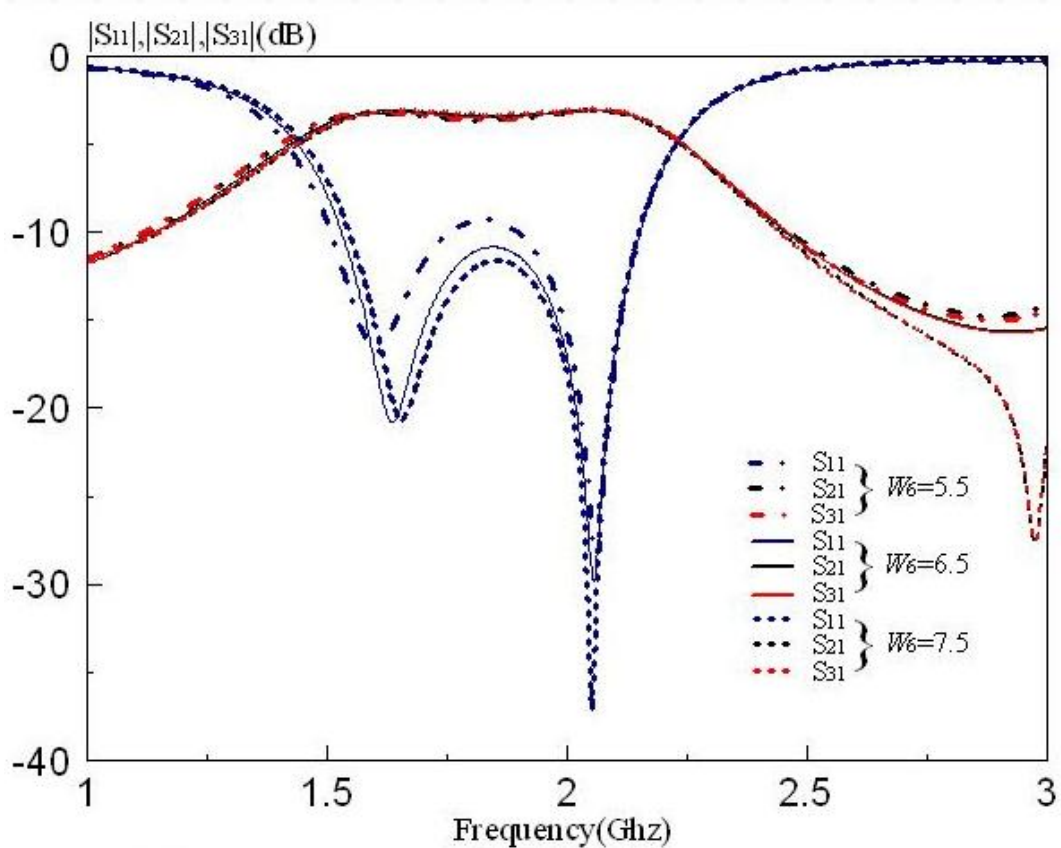


Figure 4.17 Effect of changes in width W_6 (Magnitude)

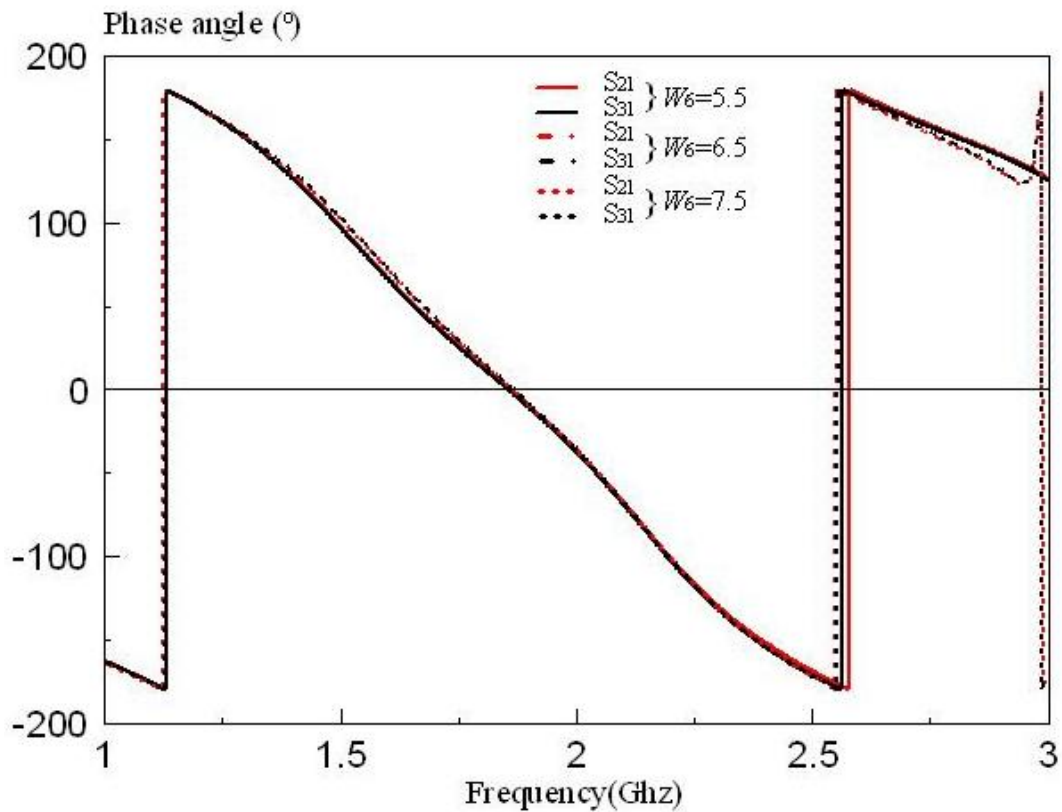


Figure 4.18 Effect of changes in width W_6 (Phase)

Effect of changes in width W_7

From the Table 4.1, when the width W_7 changes from 50 mm to 46 mm, the magnitude of S_{11} changes from -10.945 dB to -10.038 dB inside the passband ranging from 1.544 GHz to 2.161 GHz .

There is a change of modes when $W_7 = 46$ mm. The first resonant mode increases to -17.771 dB and the second resonant mode decreases to -32.375 dB. When the width W_7 changes from 50 mm to 54 mm, the magnitude of S_{11} changes from -10.945 dB to -11.325 dB inside the passband ranging from 1.544 GHz to 2.161 GHz .

There is also a phase shifting of 50 MHz with a phase difference of 10 degrees. It proves that the later changes in width W_7 to 54 mm will resulted in better matching.

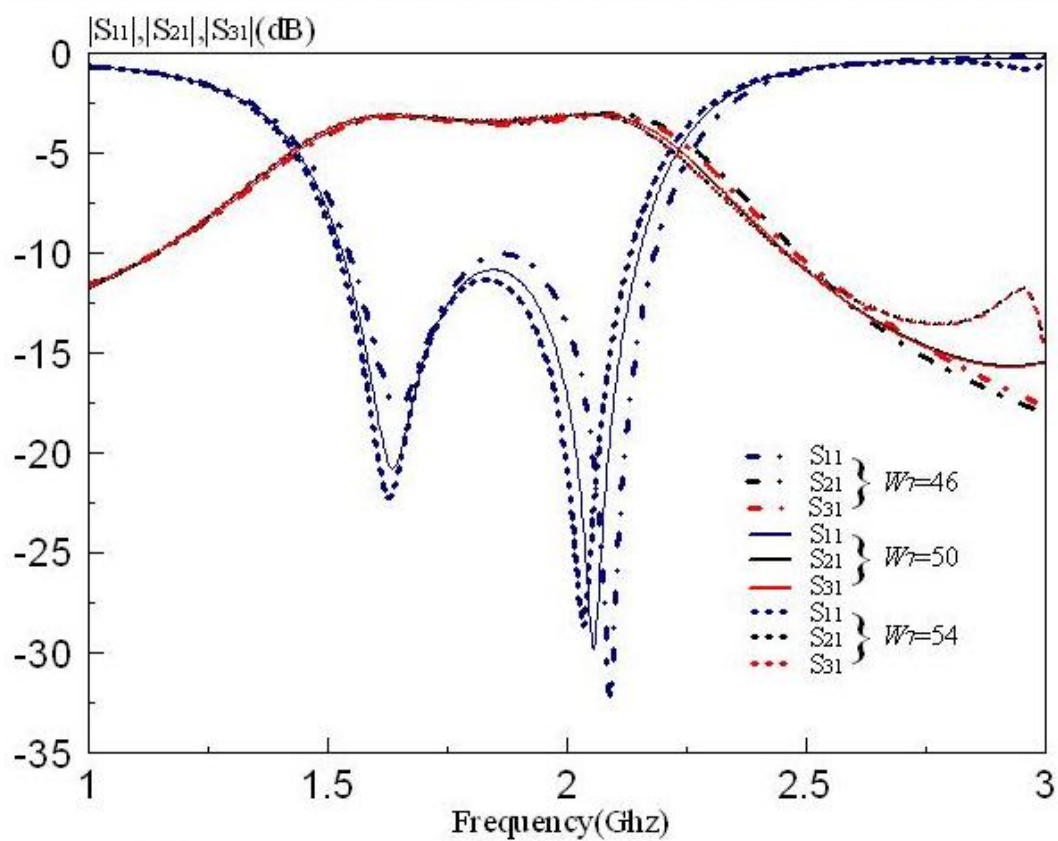


Figure 4.19 Effect of changes in width W_7 (Magnitude)

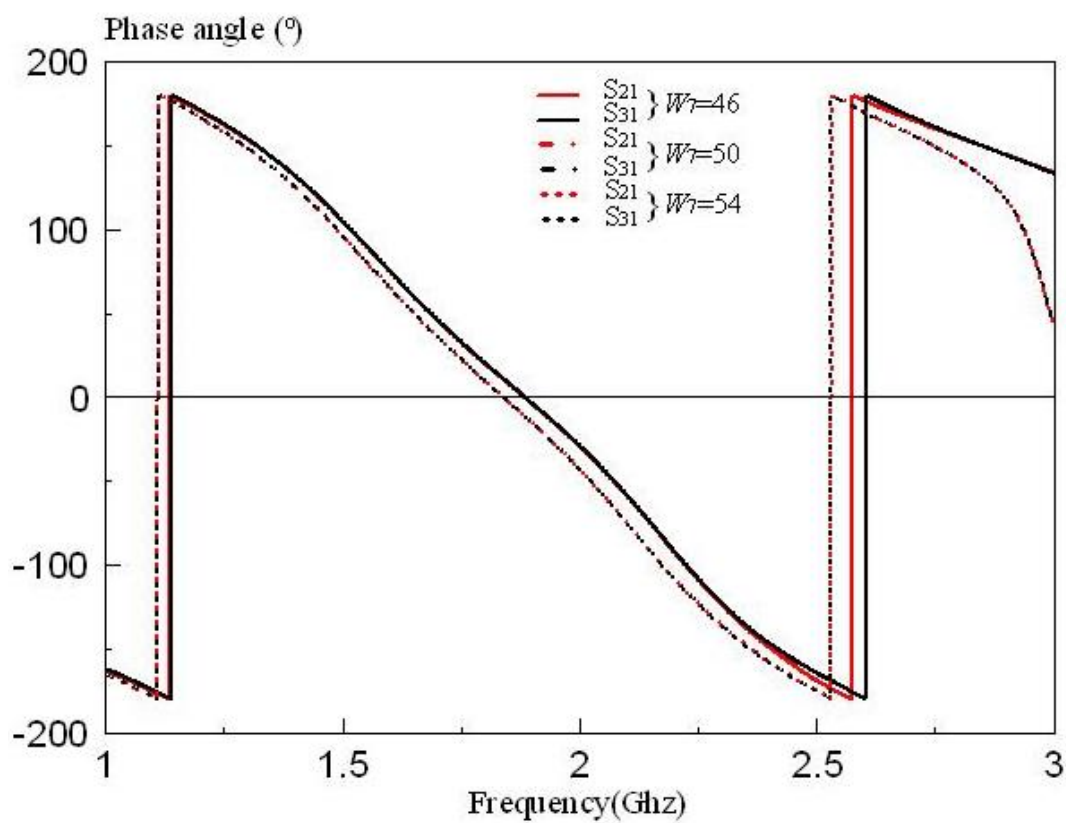


Figure 4.20 Effect of changes in width W_7 (Phase)

4.4 Discussion

This centre stub 3 ports power divider is also a new concept in microwave application and design. This multiport power divider gives a good agreement of around 3.2 dB of insertion loss, instead of 3.0 dB. The loss maybe due to the nature of the design configuration. When a slight changes in size of the patch will caused the insertion loss changed. The proposed configuration is found to be the optimised design which produce the optimum result. There is an important part of the design, which is the centre stub. When dealing with the length and width of the stub, careful measurement must be taken as slight changes of 1 mm of each of the parameter will caused the matching becomes worst.

There is an analysis by implementing lumped component such as inductor and capacitor to adjust the phase of the proposed design. Capacitor is used as the gap between the patches as coupler and inductor serves as the length of the patch. By varying the value of capacitor or inductor will tune the phase of the proposed design as well. But in return, the matching and insertion loss of the design will be affected as well. The position of the centre stub will also affect the result. It is mainly because theoretically to have equal power divided in both output ports, there must be a symmetrical dimension of port 2 and port 3. So changes of centre stub position might causes the dimension changes into asymmetrical shape with different characteristic impedance. The wave travels unequally in sinusoidal and might caused the phase in output ports to be different. In this proposed design, the desired result is in-phase. It is discussed in section 4.2.3. In short, this is still a good design with an equal power divided and negligible loss.

4.5 Four-port Microstrip Patch Power Divider

This Four-Port Microstrip Patch Power Divider is an improved version of the Three-port Microstrip Patch Power Divider by adding one port to the output. The overall dimension for the proposed design does not change, just extend the stub at the middle for output purpose. It is still proving the concept of resonance works in this proposed design.

4.5.1 Configuration

The configuration of the proposed design is as shown below;

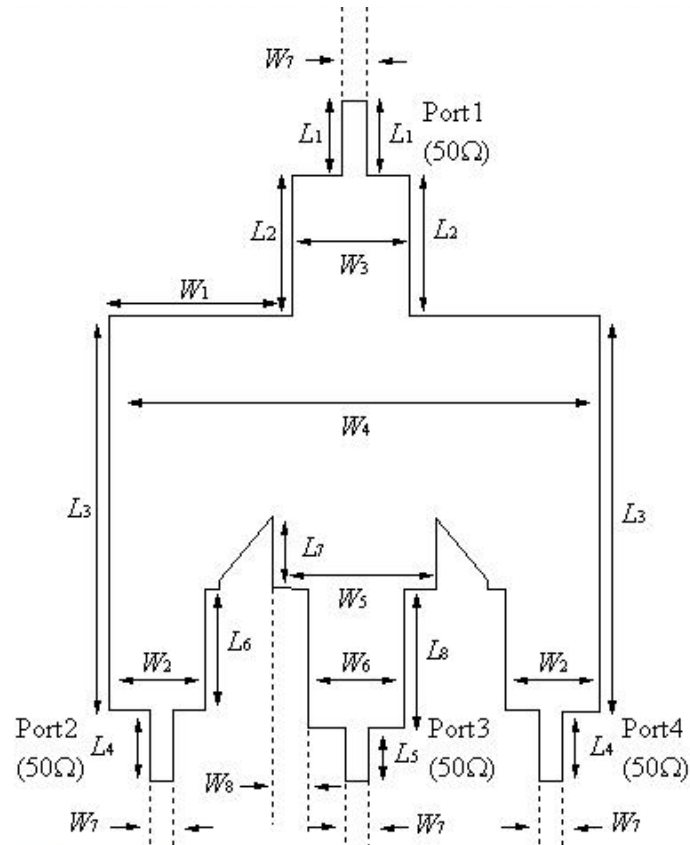


Figure 4.21 Top down view of Four-port Microstrip Patch Power Divider

L_1	13.6
L_2	15.5
L_3	40.9
L_4	11
L_5	8.9
L_6	12.7
L_7	5.7
L_8	15.1
W_1	15.65
W_2	7
W_3	10
W_4	41.3
W_5	16
W_6	7
W_7	1.8
W_8	4.5

Table 4.3 The dimension of Four -port Microstrip Patch Power Divider

4.5.2 Results

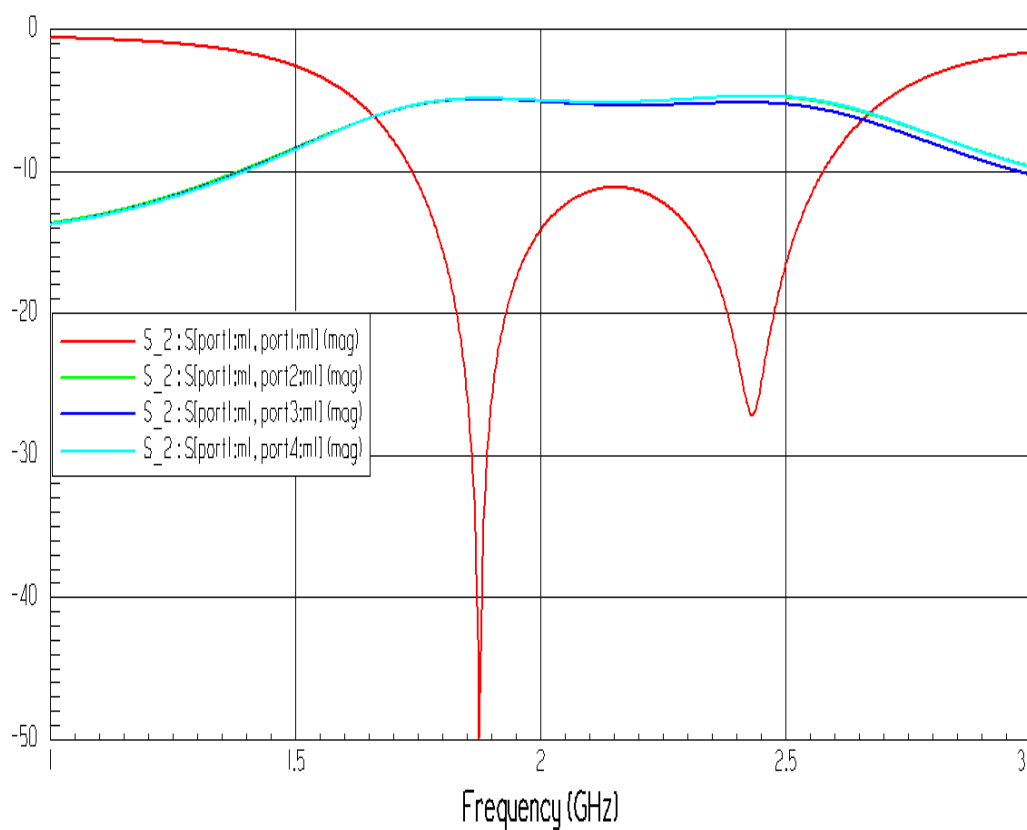


Figure 4.22 Magnitude of Four-port Microstrip Patch Power Divider (Simulation)

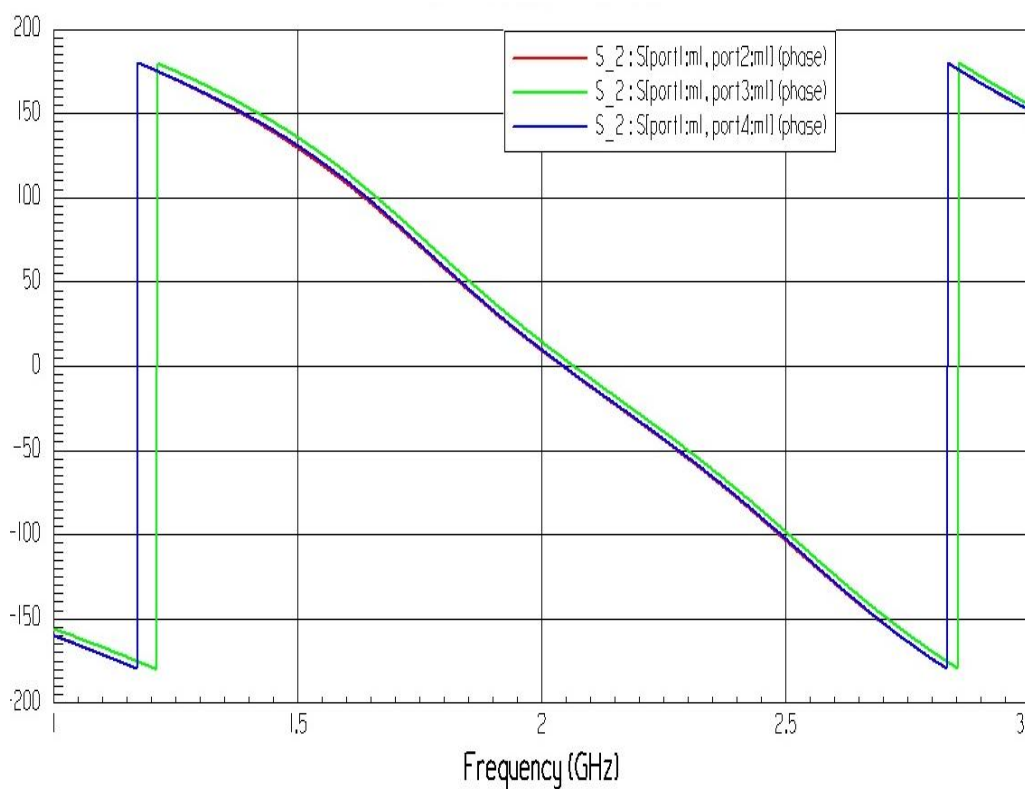


Figure 4.23 Phase of Four-port Microstrip Patch Power Divider (Simulation)

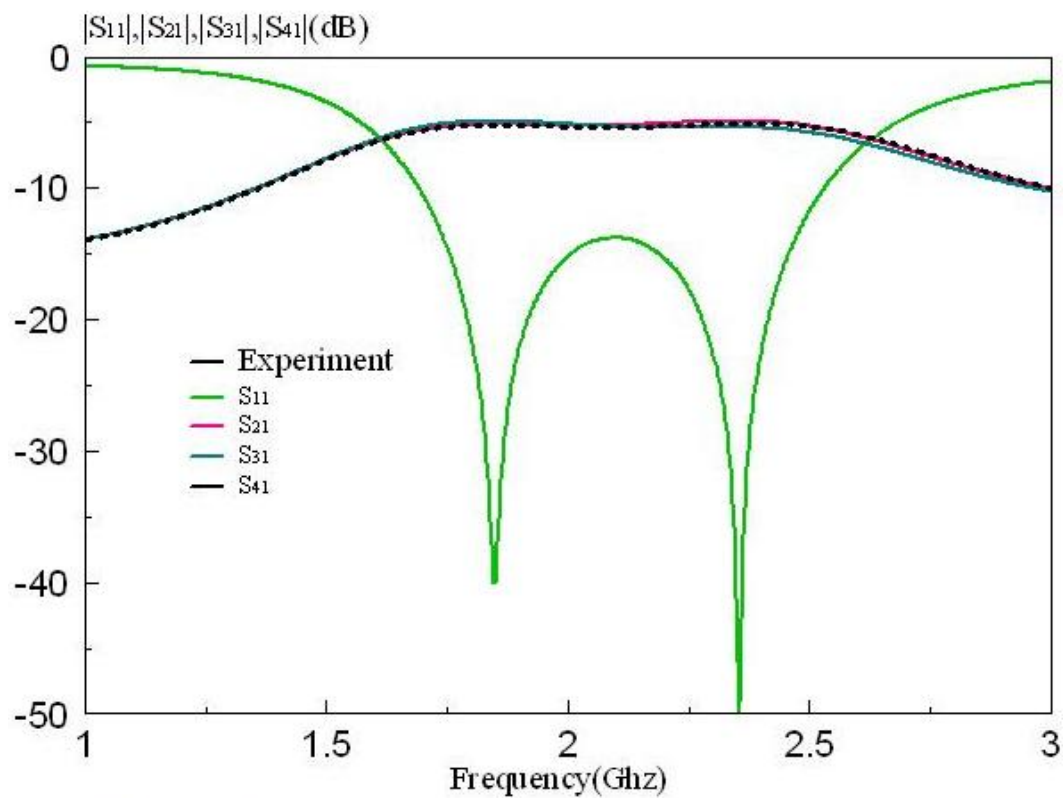


Figure 4.24 Magnitude of Four-port Microstrip Patch Power Divider (Experimental)

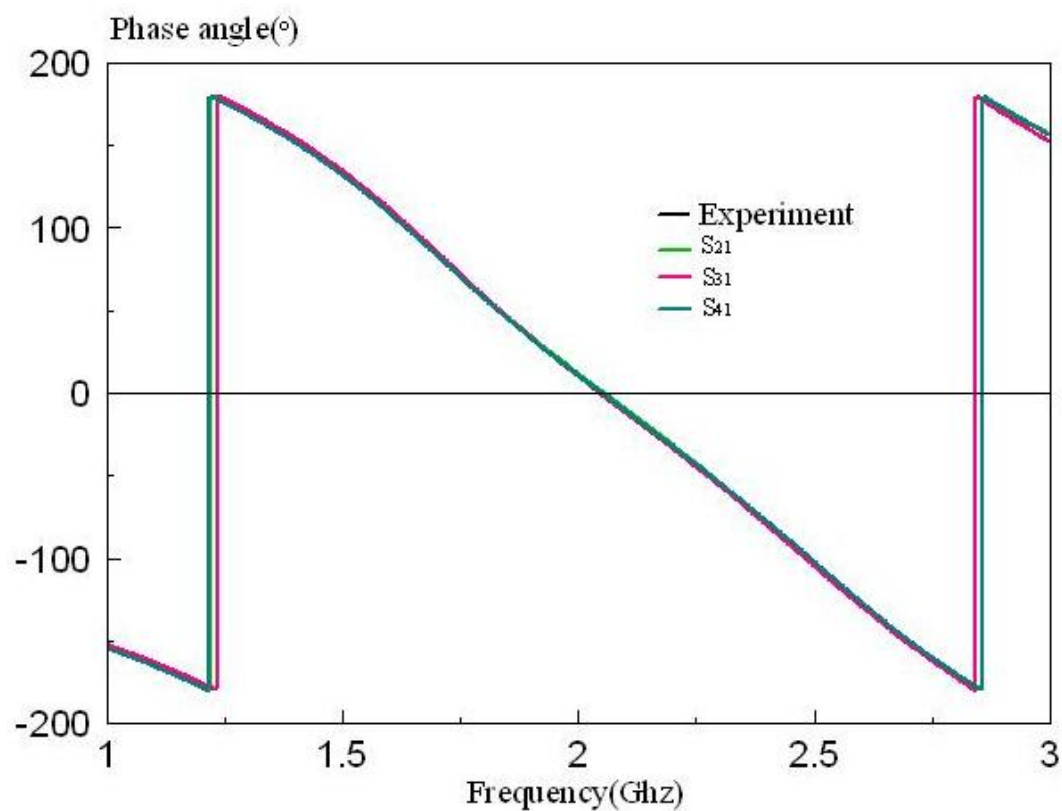


Figure 4.25 Phase of Four-port Microstrip Patch Power Divider (Experimental)

4.5.3 Discussion

Figure 4.22 and Figure 4.24 shows the comparison between measured and predicted S parameter S_{11} , S_{21} and S_{31} of the proposed prototype. The result from the experiment is quite promising as it has a better matching compared to the result from the simulation. One transmission zero can be obtained from the experimental result which proves that this proposed design power divider has a better selectivity.

From Figure 3.2, it shows that the insertion loss from -4.942 dB till -5.414 dB for S_{21} , -4.925 dB to -5.682 dB for S_{31} and -4.895 dB to -5.373 dB for S_{41} . The centre frequency for the simulated result is 2.151 GHz. From Figure 3.4, it shows that the insertion loss from -5.108 dB till -5.558 dB for S_{21} , -4.908 dB to -5.917 dB for S_{31} and -5.171 dB to -5.596 dB for S_{41} . The centre frequency for the experimental result is 2.101 GHz.

A better matching has been encountered mostly due to the centre fed line of the design. Slight changes of the fed line will affect the result. This phenomena remains unexplained due to the triangular gap at the centre fed. The assumption for implementing the triangular gap between feeder could be the capacitance and inductance effect on the proposed design.

If the triangular gap is filled with microstrip, the bandwidth that can be used inside passband is lower than the optimised result which is showed in Figure 4.26. Furthermore, the matching inside the passband is not preferable compared to the previous result and it shows that filled triangular gap does not gives a better result for the proposed filter design.

The phase of the proposed filter design will also be affected as well. The allowable gap of the In-phase design is around 5 degree and the that filled triangular gap design goes up to 11 degree difference in the passband which is not desirable. Effect of the stub will be further discussed in the next section of this chapter. The comparison between the measurement and simulation results is summarized in table 4.4.

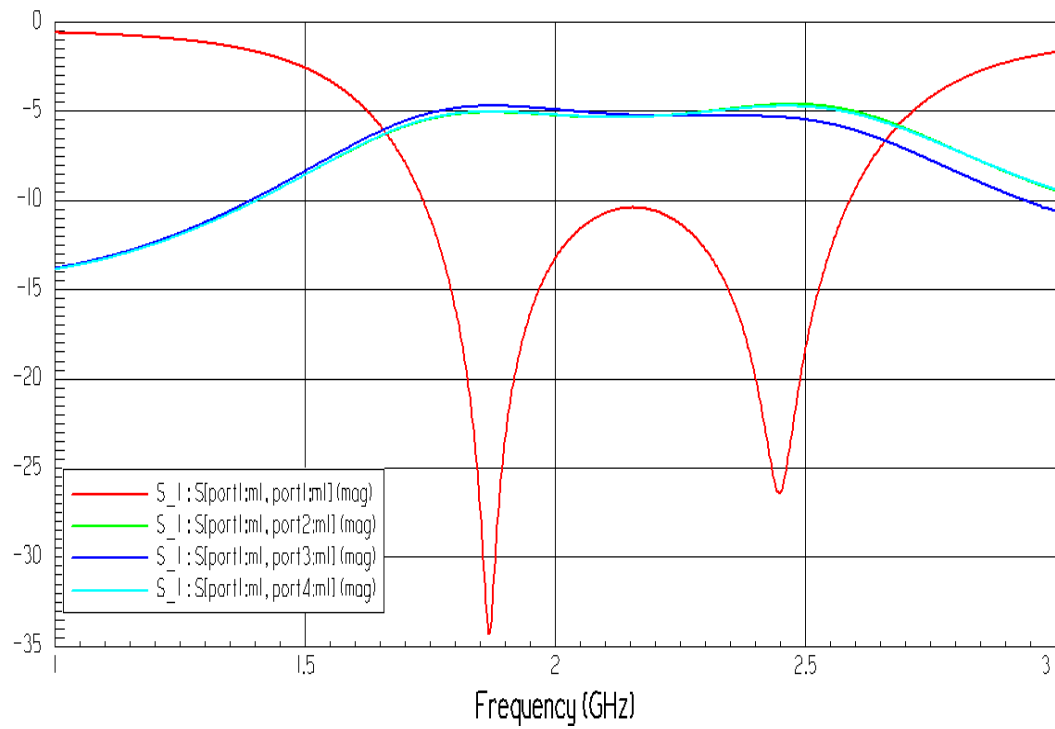


Figure 4.26 S-parameter for the triangular gap is filled

	Measured			HFSS		
	S_{21}	S_{31}	S_{41}	S_{21}	S_{31}	S_{41}
Minimum Insertion Loss (dB)	-5.108	-4.908	-5.171	-4.942	-4.925	-4.895
4.77-dB Reference (dB)	-9.878	-9.678	-9.941	-9.712	-9.695	-9.665
f_L (GHz) / f_H (GHz)	1.739 / 2.575	1.739 / 2.575	1.739 / 2.575	1.694 / 2.528	1.694 / 2.528	1.694 / 2.528
f_c (GHz)	2.157	2.157	2.157	2.111	2.111	2.111
Fractional Bandwidth (%)	38.75	38.75	38.75	39.50	39.50	39.50
Error (%)	2.13	2.13	2.13	2.18	2.18	2.18

Table 4.4 Comparison between the measure and simulated S-parameter

4.6 Parametric Analysis

This section of Chapter 4 is about the case studies on Four-port Microstrip Patch Power Divider by changing the value of the variable such as patch length and width. The main purpose of this studies being carried out is to observe the changes of the s-parameter with the changes of the variables, whether it produces a better or worst result. Other parameter such as frequency range and centre frequency will be remained. The configuration of the proposed design filter shown below ;

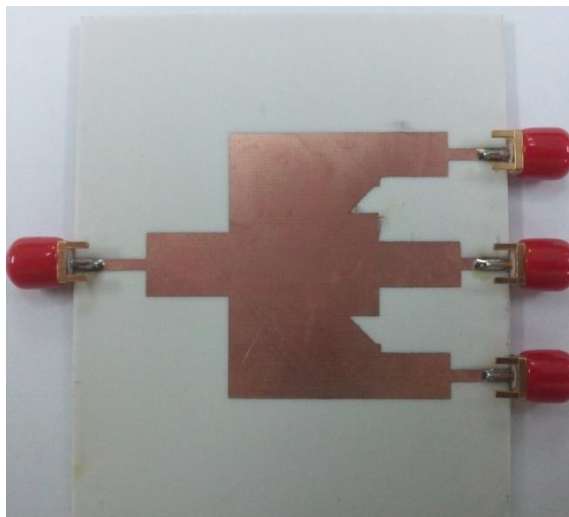


Figure 4.27 Configuration of the Four-port Microstrip Patch Power Divider

Effect of changes in length L_2

From the Table 4.2, when the length L_2 changes from 15.5 mm to 14.5 mm, the magnitude of S_{11} changes a little from -11.140 dB to -10.896 dB inside the passband ranging from 1.769 Ghz to 2.633 Ghz .

When the length L_2 changes from 15.5 mm to 16.5 mm, the magnitude of S_{11} changes a little from -11.140 dB to -9.423 dB inside the passband ranging from 1.676 Ghz to 2.463 Ghz . For $L_2 = 14.5$, the first resonant mode increases to -21.900 dB and the second resonant mode increases to -21.562 dB. For $L_2 = 16.5$, the first resonant mode increases to -22.875 dB and the second resonant mode increases to -18.311 dB. The result is ideal when the length $L_2 = 15.5$ mm.

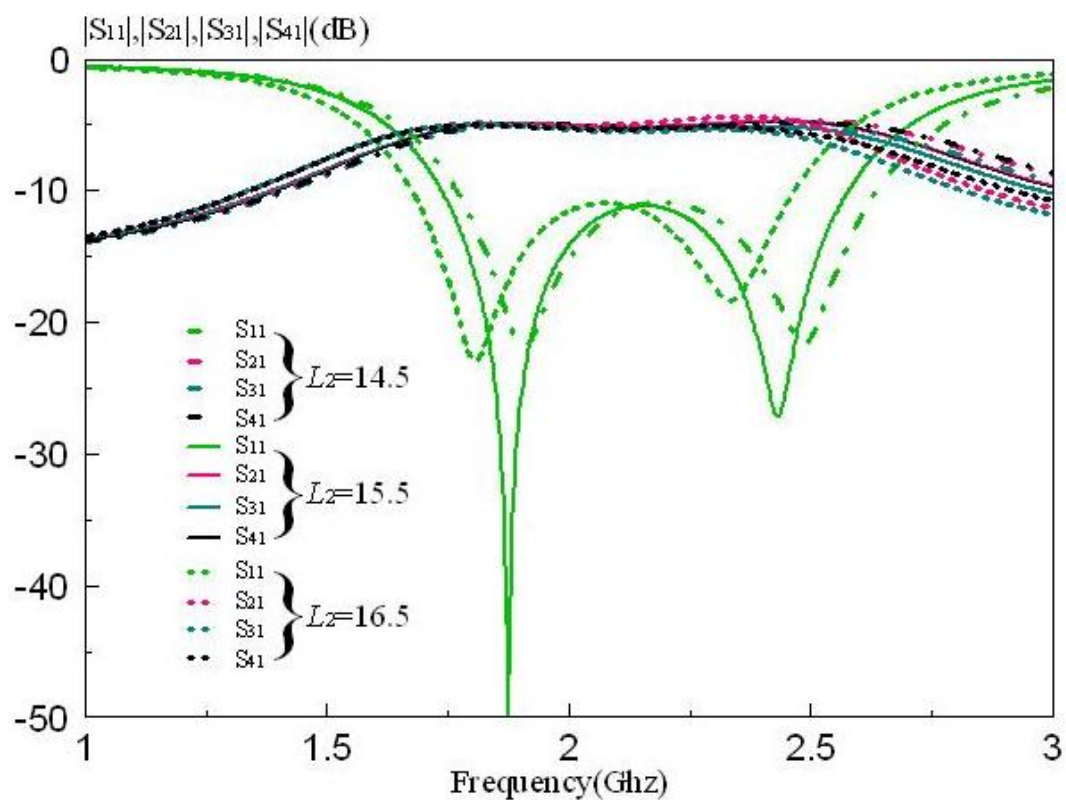


Figure 4.28 Effect of changes in length L_2 (Magnitude)

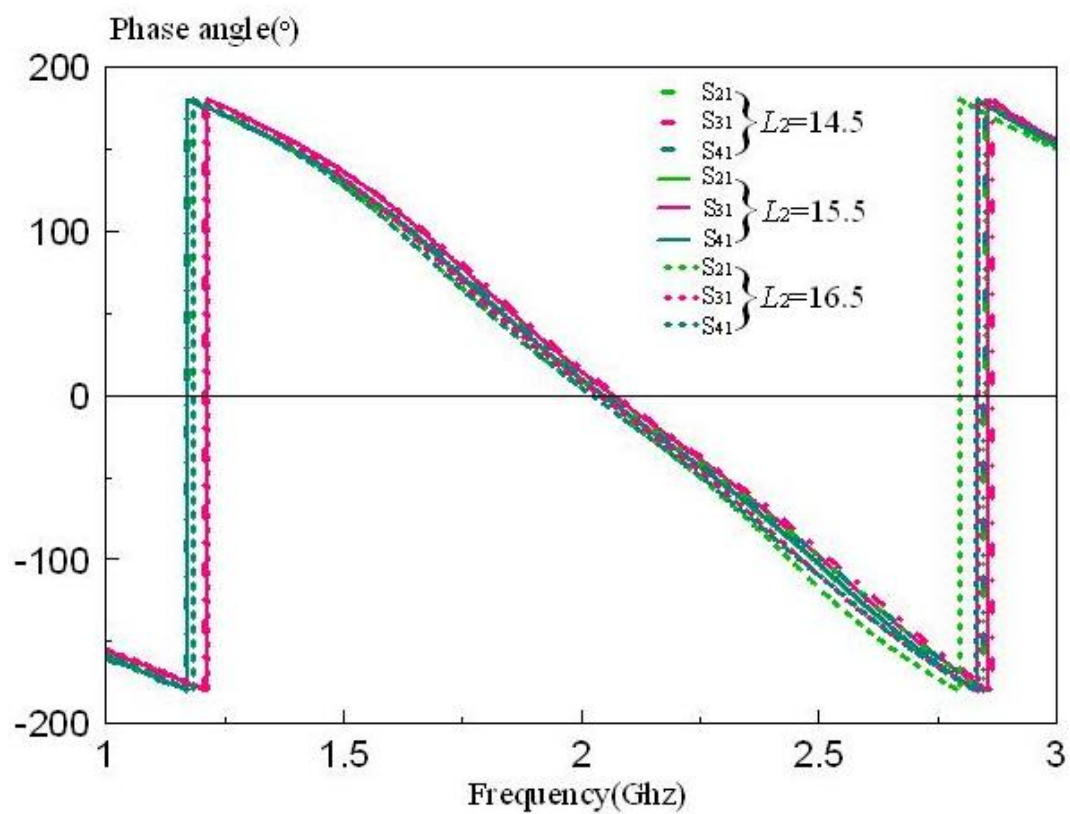


Figure 4.29 Effect of changes in length L_2 (Phase)

Effect of changes in length L_3

From the Table 4.2, when the length L_3 changes from 40.9 mm to 39.9 mm, the magnitude of S_{11} changes a little from -11.140 dB to -11.257 dB inside the passband ranging from 1.744 Ghz to 2.578 Ghz .

When the length L_3 changes from 40.9 mm to 39.9 mm, the magnitude of S_{11} changes a little from -11.140 dB to -9.423 dB inside the passband ranging from 1.709 Ghz to 2.530 Ghz .

There is a significant change of resonant mode when $L_3 = 41.9$ mm. The first resonant mode increases to -38.054 dB and the second resonant mode decreases to -45.211 dB. The result is ideal when the length $L_3 = 40.9$ mm.

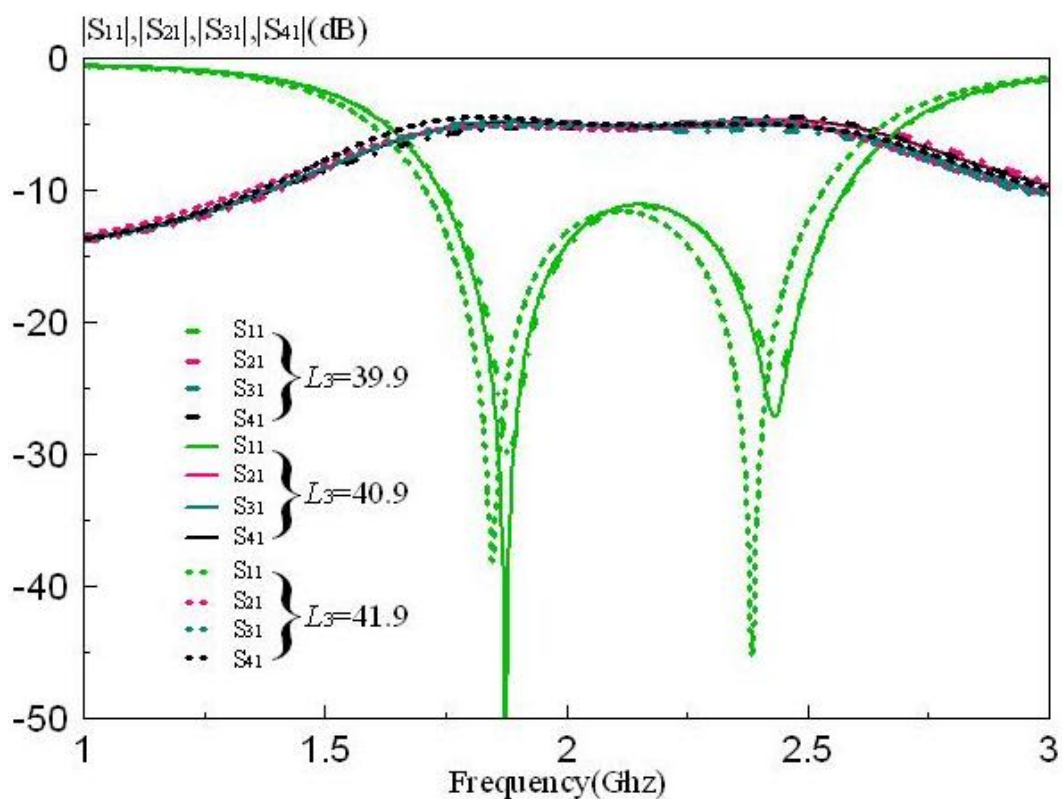


Figure 4.30 Effect of changes in length L_3 (Magnitude)

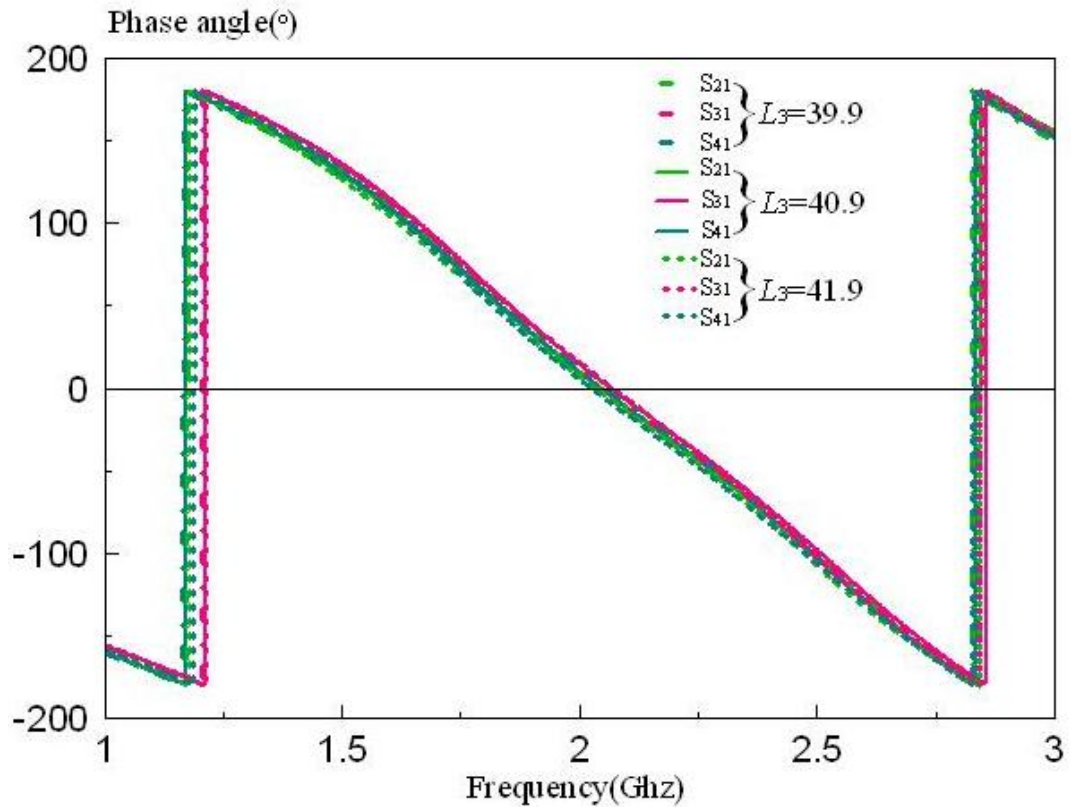


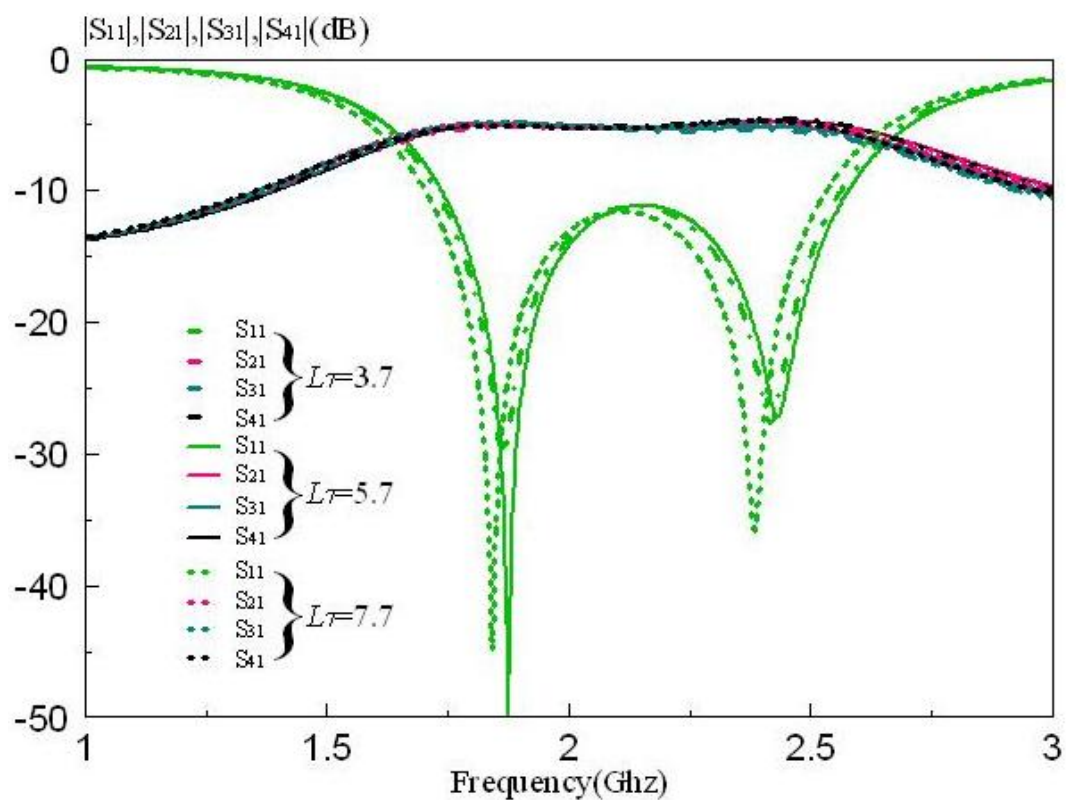
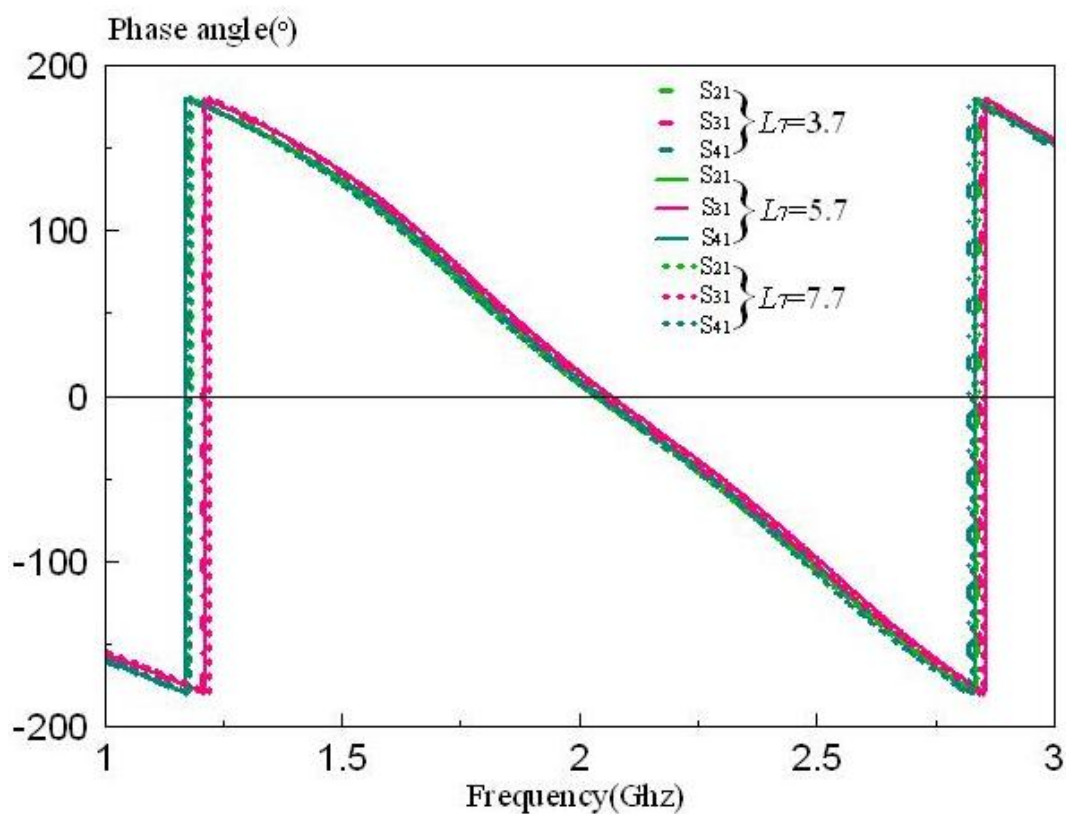
Figure 4.31 Effect of changes in length L_3 (Phase)

Effect of changes in length L_7

From the Table 4.2, when the length L_7 changes from 5.7 mm to 3.7 mm, the magnitude of S_{11} changes a little from -11.140 dB to -11.193 dB inside the passband ranging from 1.729 GHz to 2.560 GHz .

When the length L_7 changes from 5.7 mm to 7.7 mm, the magnitude of S_{11} changes a little from -11.140 dB to -11.567 dB inside the passband ranging from 1.704 GHz to 2.530 GHz .

The result is ideal when the length $L_7 = 5.7$ mm although the matching result is better when the length $L_7 = 7.7$ mm because the difference in phase is more than 5 degrees.

Figure 4.32 Effect of changes in length L_7 (Magnitude)Figure 4.33 Effect of changes in length L_7 (Phase)

Effect of changes in length L_8

From the Table 4.2, when the length L_8 changes from 15.1 mm to 14.1 mm, the magnitude of S_{11} changes a little from -11.140 dB to -11.200 dB inside the passband ranging from 1.729 Ghz to 2.565 Ghz .

When the length L_8 changes from 15.1 mm to 16.1 mm, the magnitude of S_{11} changes from -11.140 dB to -13.037 dB inside the passband ranging from 1.721 Ghz to 2.543 Ghz .

The result is ideal when the length $L_8 = 15.1$ mm although the length $L_8 = 16.1$ mm shows a better matching, but the usable bandwidth is lower than 50 %.

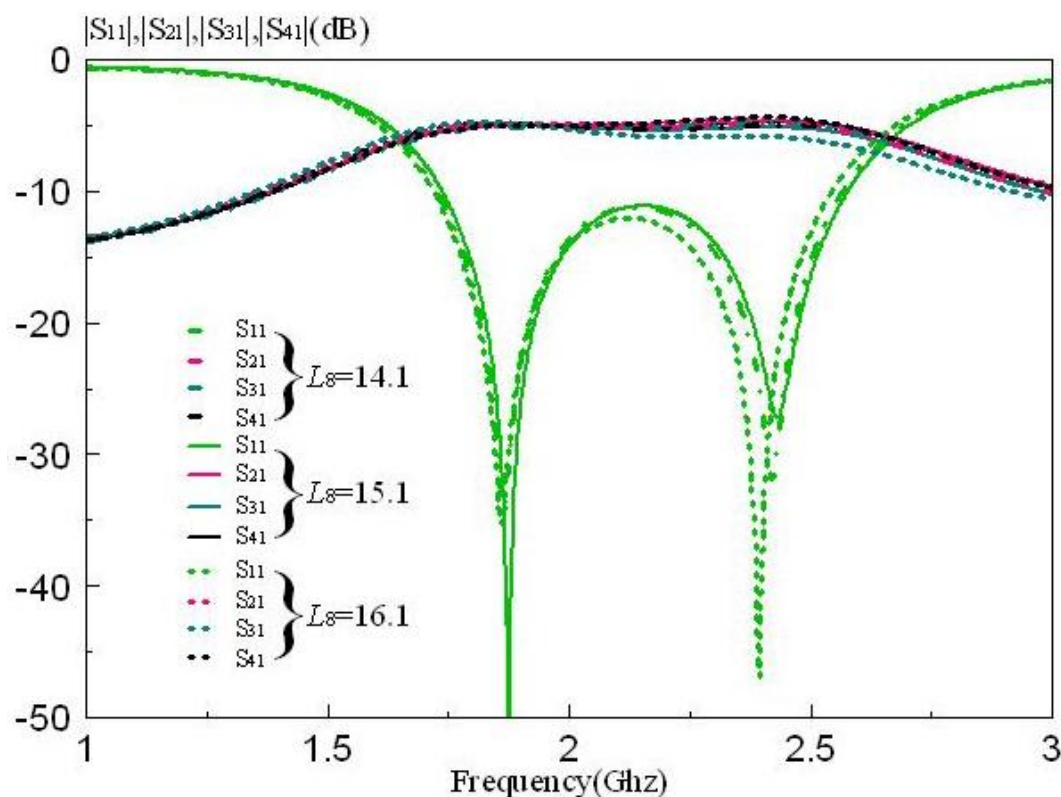


Figure 4.34 Effect of changes in length L_8 (Magnitude)

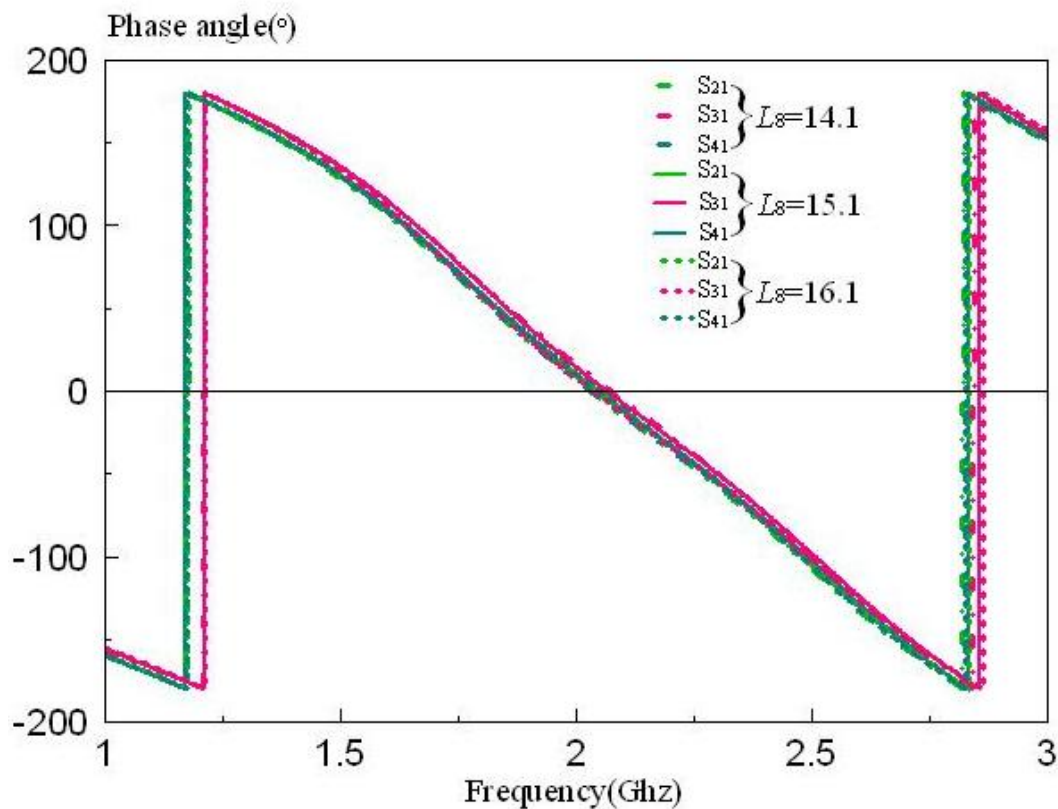


Figure 4.35 Effect of changes in length L_8 (Phase)

Effect of changes in width W_1

From the Table 4.2, when the width W_1 changes from 15.65 mm to 13.65 mm, the magnitude of S_{11} changes a little from -11.140 dB to -11.501 dB inside the passband ranging from 1.724 GHz to 2.598 GHz .

When the width W_1 changes from 15.65 mm to 17.65 mm, the magnitude of S_{11} changes from -11.140 dB to -10.933 dB inside the passband ranging from 1.716 GHz to 2.583 GHz . Changes of W_1 will affect the matching and the insertion loss. The usable bandwidth is decreasing in accordance to the changes. The result is ideal when width $W_1 = 15.65$ mm .

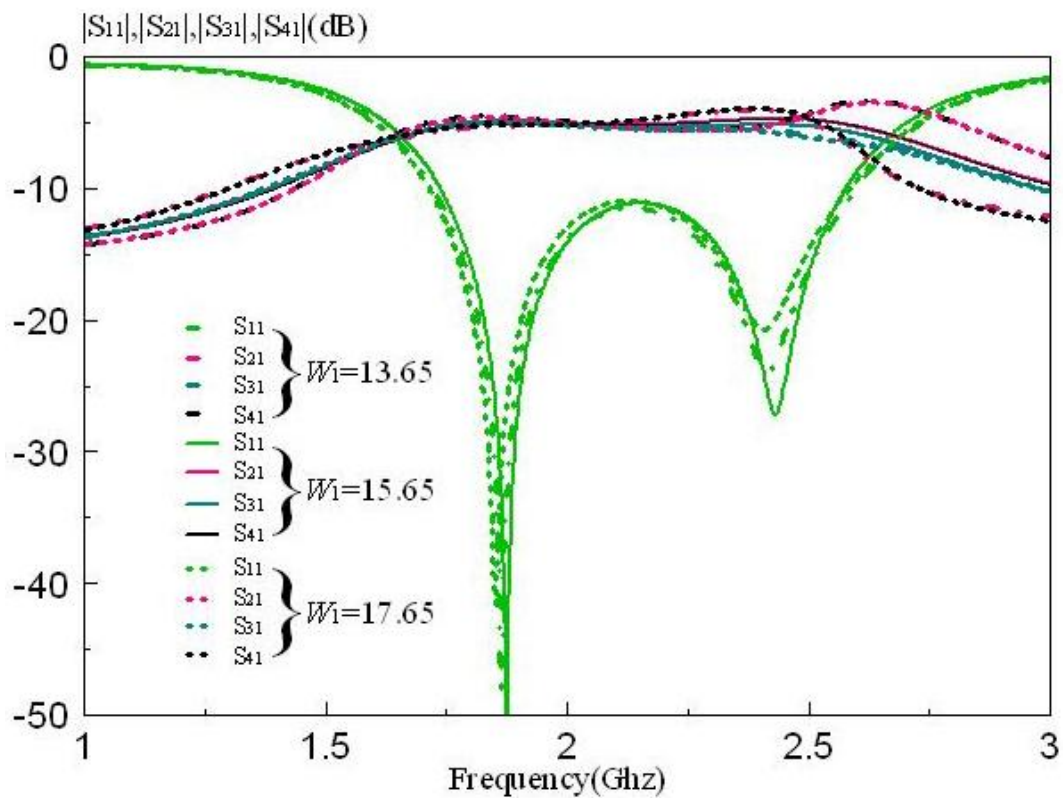


Figure 4.36 Effect of changes in width W_1 (Magnitude)

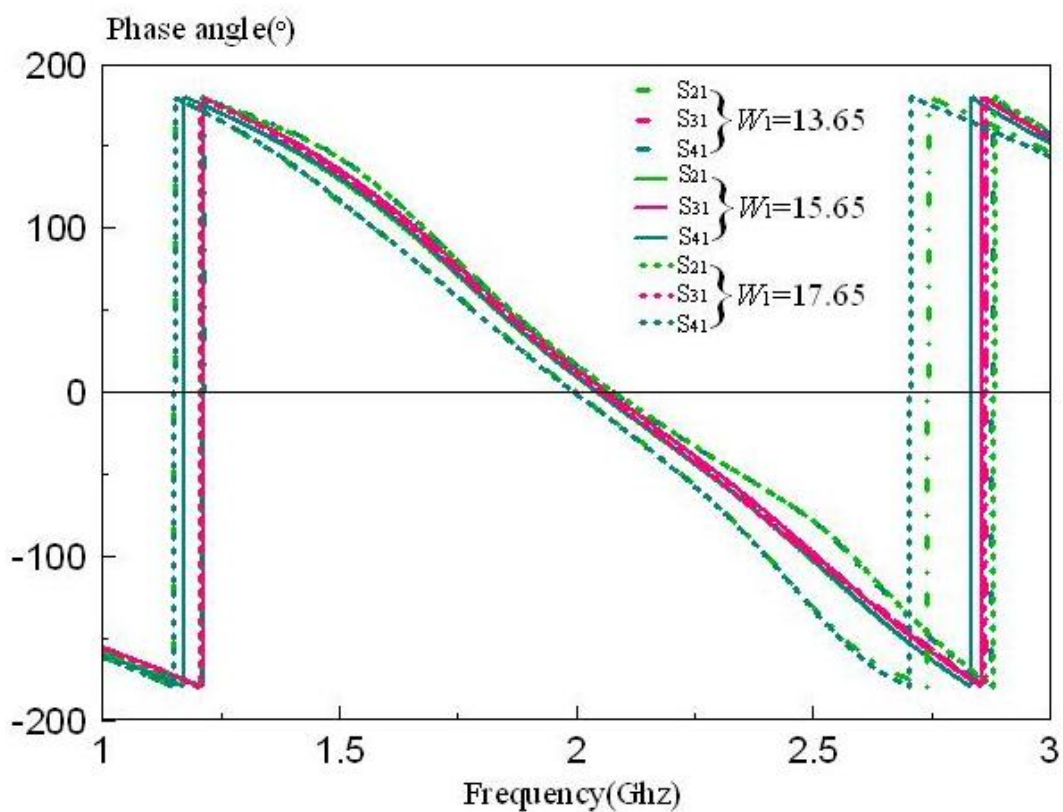


Figure 4.37 Effect of changes in width W_1 (Phase)

Effect of changes in width W_2

From the Table 4.2, when the width W_2 changes from 7 mm to 6 mm, the magnitude of S_{11} changes a little from -11.140 dB to -10.236 dB inside the passband ranging from 1.706 GHz to 2.545 GHz .

When the width W_2 changes from 7 mm to 8 mm, the magnitude of S_{11} changes from -11.140 dB to -11.903 dB inside the passband ranging from 1.751 GHz to 2.578 GHz . The result is ideal when width $W_2 = 7$ mm .

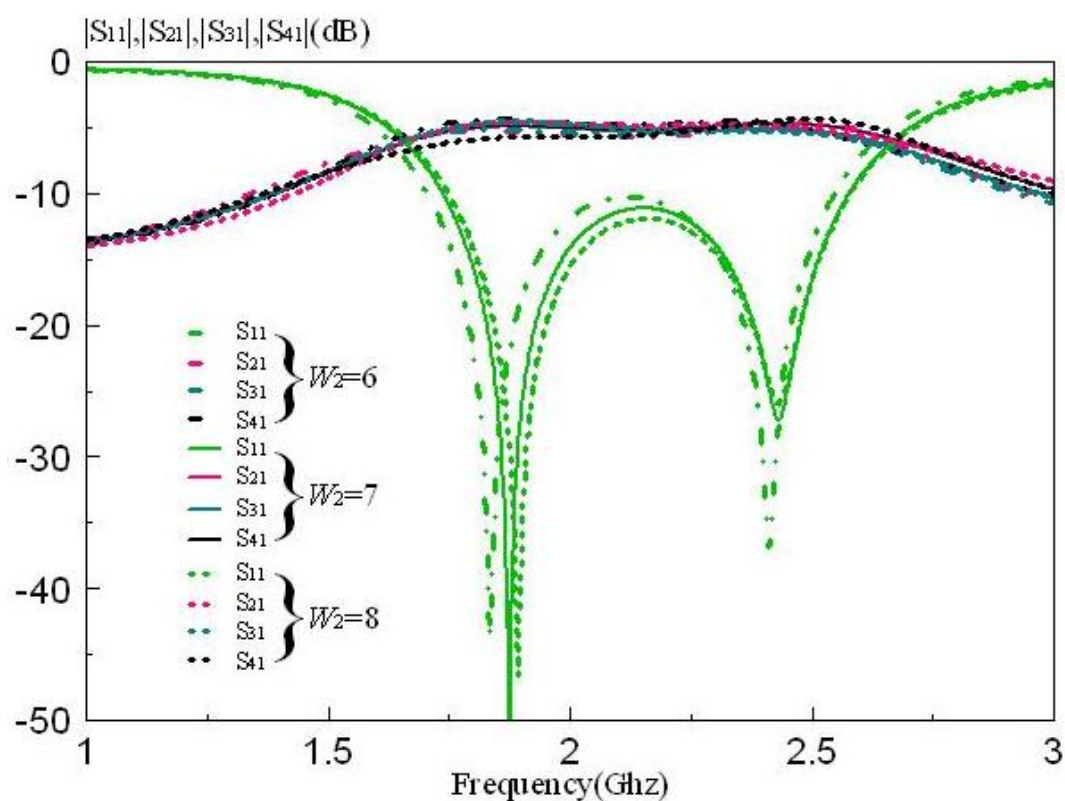


Figure 4.38 Effect of changes in width W_2 (Magnitude)

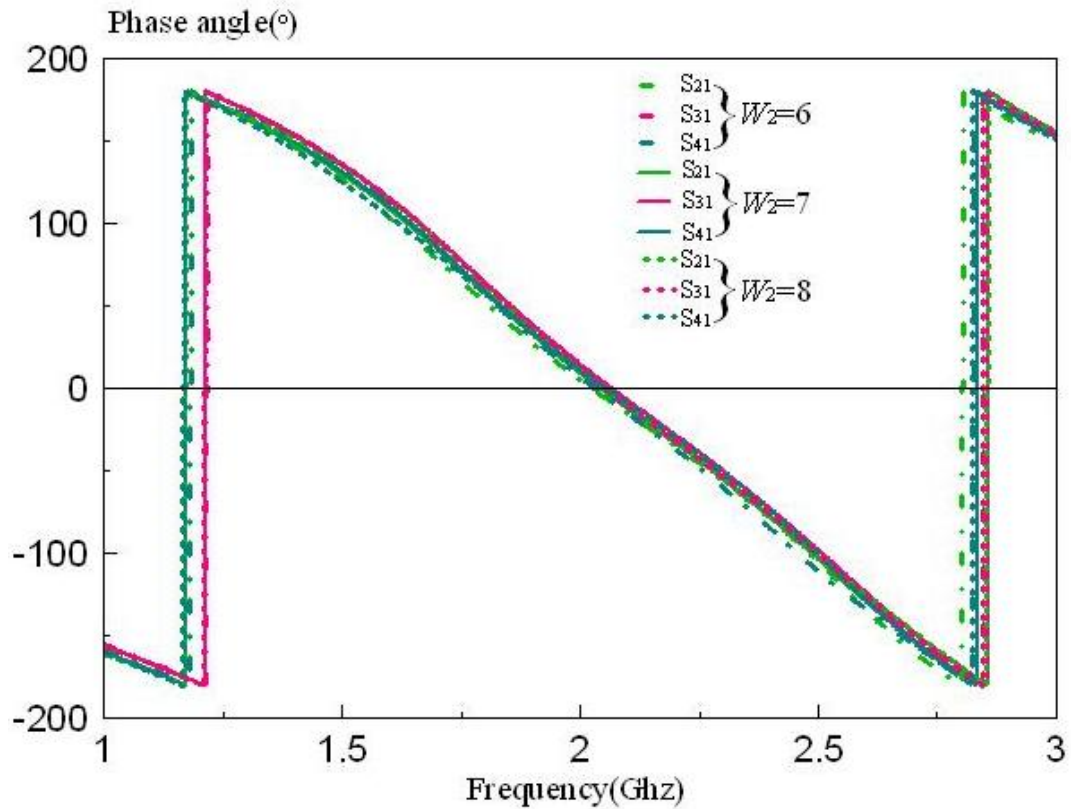


Figure 4.36 : Effect of changes in width W_2 (Phase)

Effect of changes in width W_3

From the Table 4.2, when the width W_3 changes from 10 mm to 8 mm, the magnitude of S_{11} changes a little from -11.140 dB to -18.015 dB inside the passband ranging from 1.808 GHz to 2.528 GHz . When the width W_3 changes from 10 mm to 12 mm, the magnitude of S_{11} changes from -11.140 dB to -7.531 dB inside the passband ranging from 1.679 GHz to 2.565 GHz .

There is a significant change of resonant mode as W_3 changes. For $W_3 = 8$ mm, the first resonant mode decreases to -41.424 dB and the second resonant mode increases to -20.075 dB. For $W_3 = 12$ mm, the first resonant mode increases to -26.156 dB and the second resonant mode increases to -15.919 dB.

The result is ideal when width $W_3 = 8$ mm as the matching of the proposed design is better at -18.015 dB and the difference of phase between S_{21}, S_{31} and S_{41} only -4.5 degree in the passband, which is acceptable.

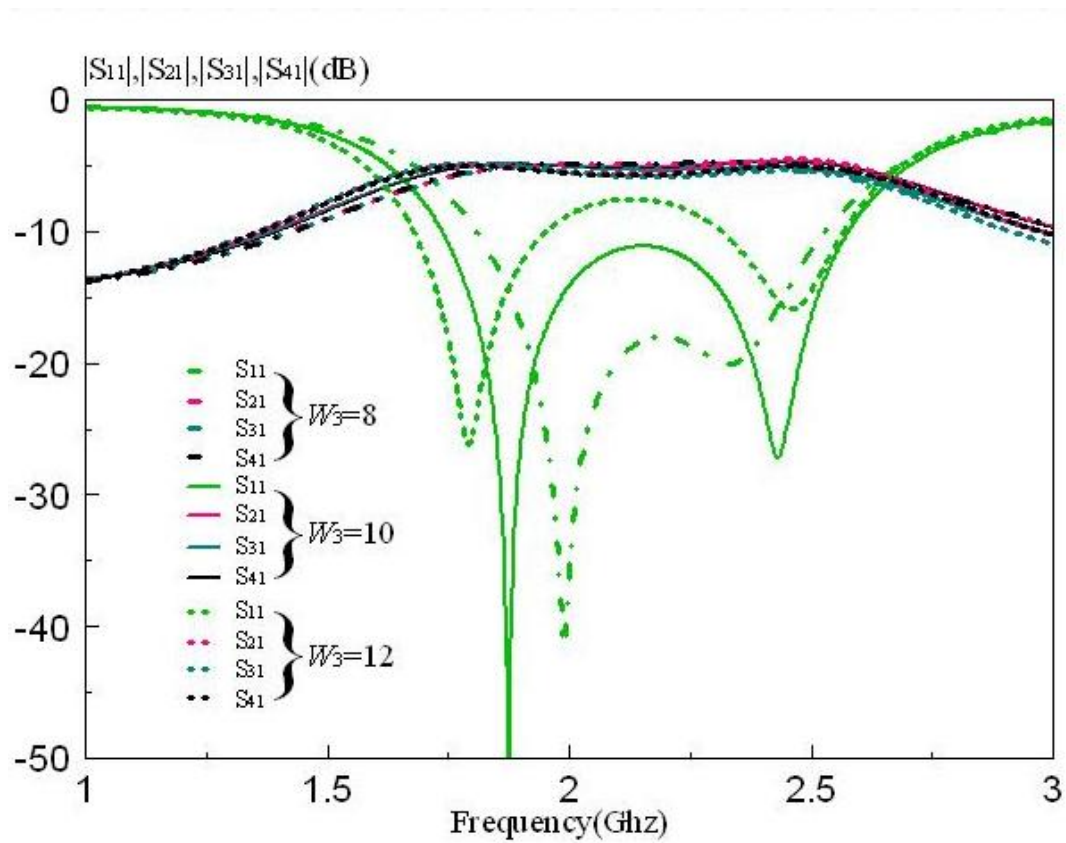


Figure 4.39 Effect of changes in width W_3 (Magnitude)

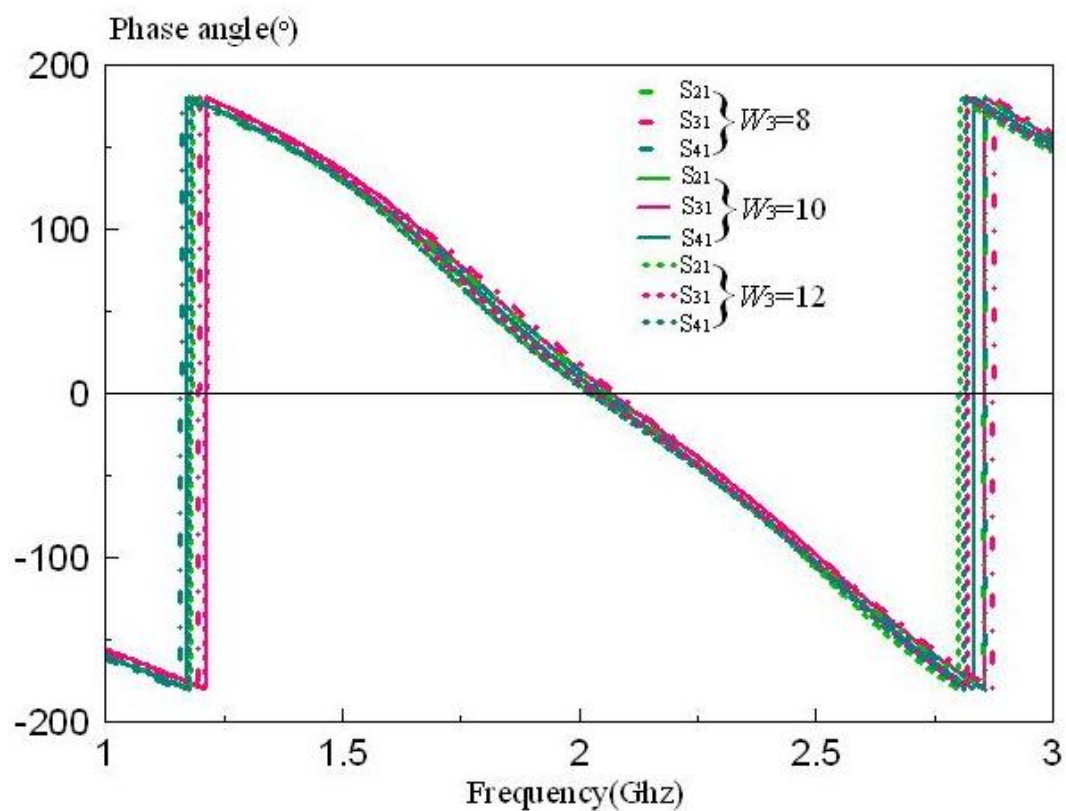


Figure 4.40 Effect of changes in width W_3 (Phase)

Effect of changes in width W_4

From the Table 4.2, when the width W_4 changes from 41.3 mm to 39.3 mm, the magnitude of S_{11} changes a little from -11.140 dB to -10.706 dB inside the passband ranging from 1.711 Ghz to 2.573 Ghz .

When the width W_4 changes from 41.3 mm to 43.3 mm, the magnitude of S_{11} changes from -11.140 dB to -12.658 dB inside the passband ranging from 1.724 Ghz to 2.518 Ghz . The result is ideal when width $W_4 = 41.3$ mm although the width $W_4 = 43.3$ mm shows a better matching, but the usable bandwidth is lower than 50 %.

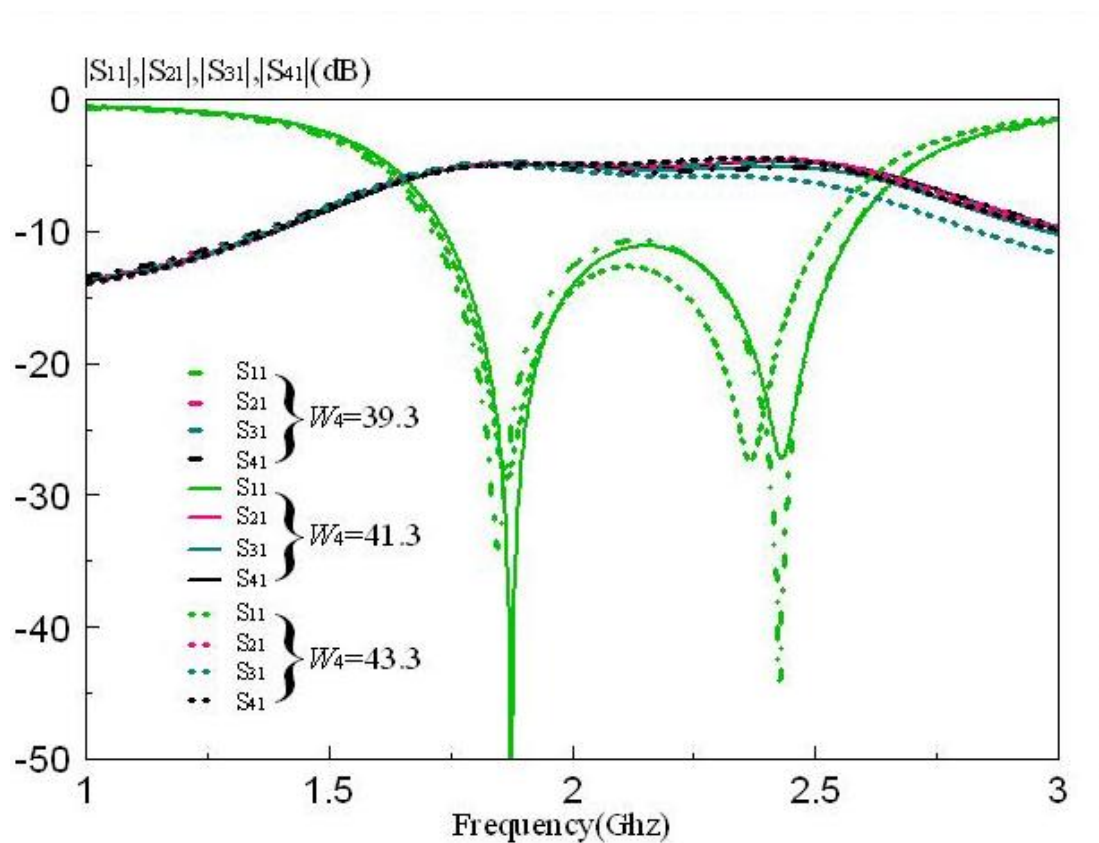


Figure 4.41 Effect of changes in width W_3 (Magnitude)

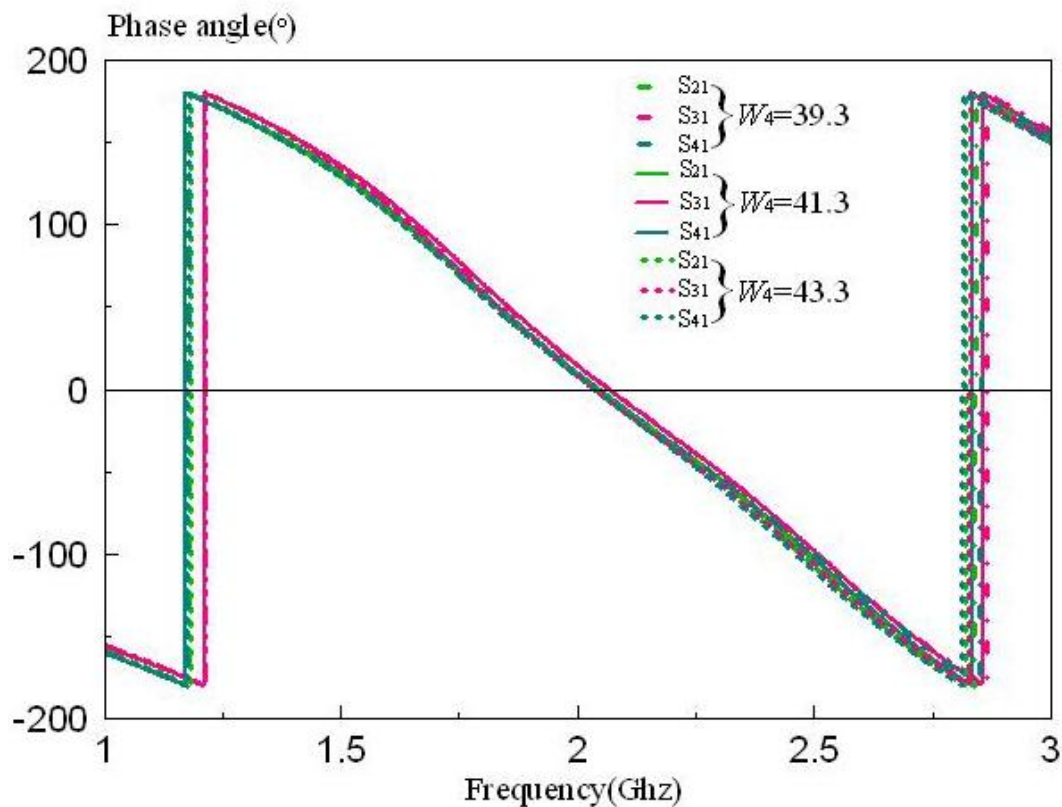
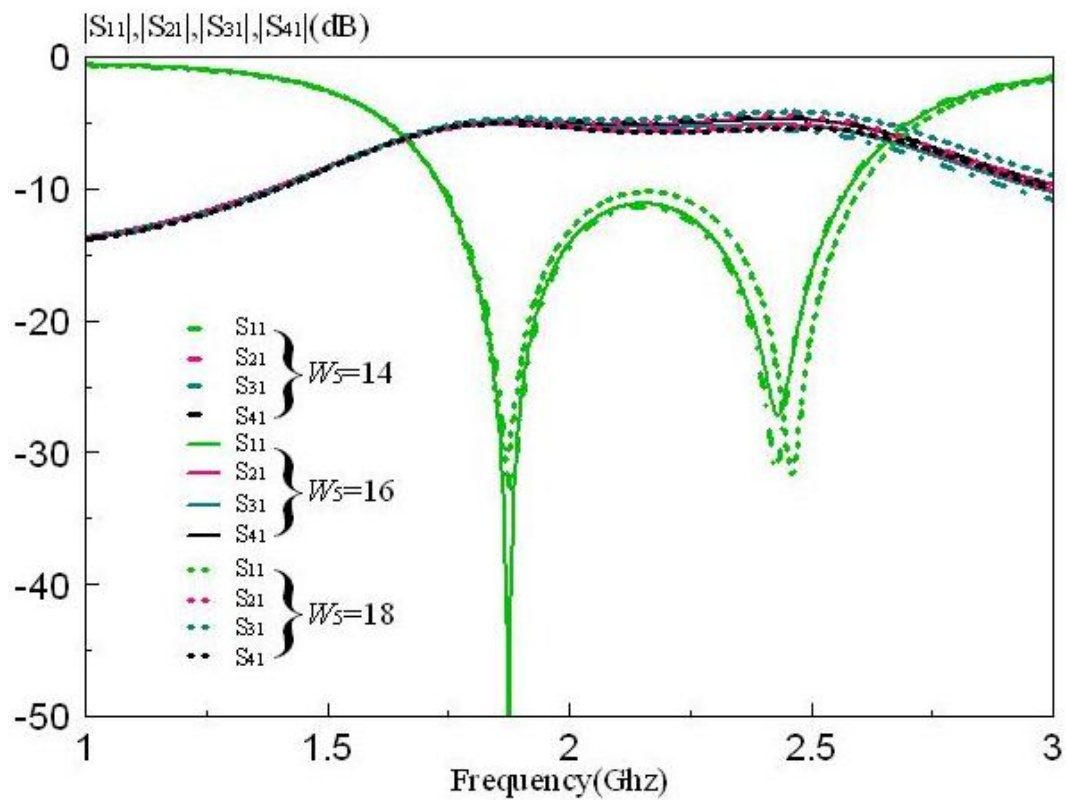
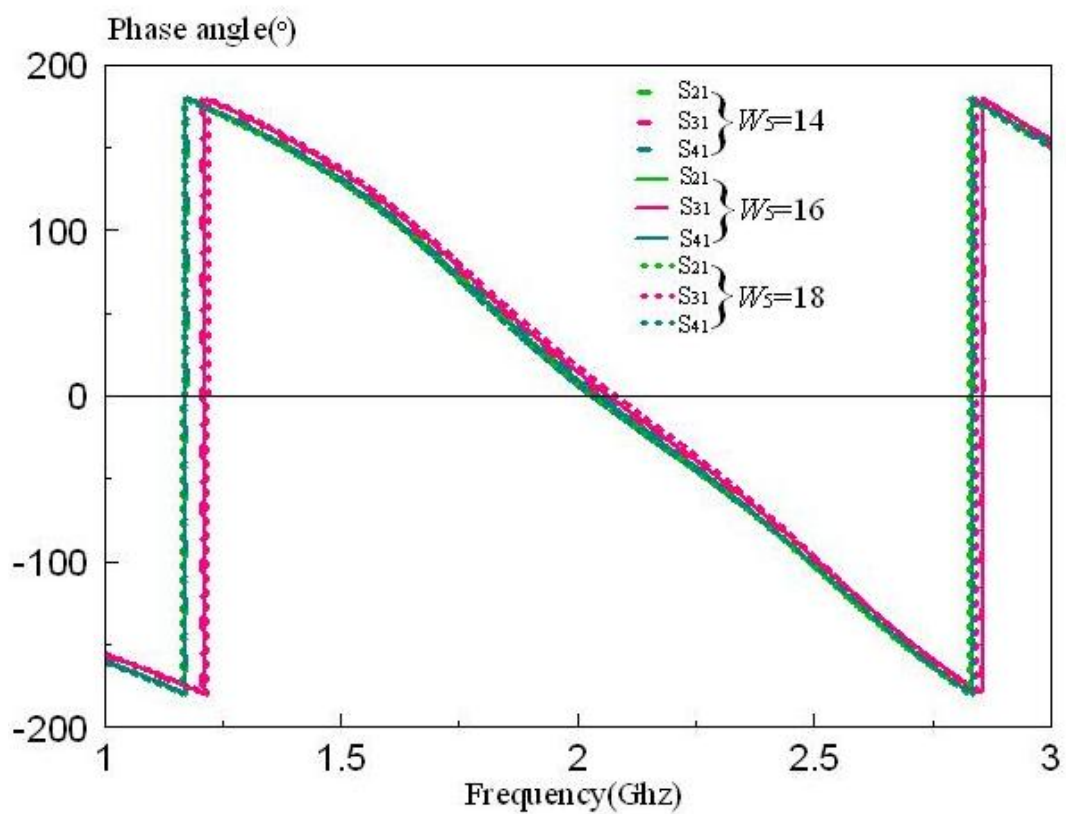


Figure 4.42 Effect of changes in width W_3 (Phase)

Effect of changes in width W_5

From the Table 4.2, when the width W_5 changes from 16 mm to 14 mm, the magnitude of S_{11} changes a little from -11.140 dB to -11.353 dB inside the passband ranging from 1.741 GHz to 2.570 GHz .

When the width W_5 changes from 16 mm to 18 mm, the magnitude of S_{11} changes from -11.140 dB to -10.216 dB inside the passband ranging from 1.739 GHz to 2.600 GHz . There is no significant changes of s-parameter when W_5 changes. The result is ideal when width $W_5 = 16$ mm.

Figure 4.43 Effect of changes in width W_5 (Magnitude)Figure 4.44 Effect of changes in width W_5 (Phase)

Effect of changes in width W_6

From the Table 4.2, when the width W_6 changes from 7 mm to 6 mm, the magnitude of S_{11} changes a little from -11.140 dB to -11.972 dB inside the passband ranging from 1.756 GHz to 2.580 GHz .

When the width W_6 changes from 7 mm to 8 mm, the magnitude of S_{11} changes from -11.140 dB to -10.740 dB inside the passband ranging from 1.706 GHz to 2.533 GHz . For $W_6=6$ mm, the first resonant mode increases to -35.764 dB and the second resonant mode increases to -22.992 dB. For $W_6=8$ mm, the first resonant mode increases to -31.371 dB and the second resonant mode decreases to -29.953 dB.

The insertion loss is not constant and stable inside the pass band. So no changes should be applied to the proposed design on this variable W_6 .

The result is ideal when width $W_6 = 7$ mm.

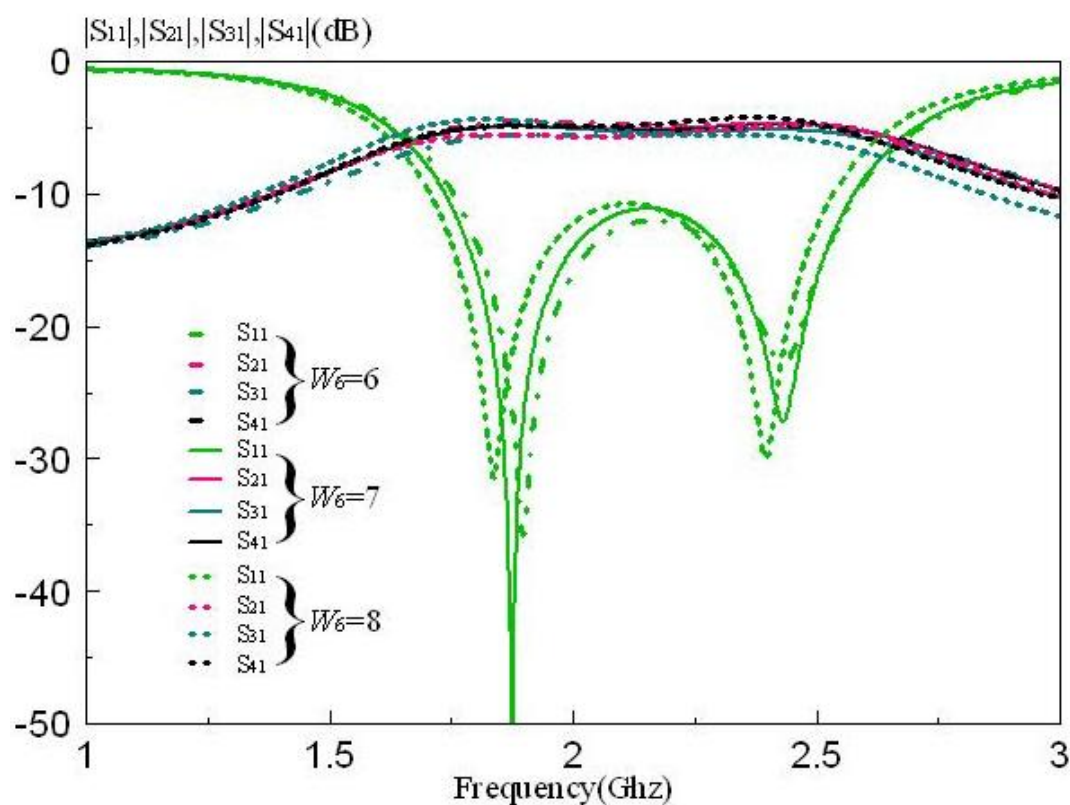


Figure 4.45 Effect of changes in width W_6 (Magnitude)

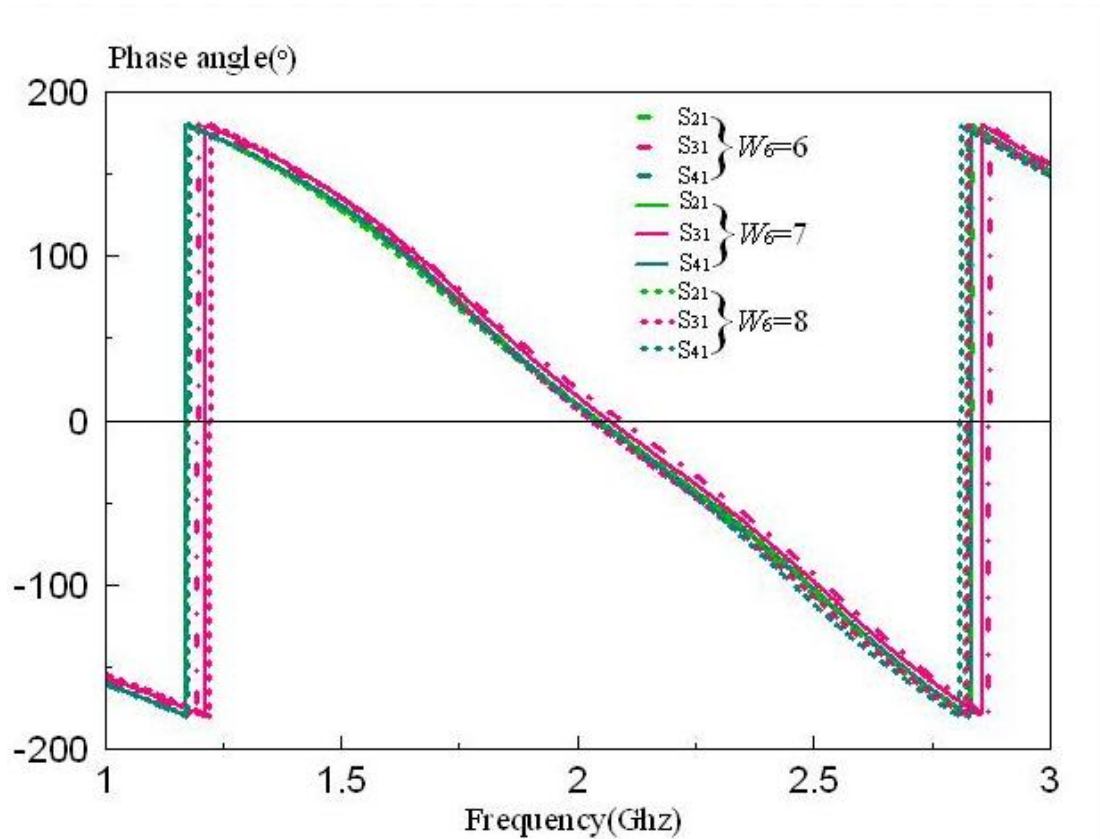


Figure 4.46 Effect of changes in width W_6 (Phase)

Effect of changes in width W_8

From the Table 4.2, when the width W_8 changes from 4.5 mm to 2.5 mm, the magnitude of S_{11} changes a little from -11.140 dB to -10.794 dB inside the passband ranging from 1.664 GHz to 2.473 GHz .

When the width W_8 changes from 4.5 mm to 6.5 mm, the magnitude of S_{11} changes from -11.140 dB to -11.403 dB inside the passband ranging from 1.664 GHz to 2.480 GHz . For $W_8 = 2.5$ mm, the first resonant mode increases to -38.753 dB and the second resonant mode increases to -28.997 dB. For $W_8 = 6.5$ mm, the first resonant mode increases to -31.371 dB and the second resonant mode decreases to -28.204 dB.

The result is ideal when width $W_8 = 4.5$ mm as the width $W_8 = 6.5$ mm has a slightly better matching but the phase are not in acceptable range.

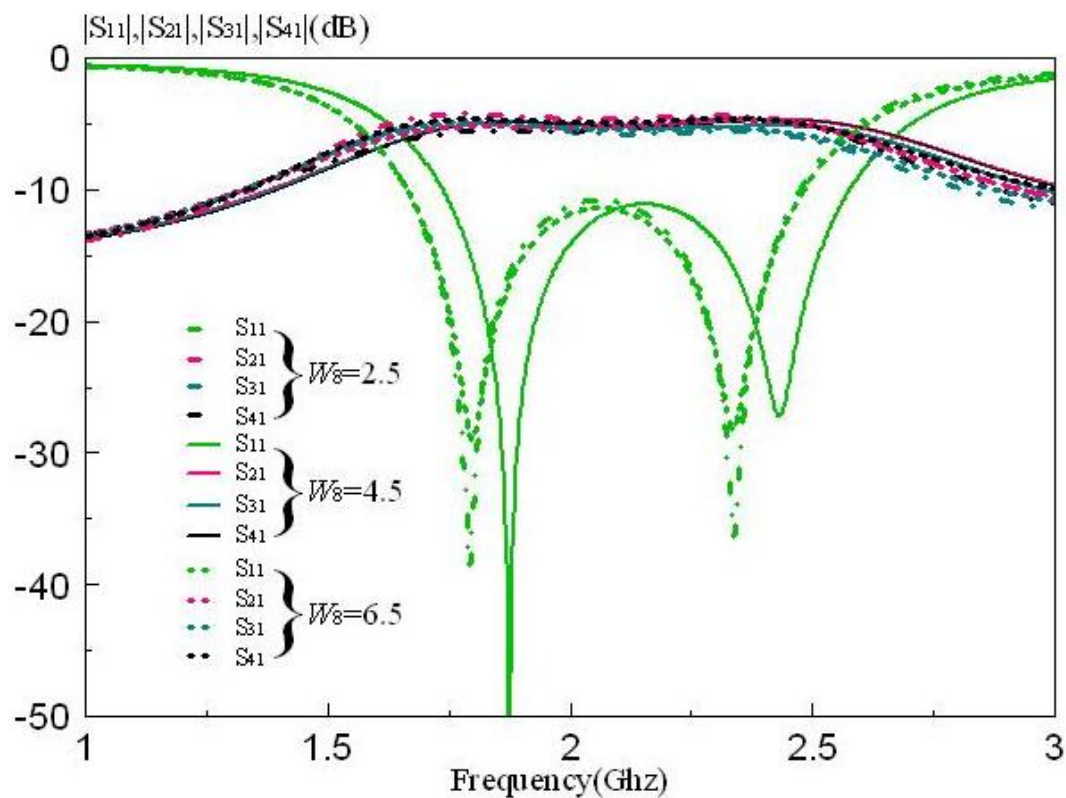


Figure 4.47 Effect of changes in width W_8 (Magnitude)

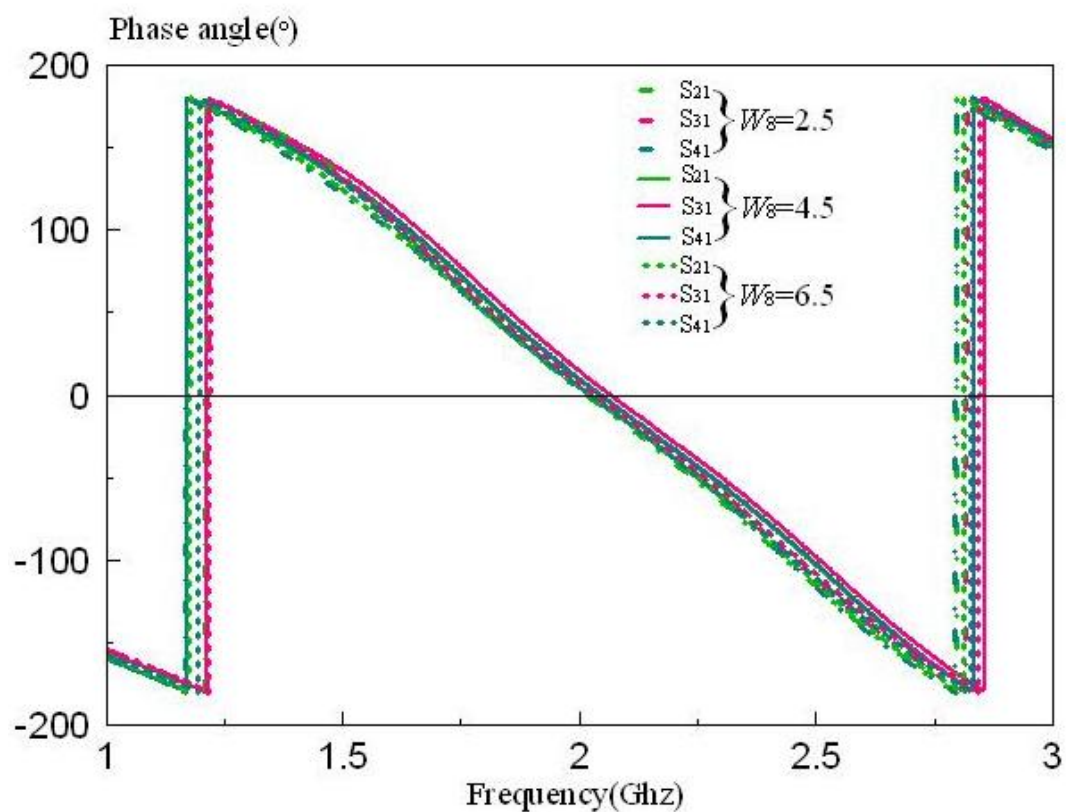


Figure 4.48 Effect of changes in width W_8 (Phase)

4.7 Discussion

One-to-three in-phase power divider is quite rare in the global market as it is not easy to obtain the optimised result for both magnitude and phase. This power divider is the improved version of the previous design by adding one more fed line through the centre stub and connected as an output port. In theory, Wilkinson Power Divider is designed to have either equal or unequal power divided, based on the usage. When one more port is connected, the characteristic impedance must be the same for all the output port if equal power divided is desired.

It shows that to have the same characteristic impedance for each port, the dimension for each patch must be symmetrical. In this design, it is just one resonator connected to all output port. So the dimension for each fed line will be different. From the analysis, it shows that the wave travels faster in the middle compared to the both sides fed line. It is due to the distance from the input port to output port. So, some delay would be applied to the middle fed line. During analysis, the delay can be increased by increasing the length or width of the fed line. Since the time of wave reaches the output port is different, the phase of the power divider should be taken care when changing the above parameter.

The result obtained is considered to be ideal although there is a 4 degree of difference (in the allowable range) in phase between S_{31} with S_{21} and S_{41} . So, this one-to-three power divider is still considered as a good power divider which has an equal power divided with negligible loss.

CHAPTER 5

Future Work and Recommendations

5.1 Achievements

The basic knowledge in the microstrip design has been learnt by the author, especially the concept of power divider. Throughout this project, several new concept of filters have been proposed and comes out as a working prototype. The 3 new working prototype filters are rotational symmetric power divider, three-port microstrip power divider and four-port microstrip power divider. All of the 3 projects are using the same board F4003C which has the dielectric constant of 3.38 and the thickness of 0.8128mm.

A new concept has been initiated by using via holes into the patches to enable the wave resonates through the guidance of the via and transfer to the respective outputs without loss. It has been applied in the 1st project as the wave guidance. With this, a rotational symmetric power divider with insertion loss of -2.92 dB till -3.17 dB is proposed . Although it does not have transmission zeros, it is preferable as it attenuate less than -40 dB and there is not second harmonic observed from 1 GHz till 5 GHz.

The second and third project is using the same concept of resonator to design the power divider. Wilkinson power divider is using the concept of the length and width to modify the impedance from the input to the output without considering much on the phase whereby in this project, the input and output dimension is the same but the patch resonator is modified to obtain the optimised result as the

Wilkinson Power Divider. The phase also can be tuned by tuning the dimension of the resonator. The 3-ways power divider has the insertion loss of -3.048 dB and the 4-ways power divider has the insertion loss of -4.925 dB, which is quite close to the conventional result of -3 dB and -4.77 dB respectively. Several studies on the proposed design has been carried out to understand the characteristic of the design and monitor the changes of the parameter.

5.2 Future Work

There are several recommendations that can be considered for future design. Whenever there is a design with via holes, it is advisable to have a proper grounding and soldering on the resonator as it affects the result a lot. A proper wire diameter must be used to fit the via hole in order to obtain more accurate result, nearer to the simulation.

Furthermore, it is also advisable to have additional port to make it one to three power divider as not to waste the additional patch. For the current design, it is found to be quite difficult to add in another port due to the limitation in time for simulation and fabrication. An additional output port can help to reduce the number of filters by having more appliances connected together. A multilayer design of power divider is also preferable as it helps to reduce space. Since all the design above are in-phase power divider, it is advisable to have out-of-phase power divider from this design. As the expectation grows higher in the market, a multipurpose power divider is definitely preferable. A standalone in-phase power divider is good but additional out-of-phase design will make it more advantages.

5.3 Conclusion

The aims and objectives of the project have been achieved. Several new concepts with new designs have been proposed such as rotational symmetric power divider and multiway power divider using the concept of resonator. Knowledge in using the simulation tool and research also a merit for the author to improve the design and even future work.

REFERENCES

- [1] Band Pass Filter. (n.d.) Wikipedia. Retrieved November 15, 2011 from http://en.wikipedia.org/wiki/Band_pass_filter
- [2] Wilkinson Power Divder (n.d.) Wikipedia . Retrieved November 15, 2011 from http://en.wikipedia.org/wiki/Wilkinson_power_divider
- [3] Microstrip (n.d.) Wikipedia . Retrieved November 15, 2011 from <http://en.wikipedia.org/wiki/Microstrip>
- [4] Microstrip Substate Equation (n.d.) Wikipedia . Retrieved November 15, 2011 from <http://www.rfcafe.com/references/electrical/microstrip-eq.htm>
- [5] Wilkinson Power Divider diagram (n.d.) Wikipedia . Retrieved November 15, 2011 from http://www.microwaves101.com/encyclopedia/Wilkinson_splitters.cfm
- [6] Pozar, D. M. (1998). *Microwave Engineering*. Canada: John Wiley & Sons, Inc.
- [7] Y. Wu, Y. Liu, and X. Liu, "Dual-frequency power divider with isolation stubs," *Electron. Lett.*, vol. 44, no. 24, pp. 1407–1408, Nov. 2008.
- [8] K.-K. M. Cheng and C. Law, "A novel approach to the design and implementation of dual-band power divider," *IEEE Trans. Microw. Theory Tech.*, vol. 56, no. 2, pp. 487–492, Feb. 2008.
- [9] Daniel G. Swanson, Jr. Grounding Microstrip Lines With Via Holes. *IEEE TRANSACTIONS ON MICROWAVE THEORY AND TECHNIQUES*, VOL. 40, NO. 8, AUGUST 1992

- [10] A Novel Design of Microstrip Square Patch Filter. Guang Xue, Dexin Qu, Jin Li, Xiaojun Qiu and Chuanjia Zheng .
- [11] Y-junction power divider based on substrate integrated waveguide. X. Zou, C.-M. Tong and D.-W. Yu
- [12] Laila K. Hady, Ahmed A. Kishk, and Darko Kajfez. Five-Way Power Divider Based on Dielectric Resonator Whispering Gallery Modes.
- [13] Y.-H. Jeng, S.-F. R. Chang, Y.-M. Chen, and Y.-J. Huang, "A novel self-coupled dual-mode ring resonator and its applications to bandpass filters," *IEEE Trans. Microw. Theory Tech.*, vol. 47, no. 10, pp. 1938–1948, Oct. 1999.
- [14] Hong J S, Li Shu-zhou. Theory and experiment of dual-mode microstrip triangular patch resonator and filters. *IEEE Trans. Microw. Theory Tech.*, vol. 52, pp. 1237-1243, Apr. 2004.
- [15] L. Wu, Z. Sun, H. Yilmaz, and M. Berroth, "A dual-frequency Wilkinson power divider," *IEEE Trans. Microw. Theory Tech.*, vol. 54, no. 1, pp. 278–284, Jan. 2006.
- [16] A. A. M. Saleh, "Planar electrically symmetric n-Way hybrid power dividers/combiners," *IEEE Trans. Microw. Theory Tech.*, vol. MTT-28, no. 6, pp. 555–563, Jun. 1980.
- [17] N. Nagai, E. Maekawa, and K. Ono, "New n-Way hybrid power dividers," *IEEE Trans. Microw. Theory Tech.*, vol. MTT-25, no. 12, pp. 1008–1012, Dec. 1977.
- [18] A. Gorur and C. Karpuz, "Compact dual-band bandpass filters using dual-mode resonators," in *IEEE MTT-S Int. Microw. Symp. Dig.*, Jun. 2007, pp. 905–908.

- [19] M. Matsuo, H. Yabuki, and M. Makimoto, "Dual-mode stepped impedance ring resonator for bandpass filter applications," *IEEE Trans. Microw. Theory Tech.*, vol. 49, no. 7, pp. 1235–1240, Jul. 2001.
- [20] J. S. Hong and M. J. Lancaster, "Bandpass characteristics of new dualmode microstrip square loop resonators," *Electron. Lett.*, vol. 31, no. 11, pp. 891–892, May 1995.
- [21] Wolff, "Microstrip bandpass filter using degenerate modes of a microstrip ring resonator," *Electron. Lett.*, vol. 8, no. 12, pp. 302–303, Jun. 1972.
- [22] K. Chang and L. H. Hsieh, *Microstrip Ring Circuits and Related Structures*. New York: Wiley, 2004.
- [23] Yongle Wu, Student Member, IEEE, Yuanan Liu, Member, IEEE, Quan Xue, Senior Member, IEEE, Shulan Li, and Cuiping Yu. Analytical Design Method of Multiway Dual-Band Planar Power Dividers With Arbitrary Power Division. *IEEE TRANSACTIONS ON MICROWAVE THEORY AND TECHNIQUES*, VOL. 58, NO. 12, DECEMBER 2010
- [24] Sha Luo, Student Member, IEEE, Lei Zhu, Senior Member, IEEE, and Sheng Sun, Member, IEEE. A Dual-Band Ring-Resonator Bandpass Filter Based on Two Pairs of Degenerate Modes. *IEEE TRANSACTIONS ON MICROWAVE THEORY AND TECHNIQUES*, VOL. 58, NO. 12, DECEMBER 2010
- [25] Roberto Sorrentino, Fellow, IEEE, Ferdinand Alessandri, Mauro Mongiardo, Gianfranco Avitabile, and Luca Roselli Full-Wave Modeling of Via Hole Grounds in Microstrip by Three-Dimensional Mode Matching Technique. *IEEE TRANSACTIONS ON MICROWAVE THEORY AND TECHNIQUES*, VOL. 40, NO. 12, DECEMBER 1992